UMENTATION PAGE

Form Approved
OMB No. 0704-0188

1. AGENCY USE ONLY (Leave blank)	2. REPORT DATE	3. REPORT TYPE AND DATES COVERED
	1992	THESIS/~~DISSERTATION~~

4. TITLE AND SUBTITLE
Predicting the Movement of Carolina Coastal Fronts

5. FUNDING NUMBERS

6. AUTHOR(S)
William Charles Tasso, Captain

7. PERFORMING ORGANIZATION NAME(S) AND ADDRESS(ES)
AFIT Student Attending: North Carolina State University

8. PERFORMING ORGANIZATION REPORT NUMBER
AFIT/CI/CIA- 92-097

9. SPONSORING/MONITORING AGENCY NAME(S) AND ADDRESS(ES)
AFIT/CI
Wright-Patterson AFB OH 45433-6583

10. SPONSORING/MONITORING AGENCY REPORT NUMBER

11. SUPPLEMENTARY NOTES

12a. DISTRIBUTION/AVAILABILITY STATEMENT
Approved for Public Release IAW 190-1
Distributed Unlimited
ERNEST A. HAYGOOD, Captain, USAF
Executive Officer

12b. DISTRIBUTION CODE

13. ABSTRACT *(Maximum 200 words)*

14. SUBJECT TERMS	15. NUMBER OF PAGES
	116
	16. PRICE CODE

17. SECURITY CLASSIFICATION OF REPORT	18. SECURITY CLASSIFICATION OF THIS PAGE	19. SECURITY CLASSIFICATION OF ABSTRACT	20. LIMITATION OF ABSTRACT

Name: William Charles Tasso

Title: Predicting the Movement of Carolina Coastal Fronts.

Rank: Captain.

Branch: USAF

Date: 1992

Pages: 116

Degree: Master of Science

School: North Carolina State University

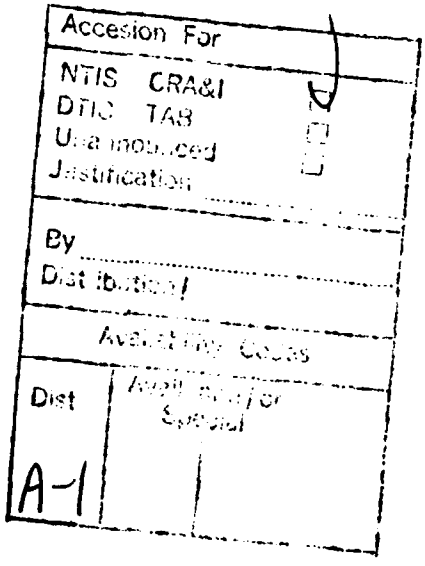

ABSTRACT

TASSO, WILLIAM CHARLES. Predicting the Movement of Carolina Coastal Fronts. (Under the direction of Allen J. Riordan)

The topic of coastal front movement has been largely neglected especially in the vicinity of the Carolinas. Since the presence and subsequent movement of the front can effect a significant change in a nearby stations' winds, temperature, and precipitation type, the accurate prediction of coastal front movement is essential to local forecast precision.

National Meteorological Center (NMC) three-hourly surface charts for the months of November to March were examined for the years 1975-1989. This search netted 51 Carolina coastal front cases which occurred coincident with Appalachian cold air damming and met additional selection criteria. Although all the cases exhibited a frontal passage at Cape Hatteras, North Carolina, it was found that only two-thirds of the fronts actually migrated inland. In addition the events were determined to have a peak frequency in the month of January, and a mean axis of stagnation, for onshore cases, that is approximated by a line from Hampton, Virginia to Myrtle Beach, South Carolina.

The use of NMC historical grid point data enabled the construction of climatic, composite, and deviation charts which suggest that offshore events are characterized by damming high pressure centers located farther west and with isobars which are oriented perpendicular to the coast for a longer duration.

The influence of Appalachian cold air damming on Carolina coastal front movement was examined in four case studies. These incorporated the analyses of ageostrophic wind angles, the Laplacian of sea level pressure, and a simple mountain-parallel pressure differential calculation. Results indicate that ageostrophy and one-dimensional pressure estimations are unsuitable for the prediction of frontal movement. Attempts to correlate frontal movement with onshore wind angles proved to be inconclusive.

PREDICTING THE MOVEMENT OF CAROLINA COASTAL FRONTS

by

William Charles Tasso

A thesis submitted to the Graduate Faculty of

North Carolina State University

in partial fulfillment of the requirements for the Degree of

Master of Science

Department of Marine, Earth & Atmospheric Sciences

Raleigh

1992

Approved by:

S. Raman

P. T. Shaw

A. J. Riordan
Chairman of Advisory Committee

DEDICATION

This thesis is graciously dedicated to:

- My wonderful wife, Elizabeth, for all her love, patience, understanding, encouragement, and endless support.

- My sons, Jason and Matthew, who keep me from taking life too seriously, but enable me to keep things in their proper perspective.

ACKNOWLEDGEMENTS

Any project of this magnitude is seldom the product of a single individual, therefore I would like to gratefully recognize the assistance of the following individuals:

Tom Anderson, whose cataloging of nine years worth of Carolina coastal fronts greatly streamlined my data searches and allowed me to extend the number of documented cases.

Steve Chiswell, a.k.a. THE computer God, for turning me into a GEM-Pack Warrior, and writing the numerous programs/subroutines which actually allowed me to finish this thesis.

John Grovenstein, my Macintosh mentor, philosophical partner in crime, and generally the one who aided and abetted my profound sense of irreverance. Semper Fi!

Dr. Riordan, who above all else taught me the significance of significance.

TABLE OF CONTENTS

LIST OF FIGURES

LIST OF ABBREVIATIONS AND SYMBOLS

AFB	Air Force Base.
AHN	Athens, Georgia.
CAD	Cola Air Damming.
CAE	Columbia, South Carolina.
CD	Compact Disc.
C-MAN	Coastal Marine Aids to Navigation.
DELMARVA	Delaware, Maryland, & Virginia.
DSLN7	Diamond Shoals Light Station.
ECG	Elizabeth City, North Carolina.
FAY	Fayetteville, North Carolina.
FLO	Florence, South Carolina.
GALE	Genesis of Atlantic Lows Experiment.
GSO	Greensboro, North Carolina.
HAT	Cape Hatteras, North Carolina.
IAD	Dulles International Airport.
ILM	Wilmington, North Carolina.
IOP	Intensive Observation Period.
LFI	Langley AFB, Virgina.
LLMPJ	Low Level Mountain-Parallel Jet.
MCAS	Marine Corps Air Station.
MQI	Manteo, North Carolina.
MYR	Myrtle Beach, South Carolina.

NEWSEX	New England Winter Storms Experiment.
NCA	New River MCAS, North Carolina.
NKT	Cherry Point MCAS, North Carolina.
NMC	National Meteorological Center.
ORF	Norfolk, Virginia.
PHL	Philadelphia, Pennsylvania.
POB	Pope AFB, North Carolina
ROM	Read-Only Memory.
RIC	Richmond, Virginia.
RWI	Rocky Mount, North Carolina.
SLP	Sea Level Pressure
UTC	Universal Time Coordinate.

C	Speed of a density current.
f	Coriolis parameter.
g	Acceleration due to gravity.
g'	Reduced gravity.
H	Depth of a density current.
K	Froude number.
P	Pressure.
R	Dry air gas constant.
T	Temperature.
T_v	Virtual temperature.
u	East-west component of the wind.
U	Speed of the less dense fluid in the density current equation.

U_r	Speed of a density current relative to the warm air.
U_w	Warm air wind speed in density current equation.
$\mathbf{V}_t$	Thermal wind (vector).
ρ	Density.
Θ_v	Virtual potential temperature.

1. INTRODUCTION.

The term coastal front is assigned to the shallow, mesoscale boundaries commonly observed along the east coast of the United States during the late fall to early spring seasons (Bosart et al., 1972). Generally associated with Appalachian cold air damming, coastal fronts have been linked to events ranging from the enhancement of local precipitation, to fostering east coast cyclogenesis. The implication then is that the influence of a coastal front spans the range of scales from meso-gamma through synoptic.

To date, the majority of the investigations of coastal fronts have dealt with occurrences in New England, and have focussed primarily on either their evolution (Bosart et al., 1972; Bosart, 1975; Ballentine, 1980; and Nielsen, 1989), or their participation in other processes (Marks and Austin, 1979; Bosart, 1981, and Bosart and Lin, 1984). Few studies, however, have broached the topic of predicting coastal front movement, and none have centered on this issue as it pertains to Carolina coastal fronts. The problem of frontal movement can be a matter of extreme importance since coastal fronts are in actuality a confluent axis typically separating a weak, cold, northerly flow from a stronger, warm, easterly flow which has an overwater trajectory. Thus, local observations of temperature, winds, and precipitation type may become drastically different from the forecasted conditions depending on the fronts' proximity and subsequent movement. Consequently, a precise understanding of the processes involved in coastal front propagation is warranted.

2. LITERATURE REVIEW.

2.1. The Coastal Front.

The first discussion of the mesoscale feature now known as the coastal front is generally attributed to Carson (1950), who referred to it as the Gulf Stream front while investigating the formation of stratus along the southeast coast of the United States. Carson's study analyzed three cases of Gulf Stream frontogenesis and described several features which have become synonomous with U.S. coastal fronts. Among these were a cold anticyclone located over northern New England and the establishment of a cold air dome and attendent high pressure "wedge" over the Atlantic coastal plain. Carson noted that west of the front the flow was characterized by northerly winds, while easterly flow dominated the seaward side. Carson found that stratus layers which formed under these conditions were initiated at the Gulf Stream and sloped upward toward the coast. Thus, he proposed that the formation of the stratus layer was due to a forced ascent of warm, maritime air over the cold dome entrenched on the coastal plain. Implicitly this would mean that the base of the stratus layer coincided with the top of cold dome.

Bosart et al. (1972) introduced the term "coastal front" and provided the first detailed analysis of this mesoscale feature. Through an examination of eight years of data for New England, they were able to outline some general characteristics for coastal fronts. Synoptically they discussed the necessity for a cold anticyclone to be centered north of New England (i.e. north of the damming area). This configuration provides for the formation of a cold air dome / pressure ridge east of the Appalachian mountains (see Fig. 2.1). The relationship between these features and coastal fronts will be examined in a subsequent section.

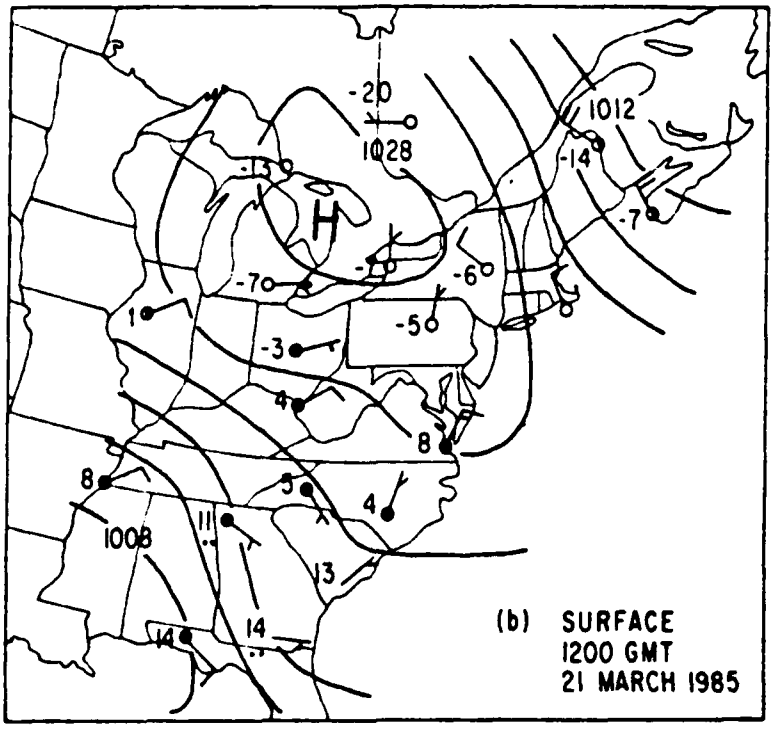

Fig 2.1. Sea level pressure analysis valid at 1200 UTC 21 March 1985. Isobar interval is 4 mb, temperatures are plotted in degrees Celsius, and wind speeds are represented in m s^{-1} with one pennant, one barb, and one half barb equal to 25, 5, amd 2.5 m s^{-1} respectively (From Bell and Bosart, 1988).

Bosart et al. stated that the coastal front forms as the boundary separating a northerly, overland flow from easterly winds off the Atlantic ocean. In addition, the fronts were found to have a length scale of 100 km and to occur on time scales of 12 hours prior to the passage of a coastal low pressure system. Also noted were temperature contrasts across the front on the order of one to two degrees C per kilometer. Furthermore, the fronts were often the dividing line between frozen and non-frozen precipitation, and displayed a distinct tendency to stagnate along a line from Boston to Providence, Rhode Island to Block Island. Dissipation of the front was said to occur after the surface low reached the latitude of New England, and the coastal winds backed to a northerly direction. Additional comments noted that the fronts were "usually not observed with

very strong offshore lows since presumably the strong cyclonic circulation over land serves to overwhelm local gradients".

Studies subsequent to Bosart et al. refined and increased the core of knowledge surrounding coastal fronts. Bosart (1975) proposed a classification system for New England coastal fronts based upon approaching synoptic cyclones. Marks and Austin (1979) determined that the front acted as a mesoscale modulator for large scale precipitation and produced a local enhancement of precipitation west of the front. Sanders (1983) found that temperature contrasts across the front could be as high as ten degrees C per kilometer. Additionally, Neilley (1984) noted that coastal fronts could extend for hundreds of kilometers and typically persisted for as much as 48 hours prior to the passage of surface cyclones.

2.2. Cold Air Damming.

It is well known that mountain ranges can obstruct or block the low level flow of cold, statically stable air (Xu, 1990; Pierrehumbert and Wyman, 1985). This type of blocking, which results in a trapping of cold air along the mountain slopes is usually referred to as cold air damming (Richwein, 1980). Cold air damming (CAD) typically manifests itself as an inverted ridge in the sea level pressure (SLP) pattern parallel to the mountains' windward side (see Fig. 2.1). Richwein (1980) stated that, given a cold anticyclone positioned north of the region, damming should be expected to begin once the layer below 850 mb attained a lapse rate less than the moist adiabatic and the winds contained some component directed toward the mountains. This, Richwein asserted, made the 850 mb pattern an excellent predictor for the onset of damming. In an elaboration he noted that since the Appalachians were oriented in a north-northeast to

south-southwest fashion, damming would be initiated as the 850 mb winds veered from northwesterly to northeasterly, and that the intensity of the damming would be directly proportional to the static stability of the layer.

The veracity of the inverted ridge analysis during damming events is often called into question. The problems arise due to the difficulties associated with the reduction of pressures from higher elevations to sea level. As is often noted, over mountainous terrain differences in pressures from station to station exist, by and large, due to differences in elevation (Wallace and Hobbs, 1977). The standard pressure reduction method further complicates the picture due to its reliance on a hypothetical temperature lapse rate. Errors introduced by the reduction method often induce artificially higher pressure values. Pielke and Cram (1987) noted such anomalies (by as much as 6 mb) over the Great Basin in Nevada. They proposed an alternate pressure correction method which they asserted reduced the "apparently excessive pressure gradients" caused by the standard methods. Dunic (1989) used their correction method on a 25 January 1986 Appalachian damming event, and found that the "corrected" analysis had only been reduced by 1 mb. Baker (1970) examined the inverted ridge pattern and concluded it was a "real atmospheric phenomenon" and that it simply reflected "changes in the inversion height aloft, or equivalently, changes in the depth of cold air".

Several investigations in both the Carolinas and New England concluded that the depth of cold air is ordinarily less than 500 m, and that the dome and overlying inversion layer was usually confined below 850 mb. Forbes et al. (1987) described a conceptual model of Appalachian CAD which was composed of an upper layer cross-mountain flow, a lower layer cold dome with a northerly mountain-parallel jet, and a frontal inversion layer in between (Fig. 2.2).

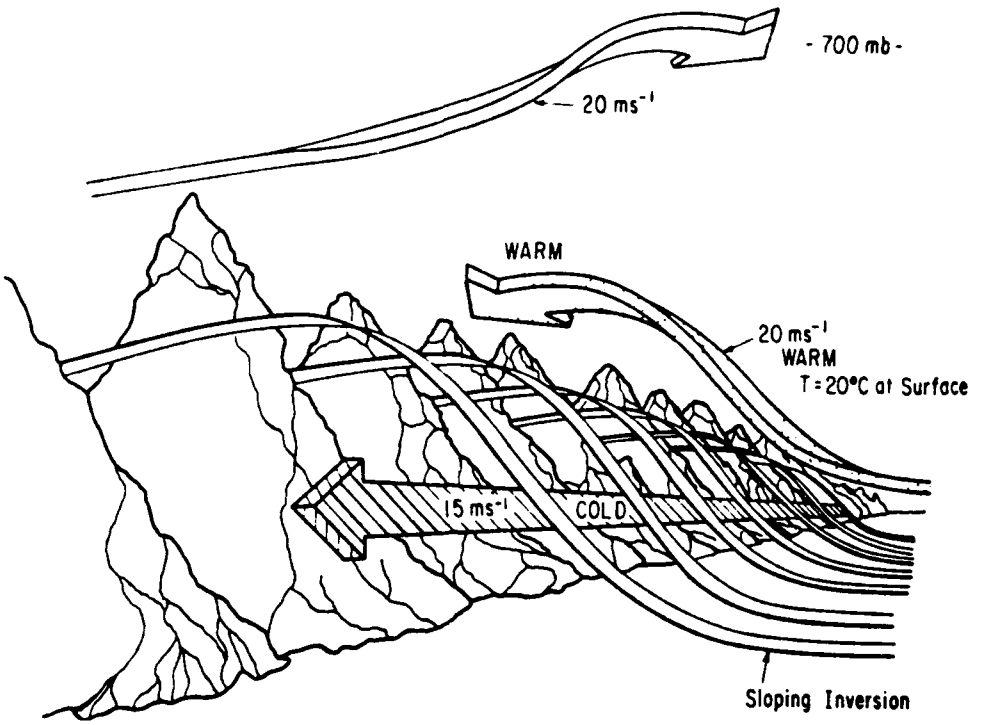

Fig. 2.2. A conceptual model of cold air damming showing a relatively strong low level mountain-parallel jet (LLMPJ) within the cold dome, the sloping inversion, and the flow aloft (From Bell and Bosart, 1988).

Bell and Bosart (1988) conducted a comprehensive examination of Appalachian CAD. Their 50 year climatology found that it was a year-round phenomena although, not surprisingly, the events were "most frequent, prolonged, and intense" during the months from December to March. According to their study, an important precursor to a CAD event is the presence of a split flow pattern in the middle and upper troposphere, typically comprised of a "leading" trough positioned over southeastern Canada, and a "lagging" trough located to the southwest, in the vicinity of the gulf coast (Fig. 2.3). This orientation is preferred since the lag time separating the troughs allows anticyclonic cold air penetrate southward along the Appalachians before cyclonic development can be initiated by the lagging system.

A prominent feature in all cases of cold air damming is the presence of a low level mountain-parallel jet (LLMPJ) (Xu, 1990; Bell and Bosart, 1988; Dunn, 1987; Forbes et al., 1987; and Parish, 1982). In the case of Appalachian CAD, the optimum conditions for formation arise when a cold anticyclone is positioned over southeast Canada or northern New England. In this configuration the air at low levels can be directed perpendicular to both the coast and the mountains. Schwerdtfeger (1975) found that when low level stable air is forced into a mountain barrier, the resulting flow will be deflected to the left, and across the isobars, in the northern hemisphere. This anomalous

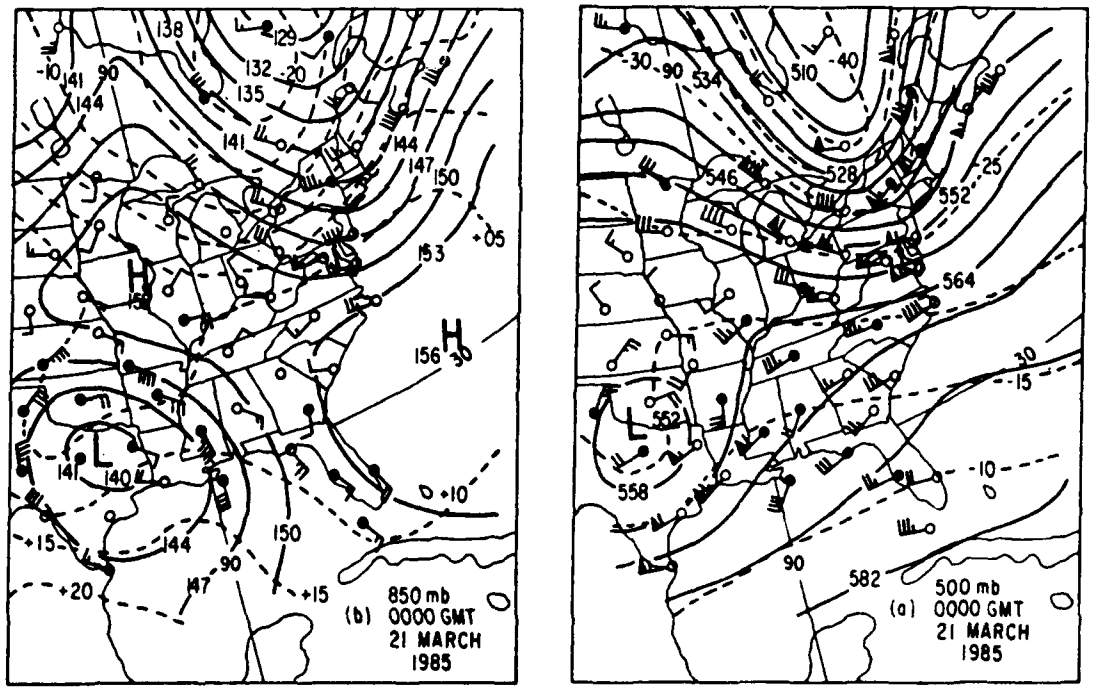

Fig. 2.3. National Meteorological Center 850 and 500 mb height (solid) and temperature (dashed) analyses valid for 0000 UTC 21 Mar 1985. Heights are contoured every 3 dm at 850 mb, and every 6 dm at 500 mb. Isotherms are every five degrees Celsius. Wind speeds are as in Fig. 2.2 (From Bell and Bosart, 1988).

flow, he suggested, was a mesoscale phenomena which was dependent upon the stability of the lower layers, and the height of the blocking terrain. According to

Schwerdtfeger one can assume that "the upper surface of the cold air mass rises in the same sense, though not necessarily at the same rate, as the terrain itself". Figure 2.4 illustrates Schwerdtfeger's concept. Referring to the figure, Schwerdtfeger stated that "the increase of pressure from level 2 to level 1 is inversely proportional to the mean virtual temperature of the layer". The fact that the pressure at level 1 is greater at point B than at point A, and that there is a difference in the mean virtual temperature between levels 1 and 2 implies the "existence of an additional horizontal pressure gradient directed outward from point B toward point A. Dunn (1987) points out that if conditions such as these were to exist on time scales greater than "a few hours, then Coriolis effects become significant and produce a wind parallel to the barrier" i.e. directed upward out of the plane of Figure 2.4. Using the concept of the thermal wind,

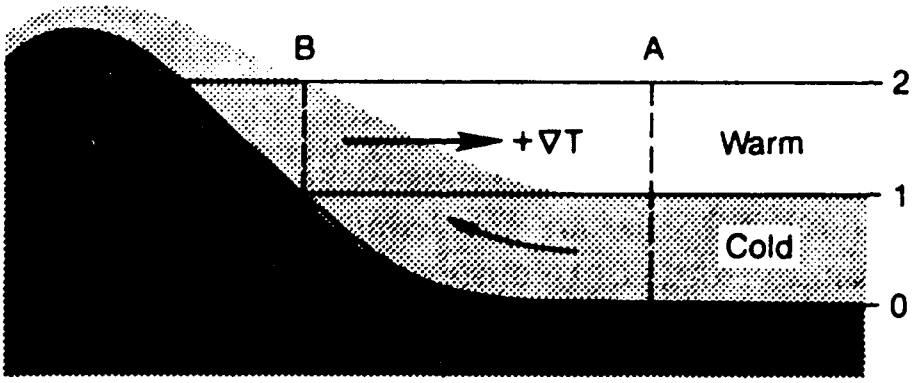

Fig. 2.4. Conceptual vertical cross section of a cold, stable air layer dammed against a mountain range (from Schwerdtfeger, 1975)

Schwerdtfeger explained the mechanics of the cross isobar flow as follows. "Whenever a layer of cold air is sloped there must exist a horizontal temperature gradient parallel to

the slope line, and hence a thermal wind parallel to the obstacle" and directed into the plane of Figure 2.4. The thermal wind is given by:

$$\mathbf{V_t} = (R/f) \ln (P_L/P_U) [\mathbf{k} \times \nabla_p T_v] \qquad (2.1)$$

Where R is the dry air gas constant, f is the Coriolis parameter, P_L is the pressure at the base of the layer, P_U is the pressure at the top of the layer, and T_v is the mean virtual temperature of the layer from P_L to P_U. Given this relationship, if the mean virtual temperature of the layer and the geostrophic wind at P_U (level 2) are known then (2.1) may be utilized to yield the geostrophic wind at the lower layer (level 1), and thus the geostrophic wind near the surface level may be determined. Richwien (1980) tested this method on 16 cases of Appalachian CAD using the 850 mb winds as an upper level geostrophic approximation. His results showed that subtracting the calculated thermal wind from the 850 mb wind yielded a surface wind which, after applying a correction for friction, was in good agreement with the observed winds.

Bell and Bosart (1988) examined the force balance structures within an Appalachian cold dome and found that the LLMPJ is generated due to the deceleration of the winds as the flow attempts to ascend the mountain slopes. In response to this decrease in velocity, there will of course be a proportional reduction in the magnitude of the mountain-parallel Coriolis force, which leads to an unbalanced pressure gradient force directed in the down gradient direction (i.e. to the left of the flow). This down gradient flow represents an acceleration toward the south along the slopes. With the increase in velocity a mountain-normal Coriolis force is developed which then attempts to turn the flow back up the mountain slope (i.e. restore geostrophic balance). Due to the decrease

in frictional influences with height the wind speeds will increase in the vertical, reaching a maximum near the top of the cold dome.

Xu (1990) noted that the intensity of the LLMPJ is limited primarily through the retarding action of friction. If the frictional forces were insufficient to hamper the flow, the LLMPJ would continue to intensify until the mountain normal Coriolis force became strong enough to push it over the mountains. Bell and Bosart also noted that the split flow pattern aloft allows the maximum pressure falls ahead of the southern system to be juxtaposed southwest of the maximum pressure rises which precede the anticyclone trailing the northern system. The result is an enhanced southward transport of cold air. Thus the northeasterly agesotrophic flow is generated by a flow forced perpendicular to the mountains at low levels, maintained through a balance between the pressure gradient and frictional forces (in the mountain-parallel direction), and is perhaps enhanced through upper level support. The decrease of friction with height leads to a relative wind maximum near the top of the cold dome, i.e. the LLMPJ. Furthermore, the damming pattern initiates cold air advection within the dome, and this advection continuously replenishes cold air lost through drainage and mixing (Nielsen & Neilley, 1990).

Richwein (1980) determined that the cold dome will begin to diminish in strength and collapse when the 850 mb winds veer from an east-northeast to a southwesterly direction, i.e. lose their upslope component. Bell and Bosart (1988) found that the dissipation of the cold dome was induced through the "synoptic scale development, intensification, and northward movement of a coastal trough and surface cyclone". These interactions produced a net acceleration of air toward the southeast and out of the cold dome. Bell and Bosart also indicated that upper level vorticity patterns may play a

role in cold dome dissipation. Given the proper orientation, upper level relative vorticity advection patterns could induce surface pressure falls in the northern portion of the damming region, and rises in the southern areas. The net result would be a decrease in the north-south height gradient, and the mountain-parallel component of the sea level pressure gradient. Ultimately this would translate into a decrease in the southward transport of cold air, thus allowing the dome to diminish through drainage and mixing. Bell and Bosart declared that processes such as these were proof that damming events were mesoscale features controlled by the synoptic scale flow.

Currently the relationship between CAD and coastal fronts is, at best, only moderately understood. Nielsen and Neilley (1990) noted that in New England, coastal fronts and CAD tend to exist as a coupled system with the coastal front forming the leading edge of the cold pool. However in the Carolinas, coastal fronts are predisposed to form along the Gulf Stream (Raman and Riordan, 1988), presumably well beyond the influences of damming. Still Nielsen and Neilley note that the equilibrium shape of the cold dome is dependent upon the land-sea temperature contrast and the large scale pressure gradient, and that the depth of the cold air then determines the location of the coastal front.

2.3. Climatology.

Anderson (1991) produced the first climatological study of Carolina coastal fronts. Using a simplified expression for frontogenesis (after Sanders, 1955), he developed an objective set of criteria to identify Carolina coastal fronts. Anderson's method required confluent winds between Cape Hatteras, North Carolina (HAT) and buoy 41001, located approximately 200 km due east, offshore. Specifically the HAT winds had to fall within a range between 330 and 050 degrees and angular differences with the buoy

had to be confined within 10 to 120 degrees. Anderson also stipulated that the buoy winds had to be at least eight knots, and that a temprature gradient, on the order of five degrees F, must be present and directed offshore. Finally he also incorporated time duration criteria to avoid high false alarm rates.

Anderson's definition enabled the identification of 161 separate events from a nine season period involving the months of November through March. A detailed examination of the data indicated that Carolina coastal fronts a) occurred most frequently in the month of January, b) remained offshore for less than 18 hours approximately 76 percent of the time, and c) moved westward passed HAT approximately 47 percent of the time. Anderson defined landfall for the coastal front as occurring when the HAT winds experienced a clockwise shift of greater than 45 degrees over a three hour period, and the temperature at HAT increased by at least 5 degrees F more than stations located further inland. Employing statistical methods, Anderson produced a frequency chart which suggested a preference for landfall between the hours of 1200 to 1800 UTC, with a secondary maximum occurring between 0000 and 0600 UTC. Using chi-square tests, Anderson found that the monthly peak for January was statistically significant, while the landfall hour peak was not.

2.4. Frontal Propagation.

Egentowich (1989) constructed a mesoscale analysis of a coastal front which occurred during the Genesis of Atlantic Lows Experiment (GALE) IOP-2. In this case he found the front formed offshore by 1800 UTC on 24 January 1986 and moved over the central outer banks of North Carolina by 0800 UTC on the 25th. The front then maintained its position and intensity until just after sunrise when the northern portion appeared to

"jump" inland. Egentowich proposed that this westward movement was likely due to either turbulent mixing or convective heating within the cold air.

Considering turbulent contributions first, Egentowich calculated values of the bulk Richardson number using three hourly sounding data for locations west of the front. The values computed for the surface layer indicated unstable air, while calculations for layers aloft showed the presence of stable air. Consequently Egentowich hypothesized that turbulent mixing was probably occurring and caused the front to move westward. To support the second conjecture, he points to the presence of superadiabatic lapse rates near the bases of two meteorological towers located on either side of the front. The existence of these strong lapse rates, he suggested, was evidence that convective eddies were destroying the eastern edge of the cold dome, and induced a westward progression of the frontal boundary.

Riordan (1990) examined the same GALE case and concluded that the initial shoreward movement was due primarily to the differential in diabatic heating which arose from differences in the underlying surfaces (i.e the sea surface temperature gradient). Huang (1990) modelled the same case using a mesoscale planetary boundary layer model developed to investigate airflow over complex topography, and found that the front moved inland "as the cold air intensity over ground weakens due to onshore warm air advection".

Nielsen (1989) produced a comparison of the factors which govern coastal fronts and land-sea breezes. He noted that typically in New England cases, heating was occurring over the water while cooling was taking place over the land. This situation is analogous to land breezes. However, unlike land breezes the flow was directed onshore as one

would find in a sea breeze. In fact aside from the thermal structure, Nielsen determined that coastal fronts exhibited characteristics that were much more reminiscent of sea breezes. Among the similiarities were the tendency to form fronts, equivalent magnitudes of thermal forcing, and the fact that the presence of an opposing flow, if not too strong, will actually serve to intensify the front. Based upon this he concluded that New England coastal fronts commonly form under conditions considered ideal for the formation of intense land-sea breeze fronts.

Many atmospheric fronts, including those associated with land-sea breezes, have been shown to possess density current characteristics (Simpson, 1982; Mitsumoto et al., 1983; Simpson and Britter, 1980; and Simpson, 1969). Nielsen and Neilley (1990), using aircraft data gathered during the New England Winter Storms Experiment (NEWSEX), noted the following characteristics pertaining to New England coastal fronts:

a) Near the ground, the cold and warm air are two separate, nearly homogeneous fluids with most of the horizontal density (virtual potential temperature) gradient confined to a narrow frontal zone.

b) Beneath the inversion there is a "feeder flow" of cold air directed from the cold pool toward the frontal zone.

c) The frontal zone rises sharply from the surface, and immediately behind the front is a region of turbulence where mixing of the warm and cold air is apparently taking place.

d) The frontal inversion levels off behind the front with typical slopes of 1:50 to 1:200.

These features are evident in the coastal front cross section shown in Figure 2.5. It is of interest to note the similarites between Figure 2.5 and the laboratory simulation of a density current shown in Figure 2.6.

Benjamin (1968) determined that the speed of a density current moving through a lighter fluid was given by:

$$C = U + K\,[g\,H\,(\Delta\rho/\rho)]^{1/2} \qquad (2.2)$$

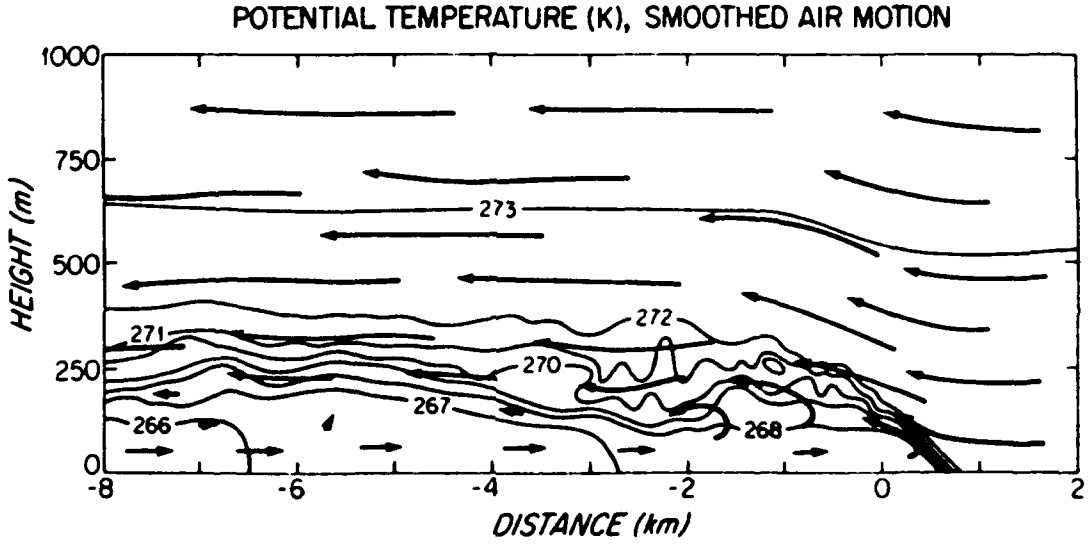

Fig. 2.5. Cross section of a 12 Dec 1983 New England coastal front. The arrows represent air parcel trajectorieswhile the solid lines pertain to potential temperature (From Nielsen and Neilley, 1990).

where U is the speed of the lighter fluid, K is the internal Froude number, g is gravity, H is the depth of the density current, ρ is the density of the heavier fluid, and $\Delta\rho$ is the density difference between the fluids. Since in atmospheric applications the density terms can be replaced by virtual potential temperature, equation (2.2) becomes

$$C = U + K\,[g\,H\,(\Delta\Theta_v/\Theta_v)]^{1/2} \qquad (2.3)$$

If the term $g(\Delta\Theta_v/\Theta_v)$, which is defined as the reduced gravity, is replaced by g', and if subscripts are added to denote warm (w) and cold (c) air, equation (2.3) reduces to

$$C = U_w + K\,[g'\,H_c]^{1/2} \tag{2.4}$$

Fig. 2.6. Shadowgraph of a density current brought to rest in a steady state where the speed of the current is equal to the opposing flow (From Simpson and Britter, 1980).

To predict the speed of a density current, equation (2.4) may be rearranged as

$$U_r = C - U_w = K\,[g'\,H_c]^{1/2} \tag{2.5}$$

Where U_r is the speed of the density current relative to the warm air and U_w is the speed of the warm air relative to the ground. Upon close inspection of equation (2.5) it can be seen that the relative speed of the front is simply a function of the normalized horizontal temperature difference across the frontal boundary, and the depth of the cold air. Since

both of these parameters are influenced primarily by the strength of the cold air damming, the value of U_f would therefore be uniquely related to the magnitude of the cold air dome.

Using a simple one-dimensional (1-D) model which incorporated the density current equation outlined above, Nielsen (1989) explored the interaction between the local winds, temperature, and subsequent coastal front movement. The model assumed a straight coastline and a constant wind speed, but the wind direction was specified to gradually veer from 270 to 90 degrees over a ten hour period. The model portrays a front which is initially located at the coast, but moves offshore "as the temperature difference rapidly grows along the front". As the onshore winds (i.e. u component) intensified, the front began moving shoreward and crossed the coast at the 7.9 hour point of the model run. The model implies that the direction of frontal movement is dependent not only on wind direction, but also on the land-sea temperature contrast (i.e. intensity of CAD). The cross-frontal temperature difference during landfall was 4.4 degrees C. Although the winds were blowing steadily onshore after ten hours, the model simulated temperature difference, or cold dome magnitude, continued to increase and the front retreated to an offshore position (i.e. "rode" the eastern edge of the dome as it moved seaward). Additional runs showed that decreasing the time interval of the wind shift resulted in earlier landfalls, while increasing the period to greater than ten hours yielded fronts which remained offshore. Similarly, increasing the value of K or H_c increased the value of U_f and shifted the frontal positions further east.

Nielsen and Neilley (1990) used equation (2.5) to compare the theoretical and observed speeds of four actual New England coastal front cases. Their results

concluded that the speeds predicted by density current theory agreed with the observed speeds to within 0.35 m s^{-1}, a value well within in the range of the instruments.

3. RESEARCH OBJECTIVES.

In view of the established connection with Appalachian cold air damming and atmospheric density currents, it is reasonable to postulate that the onshore movement of Carolina coastal fronts is directly related to the vertical and horizontal extent of the cold air dome. That is to say, the presence and strength of the cold dome constitutes an obstacle which opposes the inland propagation of the coastal front. It is hypothesized then that the coastal front will stall over the ocean or the waters immediately adjacent to the shore during those periods when the damming is strong, and or the onshore wind component is weak. Theoretically then the converse would also hold true, and inland penetration would occur as the cold dome undergoes dissipation and the maritime winds veer to a directly onshore direction.

Hence, aside from the general intent of increasing the amount of knowledge surrounding Carolina coastal fronts, the specific aims of this research are three-fold. The primary goal will be to determine whether or not the movement of Carolina coastal fronts can be correlated with the magnitudes of cold air damming, and the onshore wind component. The secondary goal is to ascertain if differences exist in the synoptic SLP pattern between onshore and offshore events. A tertiary objective would be to devise a simple predictive scheme using routinely available data, and employable by field level forecasters, to determine the liklihood of onshore movement of the coastal front.

4. DATA AND METHODOLOGY.

4.1. Climatology.

This portion of the research utilized the National Meteorological Center (NMC) Gridpoint CD ROM Version 2 program as compiled by the University of Washington in association with the National Center for Atmospheric Research. This data base contains daily (12 hourly) and monthly fields of temperature, geopotential height, and wind velocity for the northern hemisphere using a grid point spacing of 380 km. The gridded fields are available for the surface, 850 mb, 700 mb, 500 mb, 200 mb, and 250 mb levels. The period of archived data spans from 1946 to June 1989 for both surface and 500 mb levels, while the remaining levels only date back to 1962.

The software package allows the user to literally construct specified monthly climatologies for any of the available levels and parameters. The package also allows the construction of composite patterns of multiple events, which when used in conjunction with the climatological charts, can produce analyses depicting their deviation from the specified climatology. Additionally a statistical option (Student's - t test) is included to provide some measure of the significance of the deviations from the constructed climatology.

4.2. Case Studies.

The data used in this segment consists of standard surface observations augmented with data from Coastal Marine Aids to Navigation (C-MAN) sites, offshore buoys, and ship reports. Mesoscale analyses were accomplished with the aid of The Weather

Processor (WXP) program Ver. 4.2. Objective analysis fields were constructed with GEMPAK Ver. 5.0 using a two-pass Barnes' analysis on a 15 x 15 grid, where the east-west gridpoint distance equals 1.067 degrees of longitude, and the north-south gridpoint distance equals 0.67 degrees of latitude. Figure 4.1 depicts the entire data collection region, and highlights the specific area of interest for the calculations of damming magnitude. Figure 4.2 is provided as a reference for locations mentioned in subsequent sections.

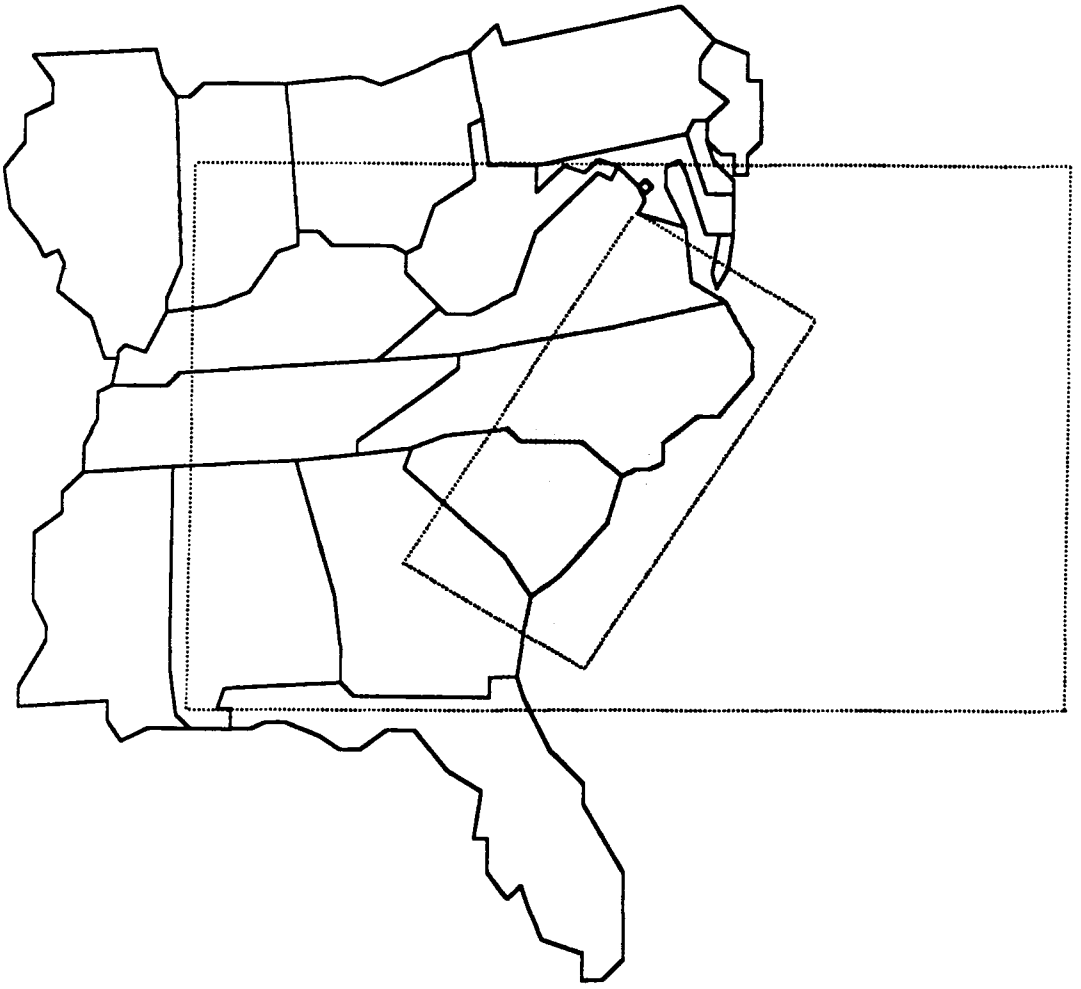

Fig. 4.1. Study region used for data collection, and analysis. The shaded box represents the specific area of interest for computations and analysis of cold air damming magnitude. Actual coordinates of the outer box is from 30N to 40N, and from 70W to 86W.

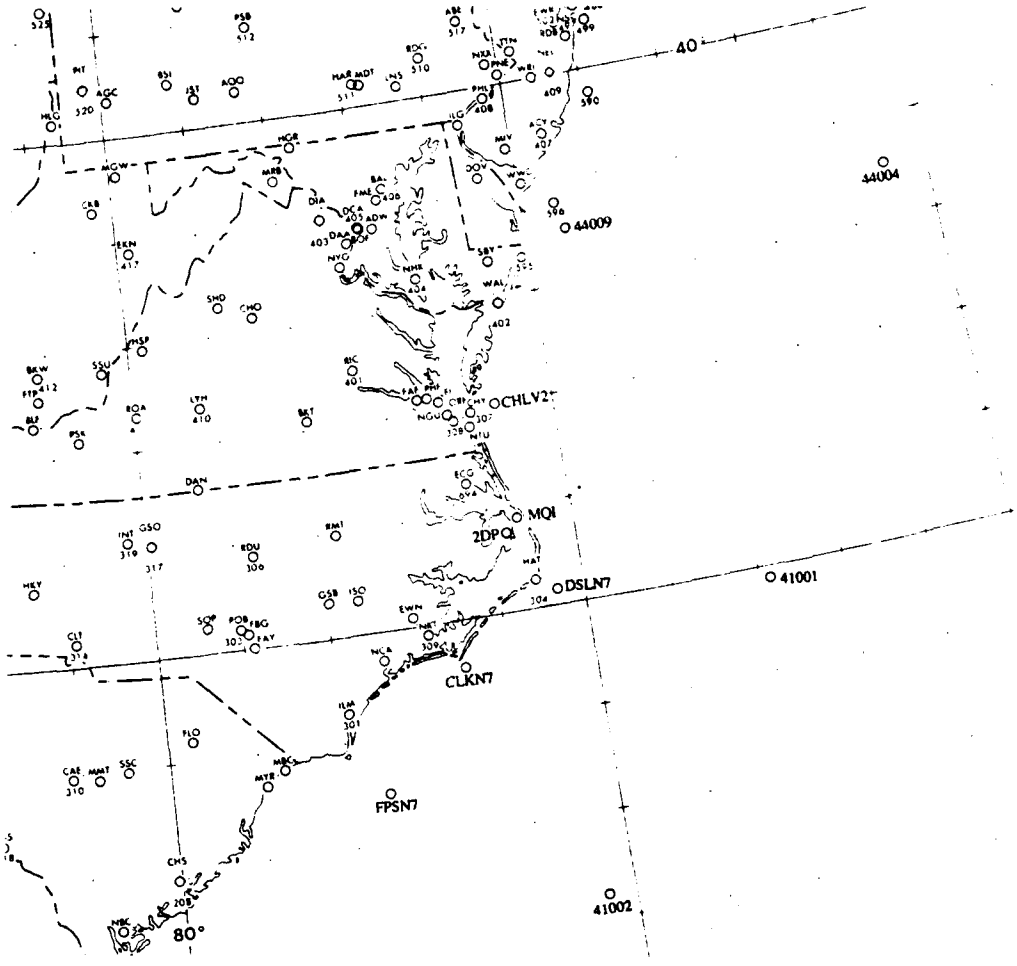

Fig. 4.2. Reference locator for stations identified in discussions.

4.3. Event Definition.

Before embarking upon a study to evaluate the relationship between damming strength and coastal front movement, a definition of what constituted a coastal front event was needed. Obviously the first requirement would be the presence of damming over the Piedmont plateau / Southeast Atlantic coastal plain as evidenced by the classic inverted ridge and ageostrophic wind flow. Although this pattern implies the existence of near-coast confluence a second criterion of offshore confluence, confirmed by any available data, and evidence of coastal front passage at HAT was also imposed. The purpose of

the latter condition was two-fold. First it helps to establish the fact that a coastal front was indeed offshore, and second it provides a simple means of normalizing all coastal front cases examined. It should be mentioned that a deliberate attempt was made to exclude coastal fronts which originated due to a northward moving coastal cyclone, and those which were associated with lows approaching from west of the Appalachians with warm fronts wrapping northward around the mountains. The omission of cases such as these represents an attempt to isolate the effects of the cold dome in the absence of strong cyclonic forcing.

Since virtually all coastal fronts form offshore and propagate toward the coast (see Nielsen, 1989), a definition of the terms onshore and offshore was also required. It has been noticed that Coastal fronts often linger in the vicinity of the outer banks of North Carolina while areas on the mainland remain under the influence of damming. Due to this fact and the narrowness of the outer banks, a coastal front was not classified as "onshore" until observations indicated a frontal passage at locations such as Elizabeth City (ECG), Cherry Point MCAS (NKT), New River MCAS (NCA), and or Wilmington (ILM) (see Fig. 4.2). This is an admittedly imperfect system, but unavoidable given the data density of the coastal region.

5. CLIMATOLOGICAL INVESTIGATION.

5.1. Comparitive Analysis.

Working with the definition outlined in the previous section, NMC three-hourly SLP charts for the months of November to March were examined for the period 1975 to 1989. This search netted a total of 51 cases which met the established criteria (see Appendix 1). Of these at least 23 were not identified by Anderson simply due to the fact that the current study covered a longer period than Anderson's, and the definition used was not hampered by a lack of data from buoy 41001.

The 51 cases were examined in a climatological fashion and yielded some interesting results. First, the frequency of occurrences was determined by month and plotted in Fig. 5.1. As with Anderson's work, a peak was found for the month of January. In fact the current study's bar chart is remarkably similar in appearance to the one produced by Anderson, with frequencies within four to sixteen percent of his values. Frontal passage hour at HAT was also charted, again with results similar to Anderson's (Fig. 5.2). Here the trend is roughly equivalent to that found by Anderson and the frequencies are all within fourteen percent of his values. Thus, even though the current study's cases represent less than one third of those examined by Anderson, from the results in fig. 5.1 and 5.2 it would appear that the 51 cases used are a reasonable cross section.

Bosart et al. (1972) noted that New England coastal fronts tended to stagnate along a line from Boston to Providence, Rhode Island to Block Island. Given this trait, the terminal positions of Carolina coastal fronts were examined to determine if they

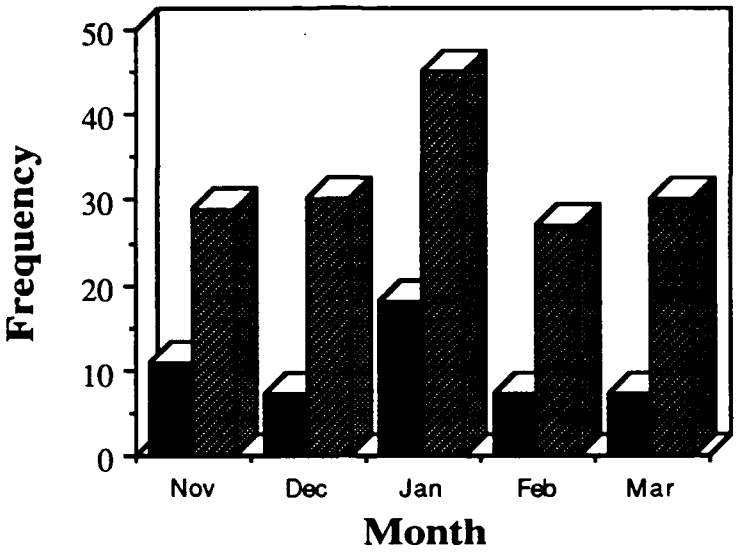

Fig. 5.1. Monthly frequency of coastal front occurrences. Current study's values (solid) based on 51 cases, while Anderson's values (hatched) are based upon 161 cases.

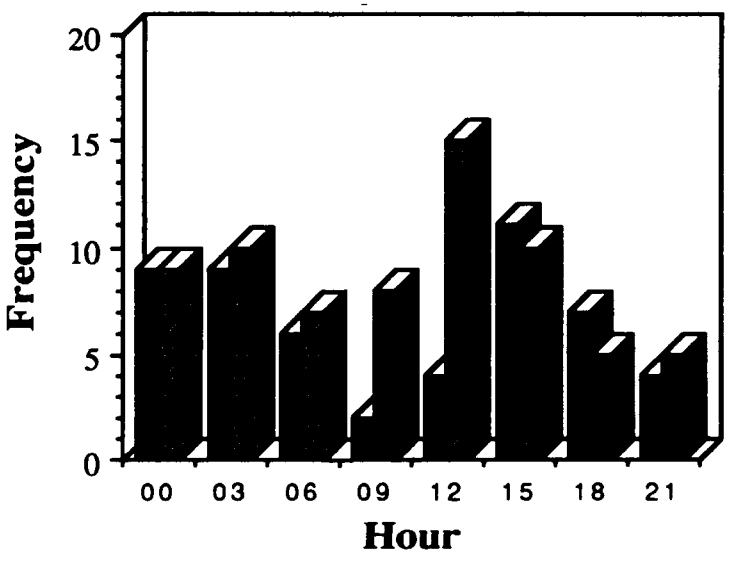

Fig. 5.2. Frequency of hour of frontal passage at Cape Hatteras, NC. Values for the current study (solid) are based upon 51 cases, while Anderson's values (hatched) are based upon 69 cases.

displayed a similar behavior. The current study's 35 onshore cases were divided into two groups (see section 12.1), those whose final onshore frontal positions were suspected of being influenced by a coastal cyclone, and those which were not. For the cases involving a cyclone (Fig 5.3) there appears to be a good deal of variability, as might be expected, although the fronts almost always remain east of a line from Richmond, Virginia (RIC) to Florence, South Carolina (FLO).

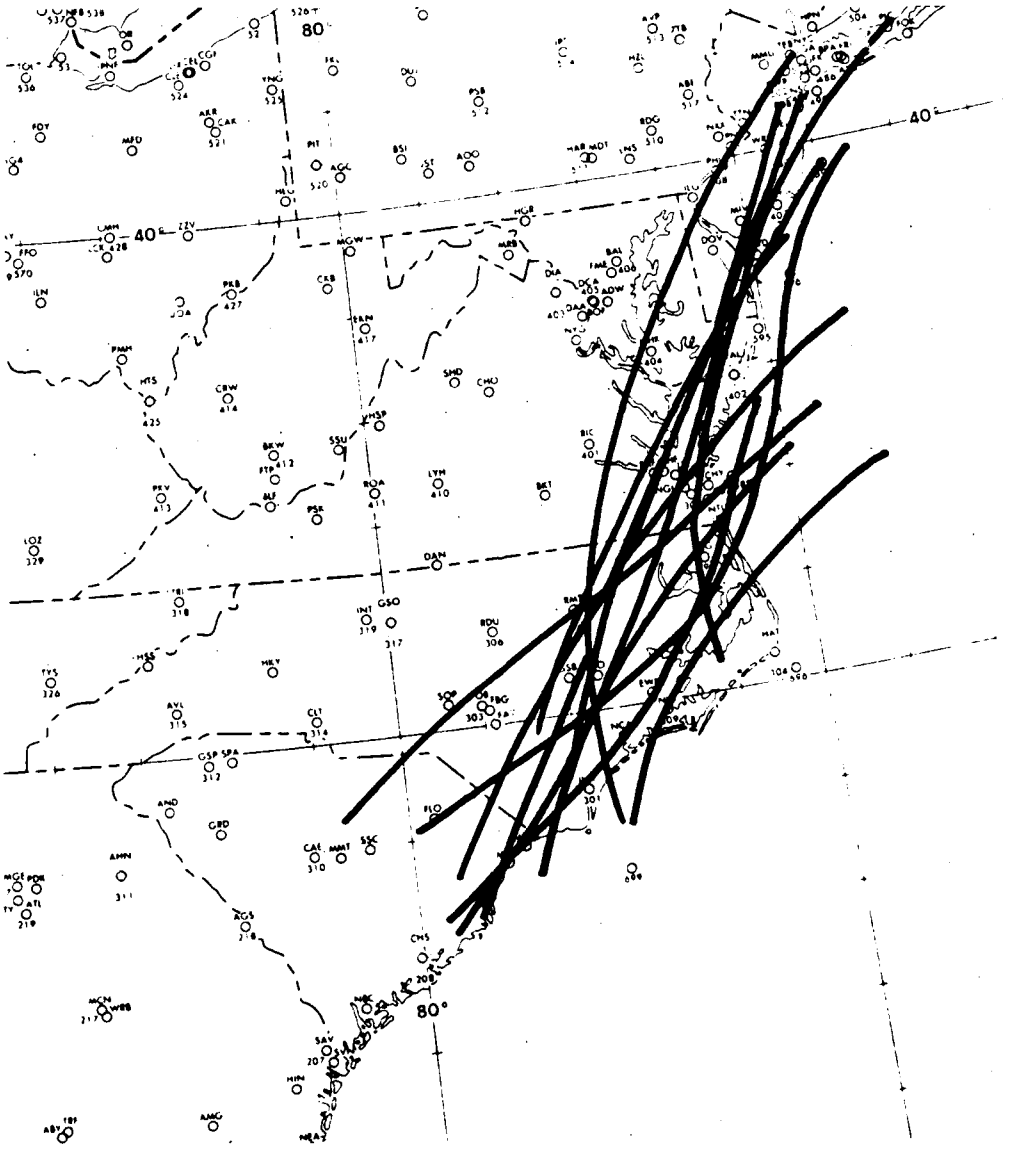

Fig. 5.3. Terminal positions of Carolina coastal fronts for 11 events involving a cyclone.

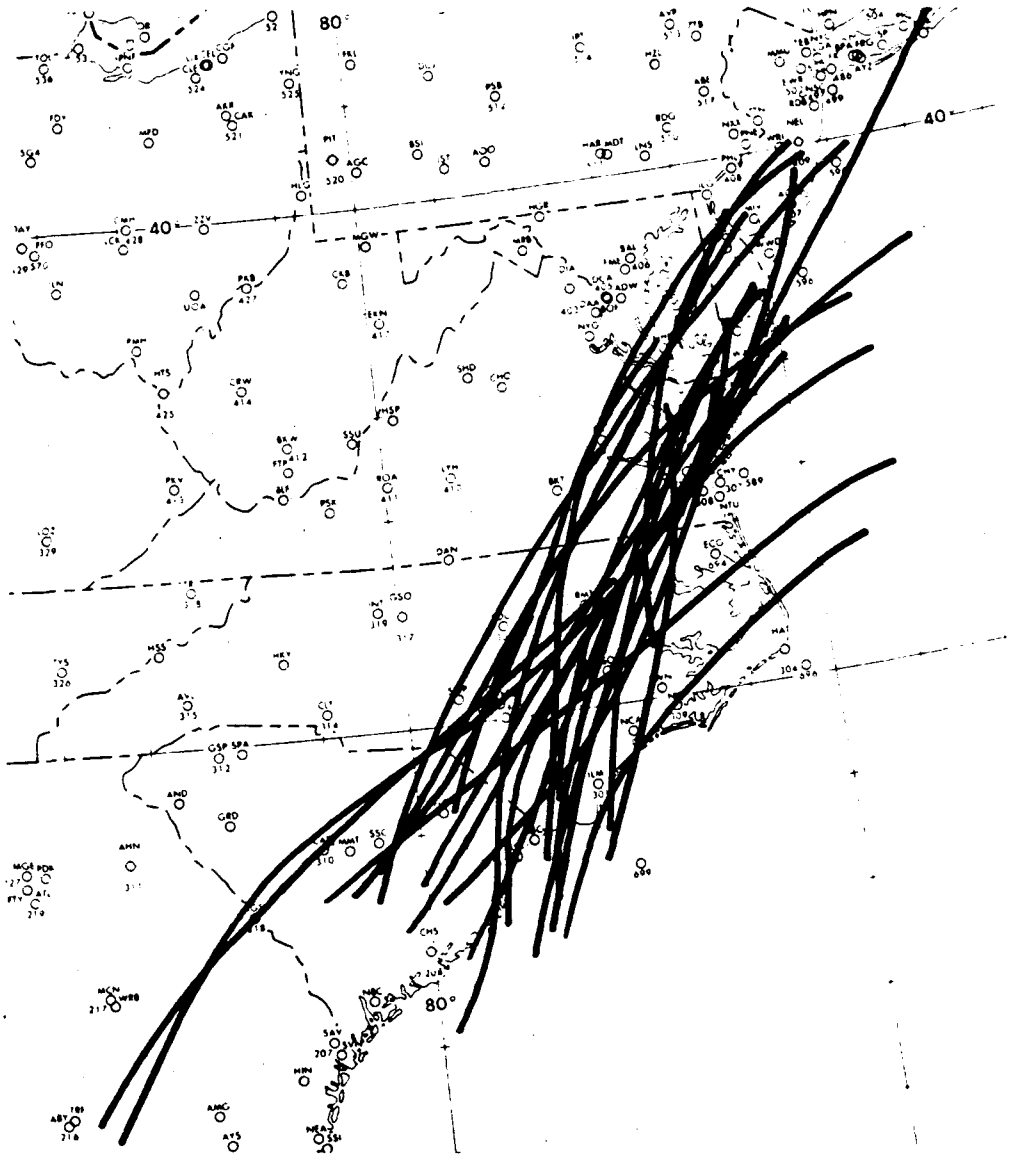

Fig. 5.4. Terminal positions of Carolina coastal fronts for 24 events not involving a cyclone.

The non-cyclone cases (Fig. 5.4) seems to show a bit less variability, and a concentration of activity along a line from Hampton, Virginia (LFI) to Goldsboro, North Carolina (GSO). This is suggestive of a stagnation line but perhaps more importantly in terms of forecasting, is the observation that 80 percent of all onshore cases in North Carolina remained east of Rocky Mount (RWI), while the remaining 20

percent reached all the way to Pope AFB (POB). Also note that only one case appears to have passed Raleigh-Durham Airport (RDU).

Another interesting observation from Figs. 5.3 and 5.4 is the fact that "Carolina" coastal fronts generally range from New Jersey to South Carolina, and sometimes affect Long Island and Georgia. One may then infer that coastal fronts exert an influence over a much larger area than previously recorded. This would contrast with discrete classifications such as "New England" or "Carolina" set forth by Bosart et al. (1972) and others.

Given the work done by Marks and Austin (1979) this would suggest that precipitation maximums and perhaps the greatest threat of freezing precipitation in North Carolina should occur in the region between Rocky Mount and Greensboro (GSO). In a forty year climatology of North Carolina sleet events, Musick (1991) found the greatest number of events occurred west of Fayetteville (FAY) with the most frequent reports coming from Greensboro and Raleigh-Durham. It must be noted however that freezing precipitation can and does occur independent of coastal fronts and that station operating hours may have influenced the data used by Musick.

5.2. Surface Grid Point Analysis.

NMC historical grid point data was used to determine if specific climatic patterns were common to Carolina coastal front events. Again the cases were divided into two groups, those where the fronts moved inland (onshore) and those where it remained east of the mainland (offshore). The cases in each group were then used to construct mean climatological patterns and to derive hemispheric composite and deviation charts for the

time of HAT frontal passage and a point twelve hours before and after. Since the historical data is limited strictly to 12 hourly charts, all times used had to be adjusted to either 0000 or 1200 UTC whichever was closer. The climatological chart shown in Figure 5.5 represents monthly averaged patterns from 1946 to 1988 and are weighted to the specific months and years for the 51 events examined in this study. As can be seen, the climatology charts depict a normal winter pattern with well developed Aleutian and Greenland lows, and generally weak high pressure extending over the United States.

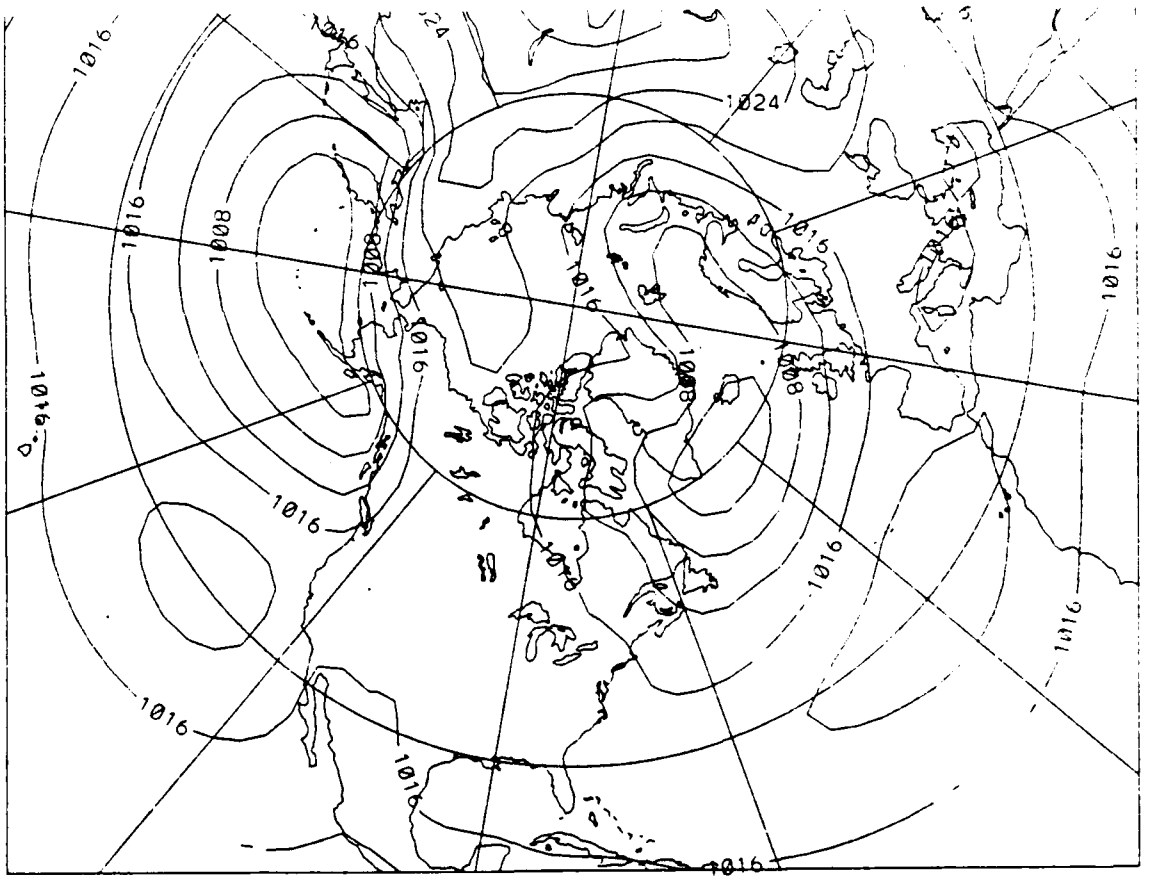

Fig. 5.5. Climatological sea level pressure pattern for the months of November to March, 1946 to 1989, and weighted to the specific months and years used in this study.

The composite charts are a compilation of the 12 hourly charts for all events in each group. At first glance the charts for both on and offshore cases appear nearly identical, (Figs. 5.6 and 5.7), however subtle differences do exist. First, the apparent center of the high pressure cell over the northeast United States is positioned approximately three degrees further west for the offshore cases. Secondly the analyses shows that at 12 hours after frontal passage at HAT the isobar orientation in the offshore cases is still nearly perpendicular to the coast, while the onshore cases show isobars more parallel with the shore These may be indicative of a stronger or more persistant damming during offshore, or perhaps just slower moving anticyclones during offshore events.

Lastly, the onshore composites show a trough of low pressure building into the central United States from Louisianna (note the similarity with Fig. 2.3). A similarly weak area of low pressure is also present in the offshore composites, but again it is located further west. Also note the stronger high pressure over the west coast for the onshore cases and the ridge axis which extends from the mid-Atlantic states to the Gulf of Mexico for the offshore cases.

Similar in appearance to the composites, the deviation charts (Figs. 5.8 and 5.9) all exhibit a strong positive SLP anomaly over the northeast United States corresponding to the damming high pressure. As before with the composites, the apparent centers of the anomalies are situated farther to the west for the offshore cases. Additional deviations include the presence of a negative anomaly centered on the Texas-Louisiana Gulf coast at 12 hours prior to HAT frontal passage in onshore events. This anomaly can be seen to spread northward up the Mississippi Valley over the ensuing 24 hour period. Note that a maximum deviation isopleth of 6 mb below normal appears over Louisiana at the approximate time of HAT frontal passage. This negative anomaly does not appear on

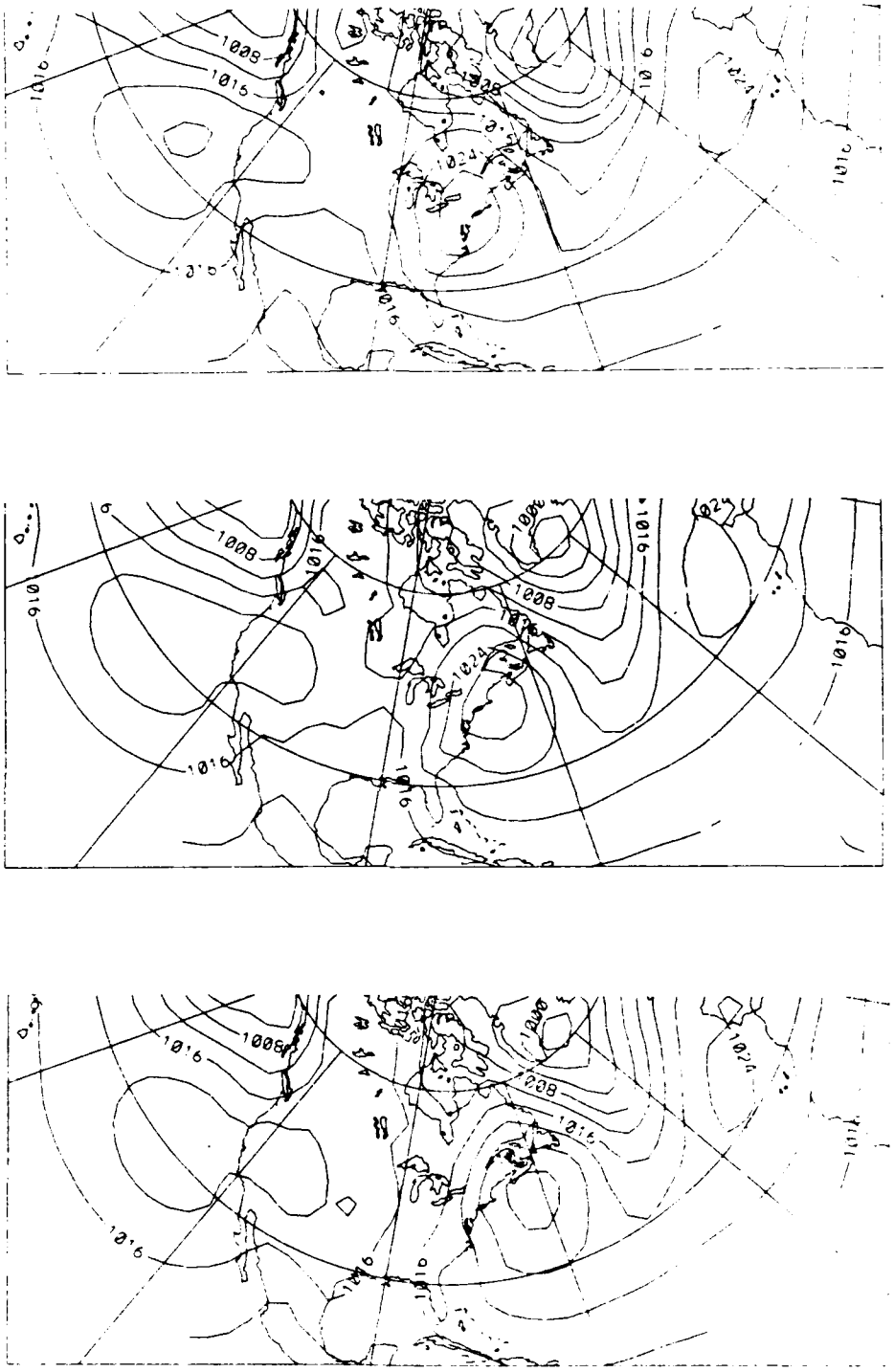

Fig. 5.6. Composite sea level pressure pattern for onshore events at 12 hours prior to HAT frontal passage, at frontal passage, and 12 hours subsequent to frontal passage.

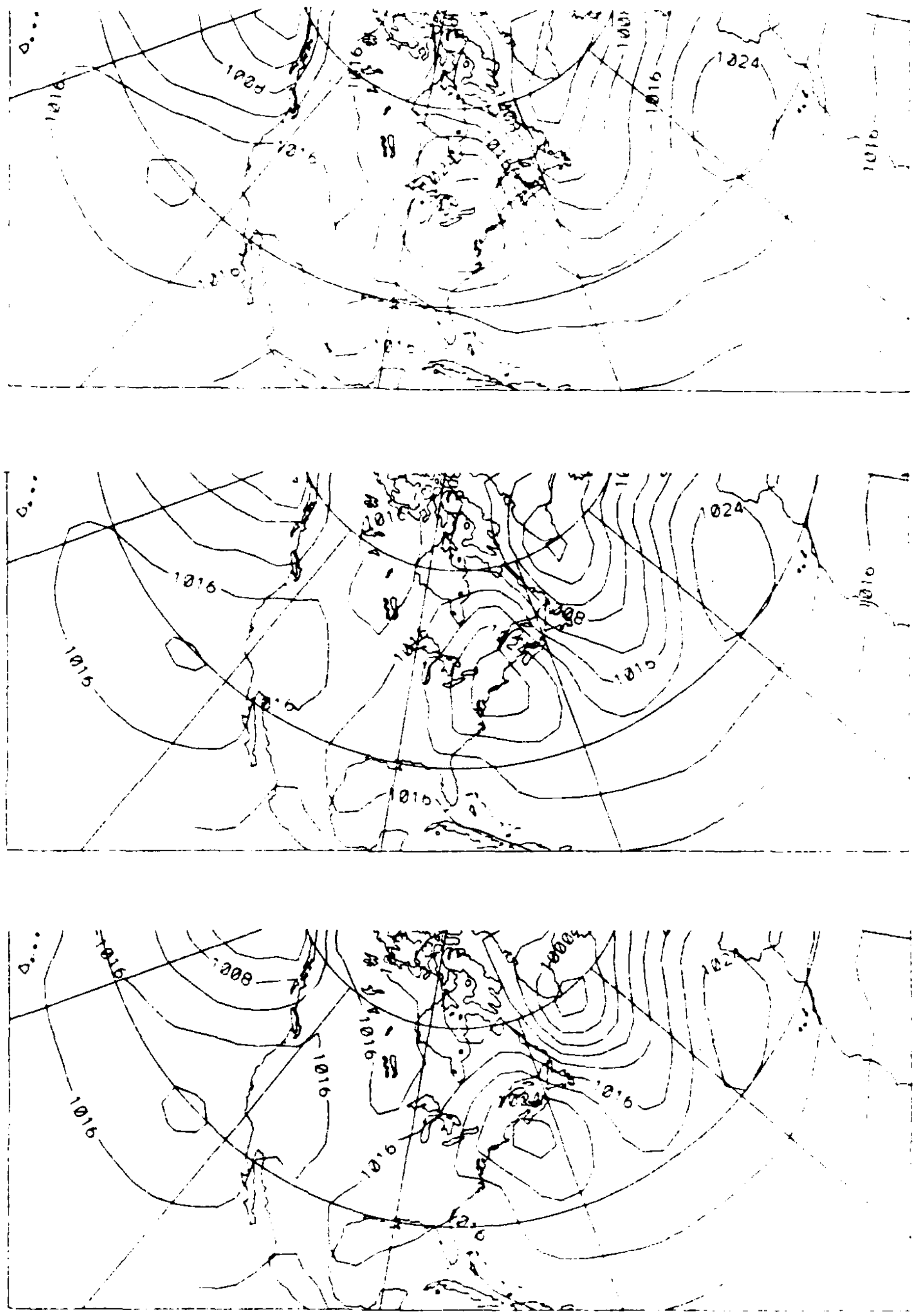

Fig. 5.7. Composite sea level pressure pattern for offshore events. Time sequence is the same as given in figure 5.6.

the charts for the offshore cases, although a much weaker one is indicated near the west coast of Florida. Also of note is the anomaly pattern over the west coast. The onshore cases depict a positive anomaly, associated with the western high pressure which moves in off the Pacific Ocean (Fig. 5.6). In the offshore cases this positive anomaly is not only absent but is replaced by a broad negative anomaly extending from the central United States across the northern Pacific.

Analysis of the statistical significance of the SLP deviations are given in Figs. 5.10 and 5.11. The significance was determined through a Student's-t test where areas within the contoured lines of 1 and 2 refer to a confidence level of greater than 85 and 90 percent respectively. That is to say, there is a high degree of confidence that the deviations within these areas are significant departures from normal and are not occurring due to chance. Note in Fig. 5.10 that areas of significant deviation occur over the eastern and southwest coasts.of the United States, as well as the western Gulf of Mexico. These areas correlate to the positive SLP anomalies on both coasts and the negative anomaly centered on the Gulf coast. It is certainly interesting to note that the only area of significance for offshore cases occurs in conjunction with the high pressure cell (positive anomaly) over the northeastern United States. The lack of significant areas corresponding to the Aleutian and Greenland lows is apparently due to the fact that these are semi-permanent features whose presence would not be considered a deviation from normal.

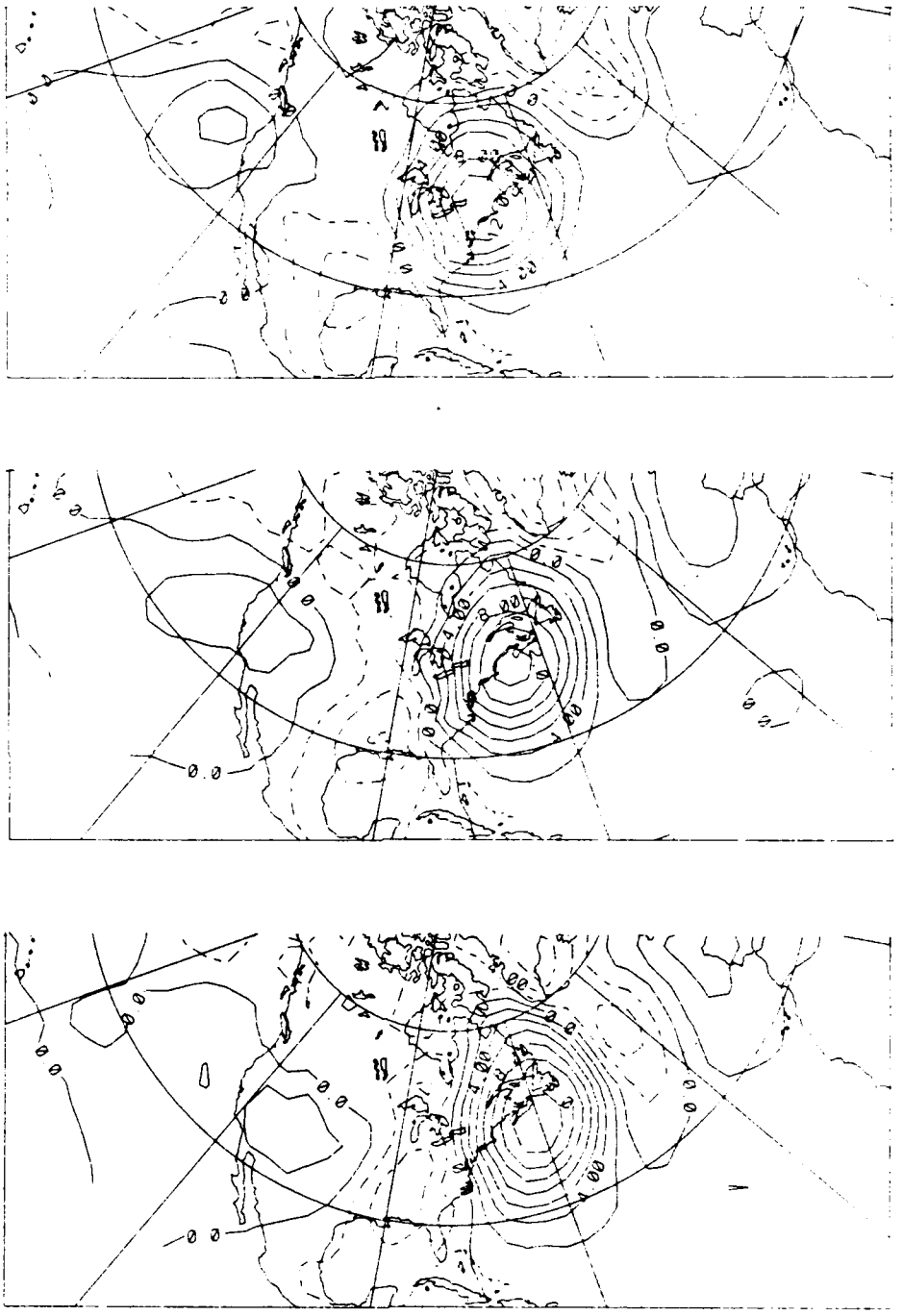

Fig. 5.8. Sea level pressure deviations from climatology for onshore events. Time sequence is the same as given in figure 5.6.

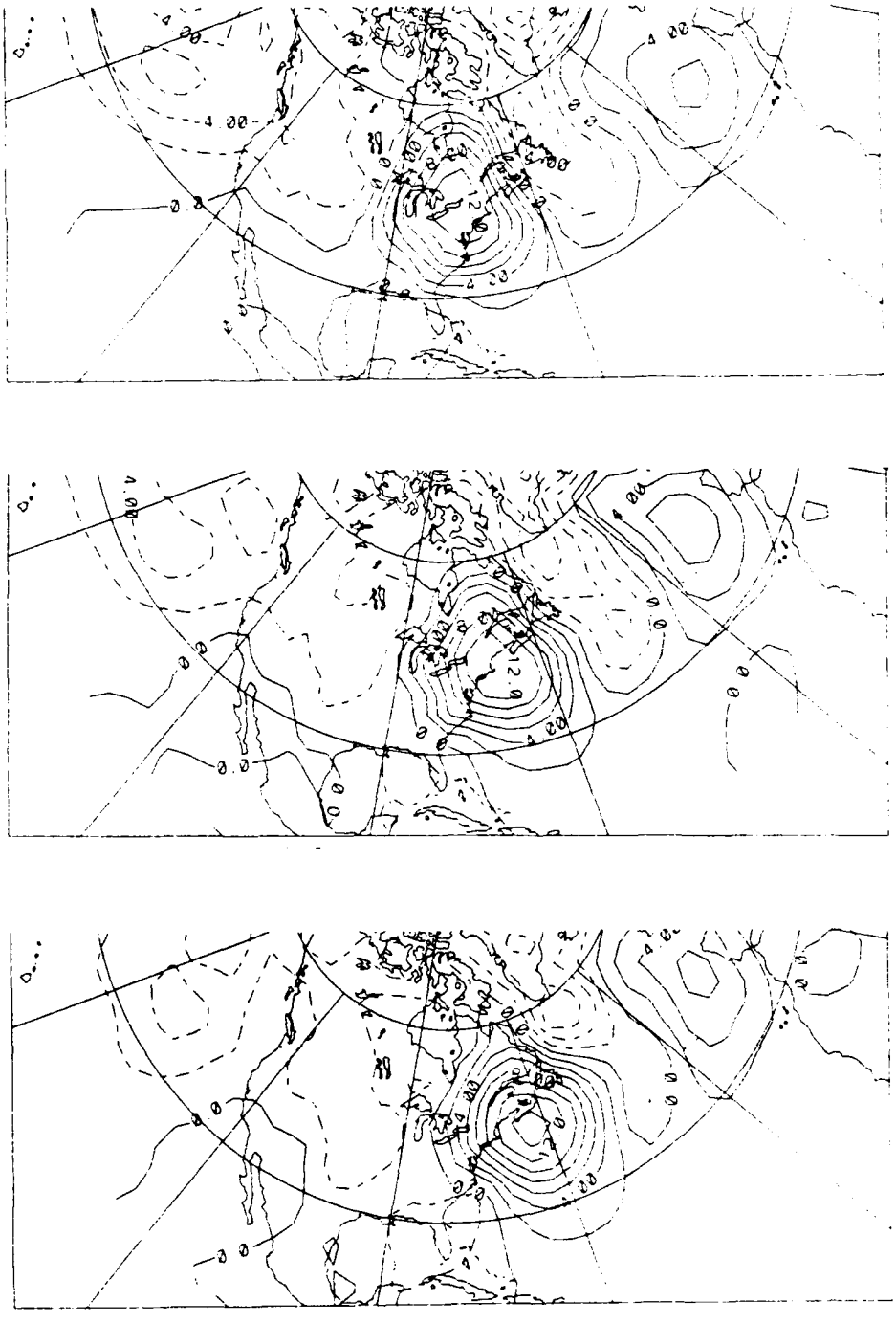

Fig. 5.9. Sea level pressure deviations from climatology for offshore events. Time sequence is the same as given in figure 5.6.

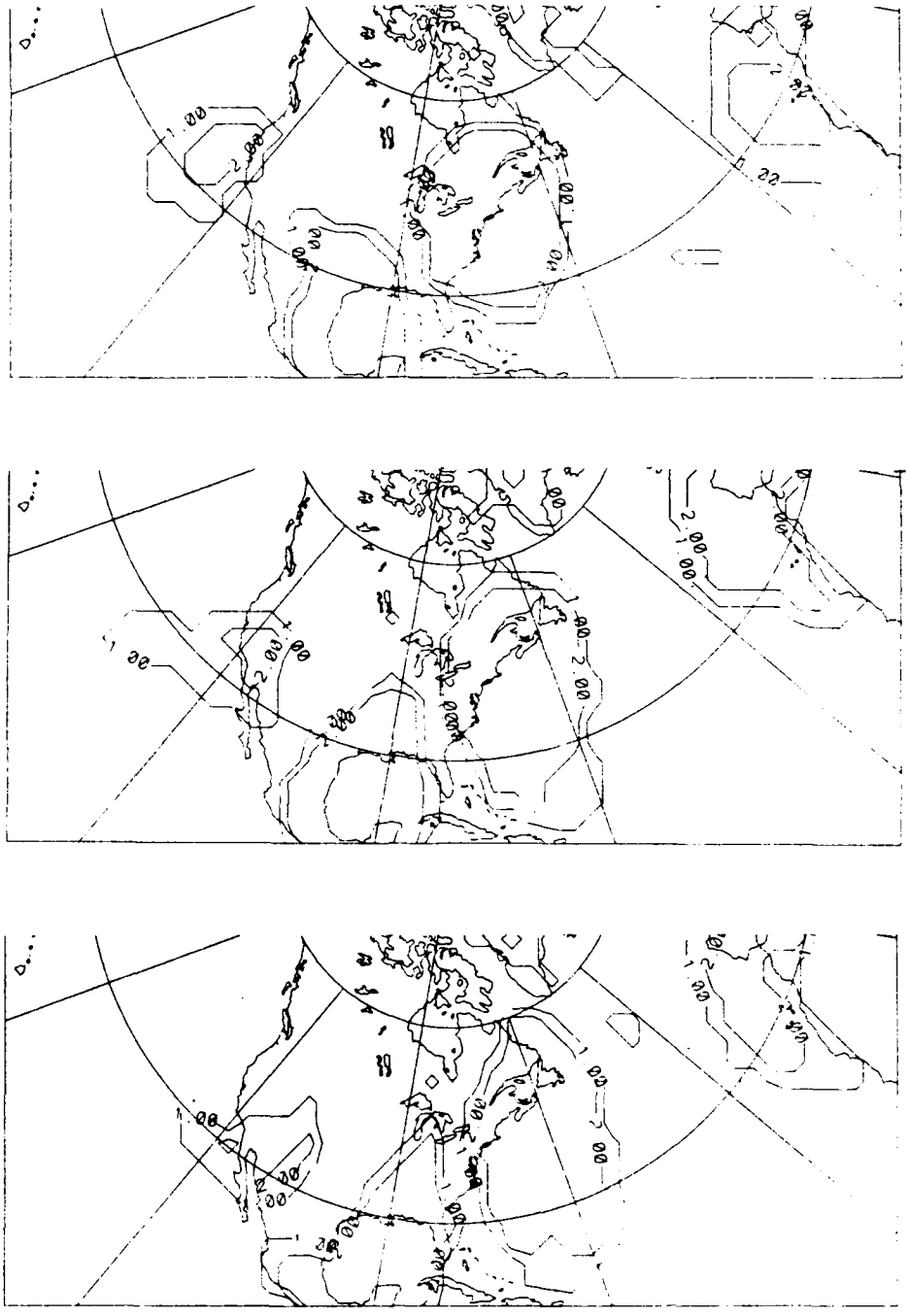

Fig. 5.10. Significance of sea level pressure deviation from climatology for onshore events. Time sequence is the same as given in figure 5.6.

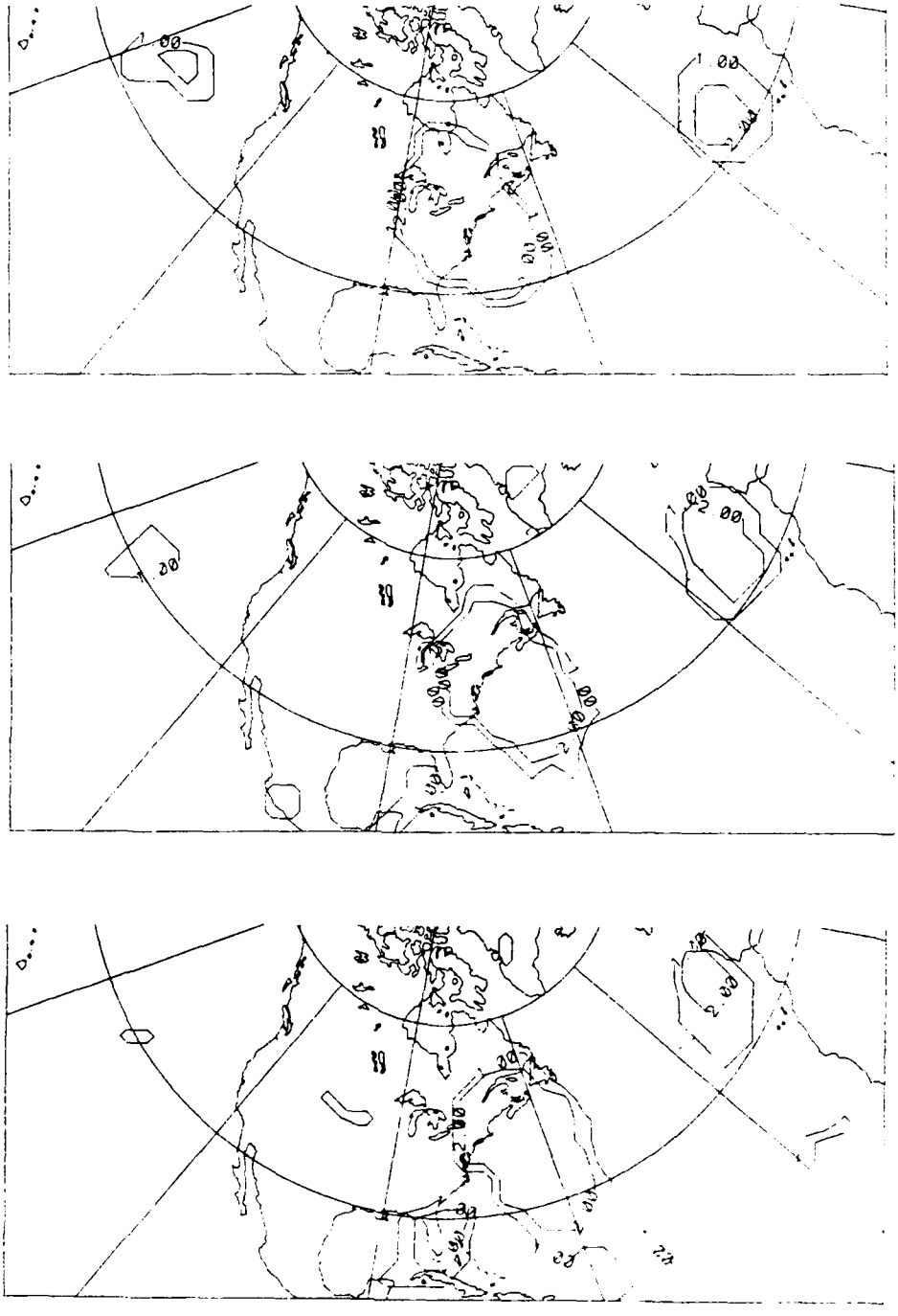

Fig. 5.11. Significance of sea level pressure deviation from climatology for offshore events. Time sequence is the same as given in figure 5.6.

5.3. 850 mb Grid Point Analysis.

Given Richwein's (1980) earlier assertion that the 850 mb pattern would be an excellent indicator of damming, additional climatological, composite, deviation, and significance charts were produced for the 850 mb level.

As with the surface charts, the 850 mb weighted climatic pattern (Fig 5.12) appears normal. Similarly, the composite charts (Figs 5.13 and 5.14) appear virtually identical, but once again differences do exist. Note that in Fig. 5.13 the trough over the central United States appears to be both deeper and more amplified, and is accompanied by stronger ridging on both coasts. In the composites for the offshore cases (Fig. 5.14) the trough shown over the north-central Atlantic Ocean has approximately the same amplitude as that for onshore cases, but appears to be slightly deeper.

The 850 mb deviation patterns (Figs. 5.15 and 5.16) echo those seen on the surface pressure deviation charts, i.e.stronger negative anomalies over the United States for onshore cases, versus over the Atlantic for offshore events. Finally, the significant deviations at the 850 mb level (Figs 5.17 and 5.18) are remarkably consistent with that seen on the surface charts. Once again the onshore cases show significant departures from normal occurring over the eastern seaboard, the Gulf coast, and the southwest coast.

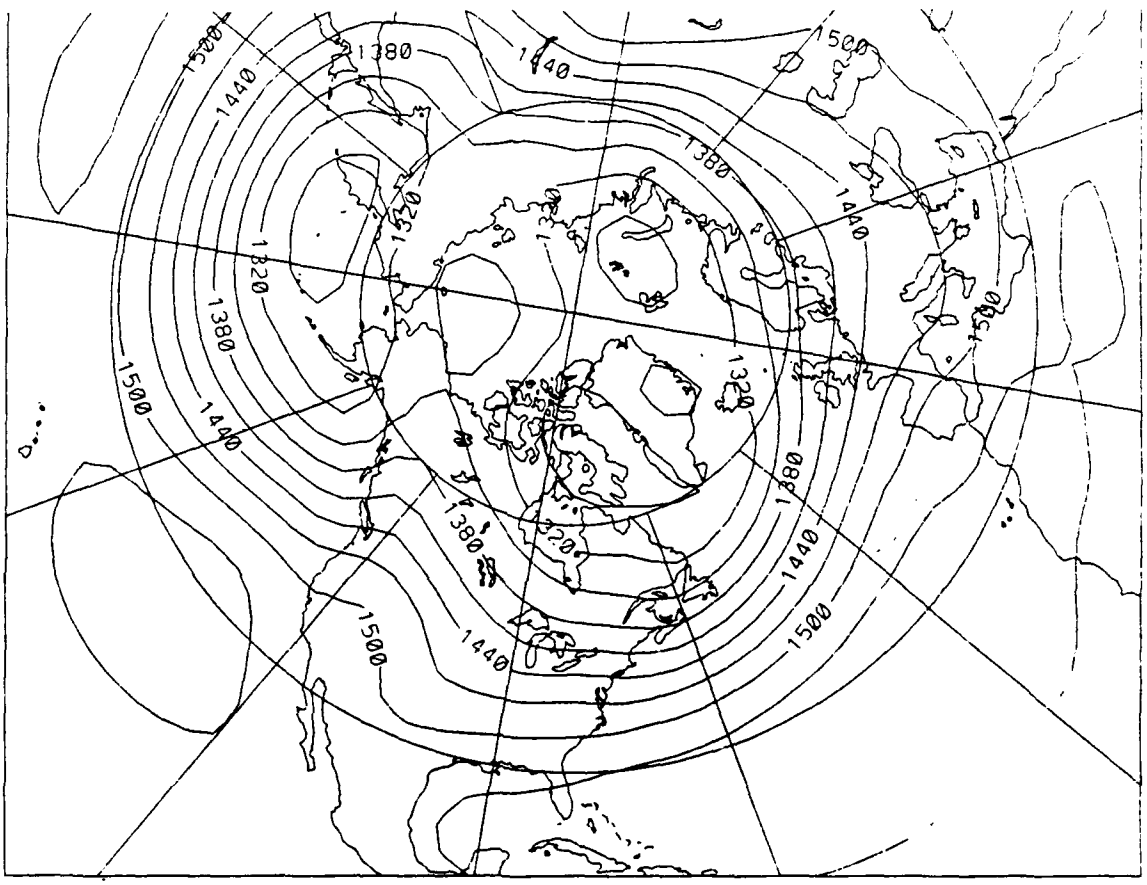

Fig. 5.12. Climatological 850 mb height pattern for the months of November to March, 1946 to 1989 and weighted to the specific months and years used in this study.

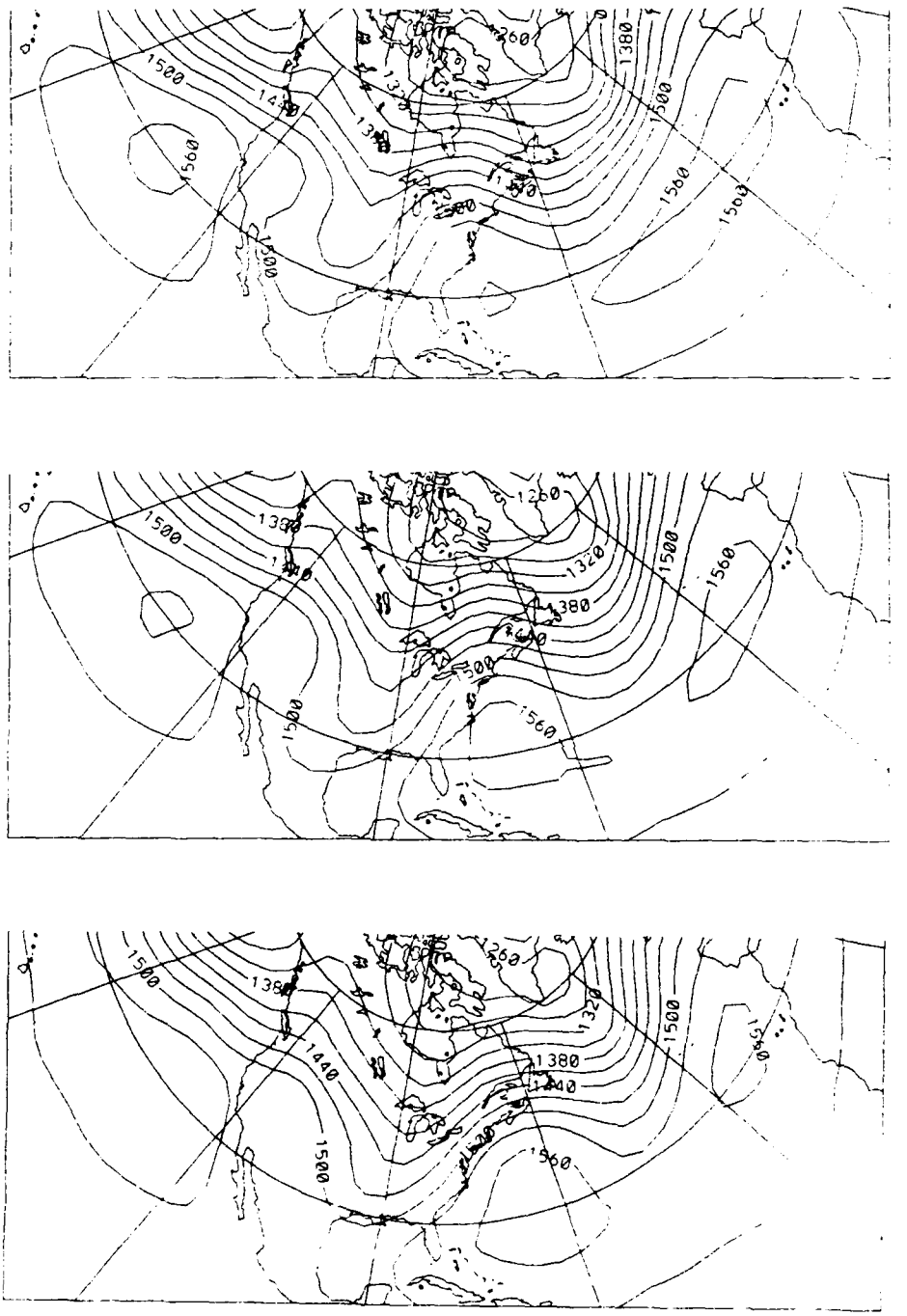

Fig. 5.13. Composite 850 mb height pattern for onshore events at 12 hours prior to HAT frontal passage, at frontal passage, and 12 hours subsequent to frontal passage.

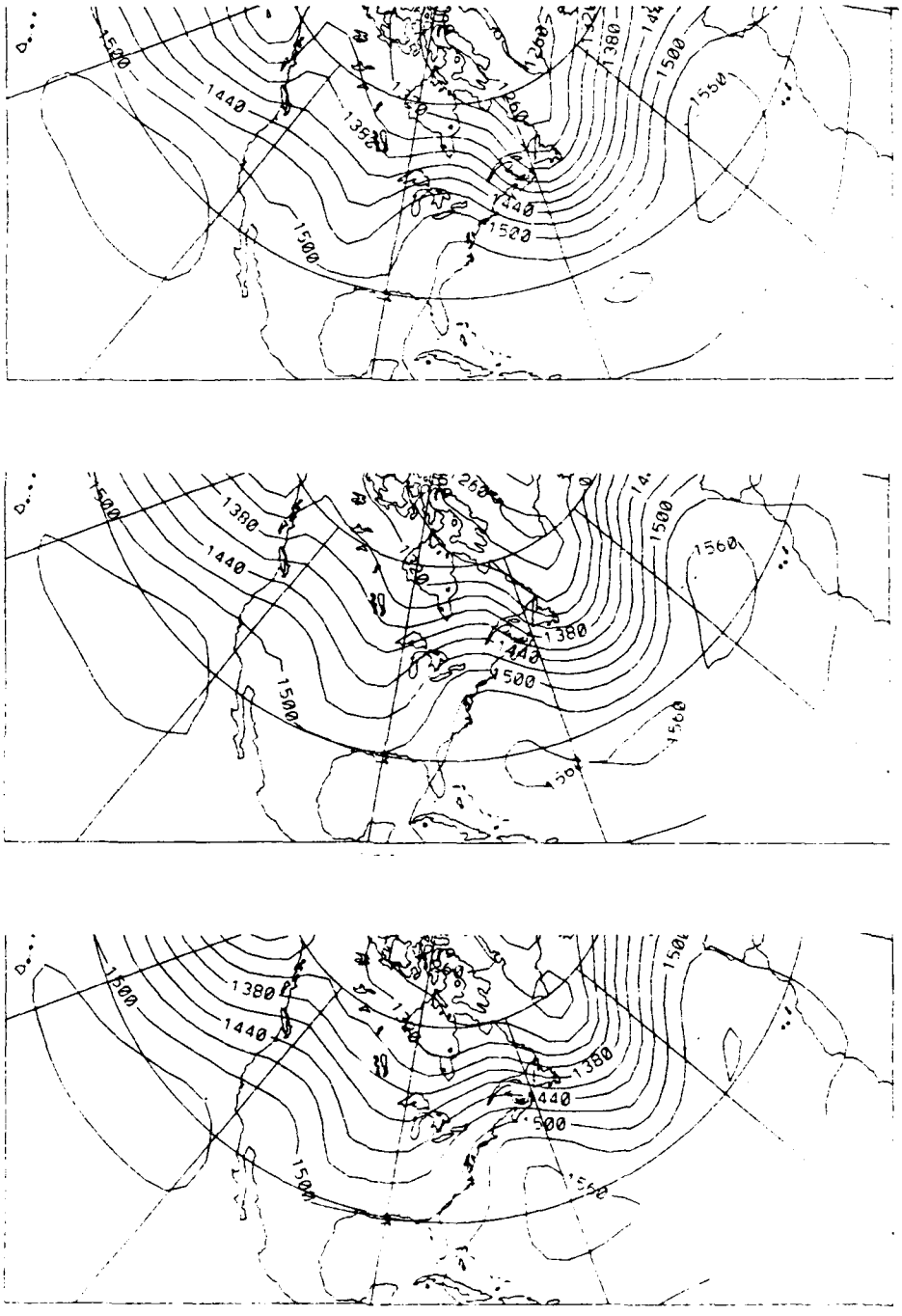

Fig. 5.14. Composite 850 mb height pattern for offshore events. Time sequence is the same as given in figure 5.13.

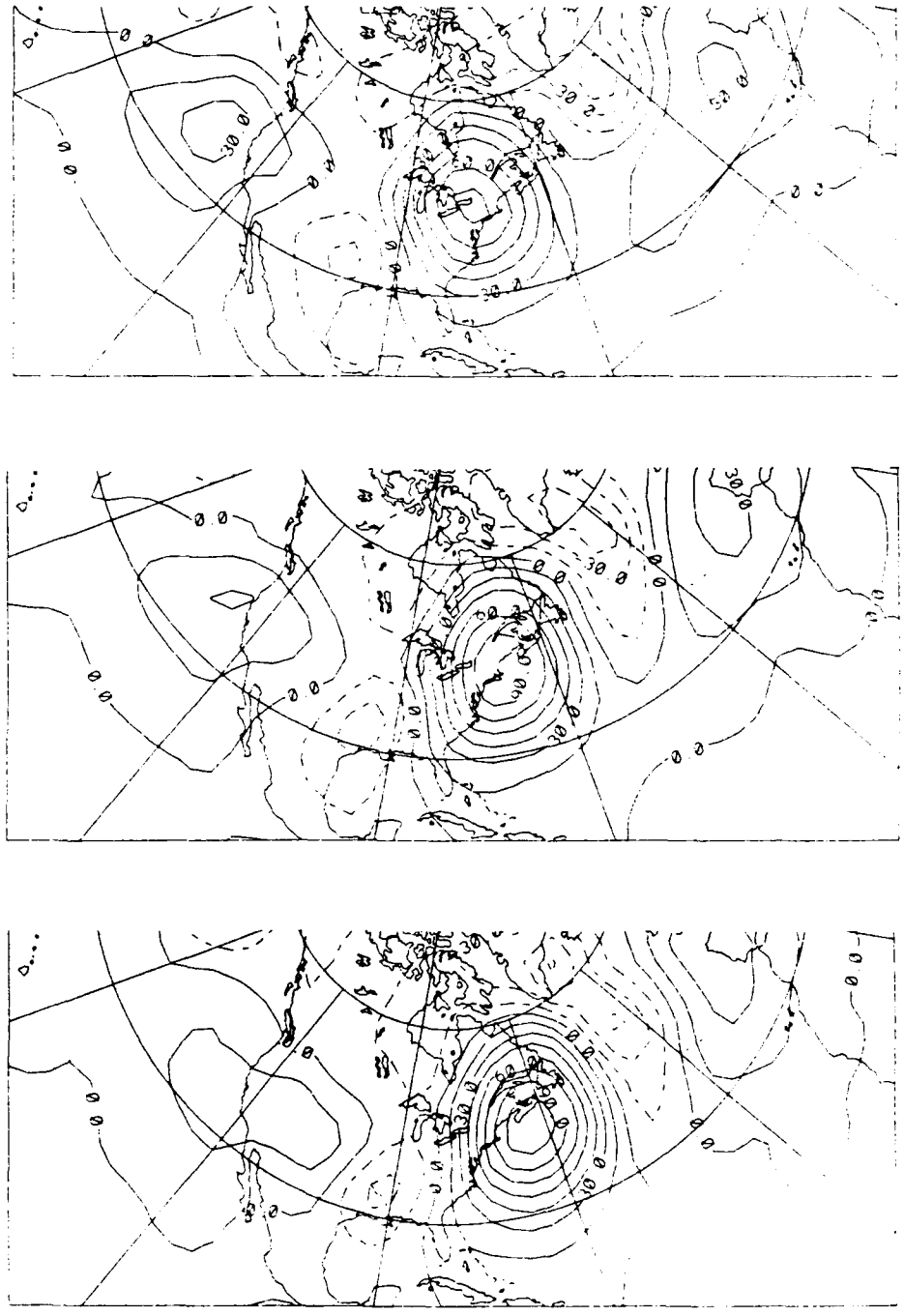

Fig. 5.15. Deviation of 850 mb height pattern from climatology for onshore events. Time sequence is the same as given in figure 5.13.

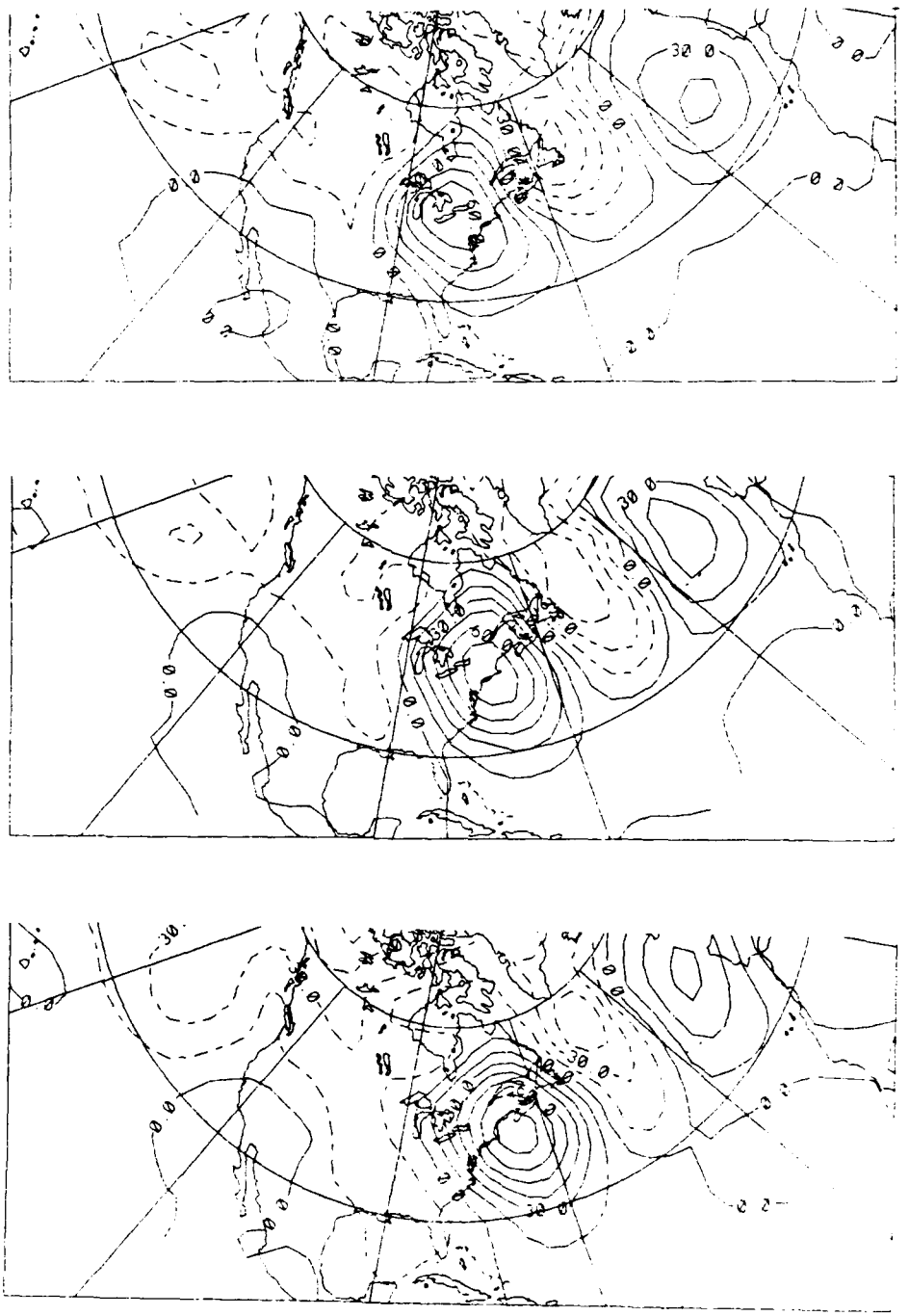

Fig. 5.16. Deviation of 850 mb height pattern from climatology for offshore events. Time sequence is the same as given in figure 5.13.

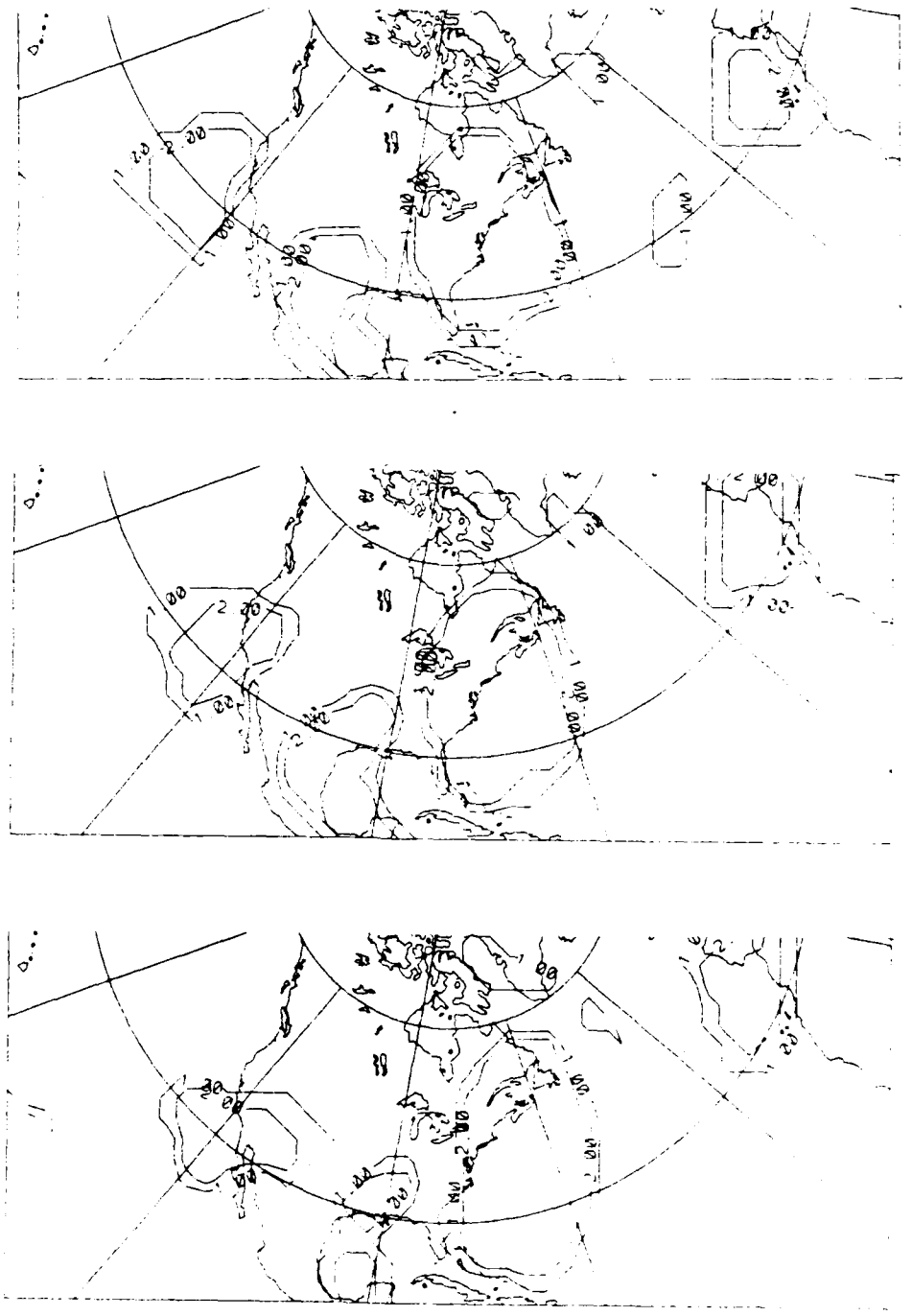

Fig. 5.17 Significance of 850 mb deviation from climatology for onshore events. Time sequence is the same as given in figure 5.13.

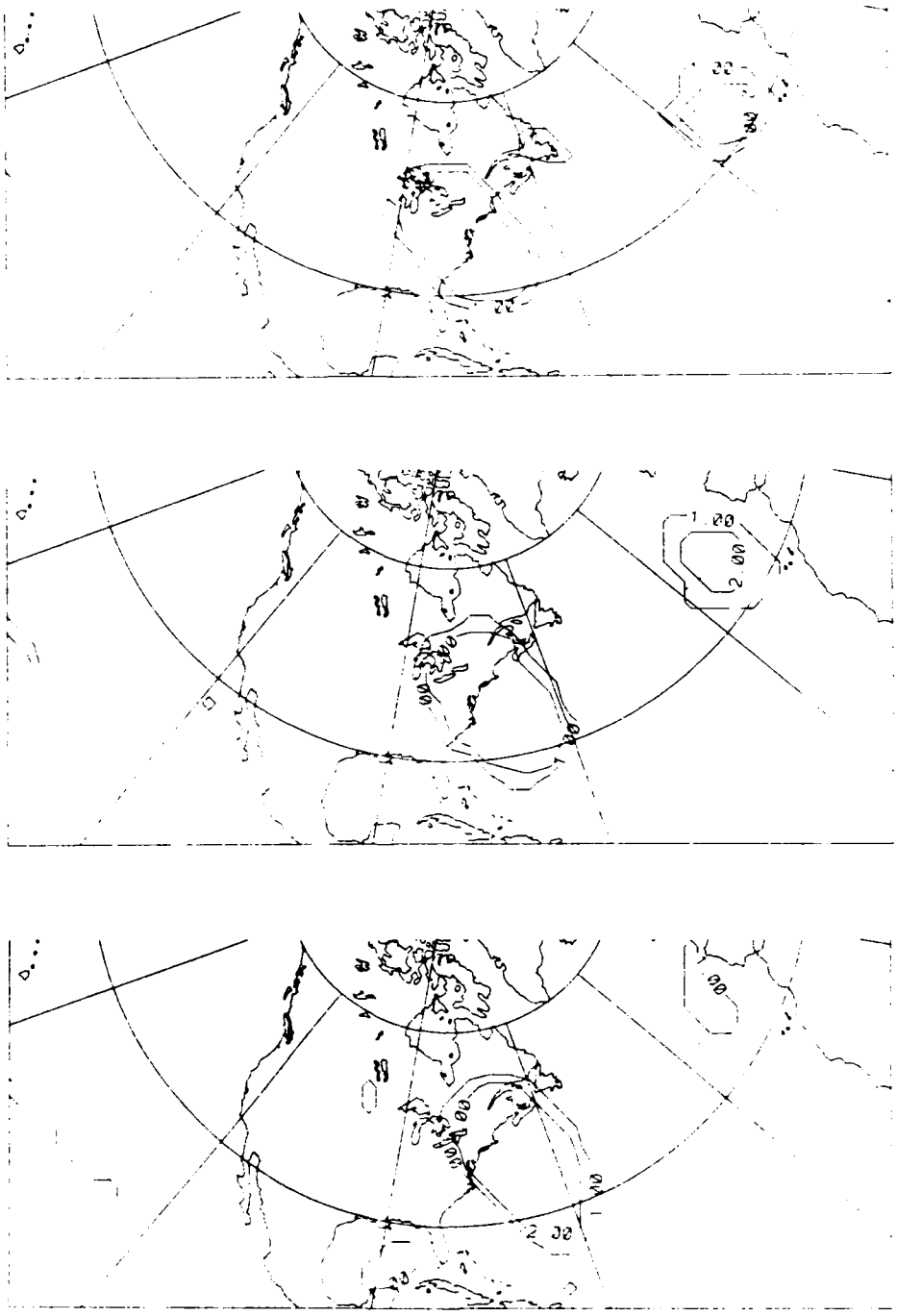

Fig. 5.18. Significance of 850 mb deviation from climatology for offshore events. Time sequence is the same as given in figure 5.13.

6. CASE STUDIES.

6.1. Overview.

The intent of this section is to provide a general discussion of each case accompanied by pressure analyses at key points, rather than an exhaustive review of each event. The following cases were selected to grant an equal representation between onshore and offshore events, and because collectively they contain the features which are common in Carolina coastal front cases. Specifically these features include (a) an approaching coastal cyclone/synoptic front, (b) cyclogenesis in the near-shore region, and (c) a coastal front which oscillates over the outer banks of North Carolina. All depictions of the coastal front employ the mesoscale analysis convention proposed by Young and Fritsch (1989).

6.2. Case of 24 January 1984.

Figure 6.1 shows the synoptic conditions for 21 January at 1200 UTC. At this time a high pressure center is centered over extreme western Kentucky. Classical CAD scenarios would lead one to believe that damming situations arise from anticyclones moving eastward along the United States-Canadian border. However, in this instance the high pressure center takes a "U" shaped path from southern Saskatchewan through the Dakotas and Missouri to its present position. By 0000 UTC on the 23rd (Fig. 6.2) the high center has taken up station over the Delmarva peninsula. At this time the characteristic pressure ridge is already becoming evident although in the Carolinas the northerly wind component usually expected with damming is still largely disorganized. Nevertheless, observations at North Carolina coastal stations and buoys 41001 and 41002 suggest the existence of confluence in the near-shore region. Six hours later

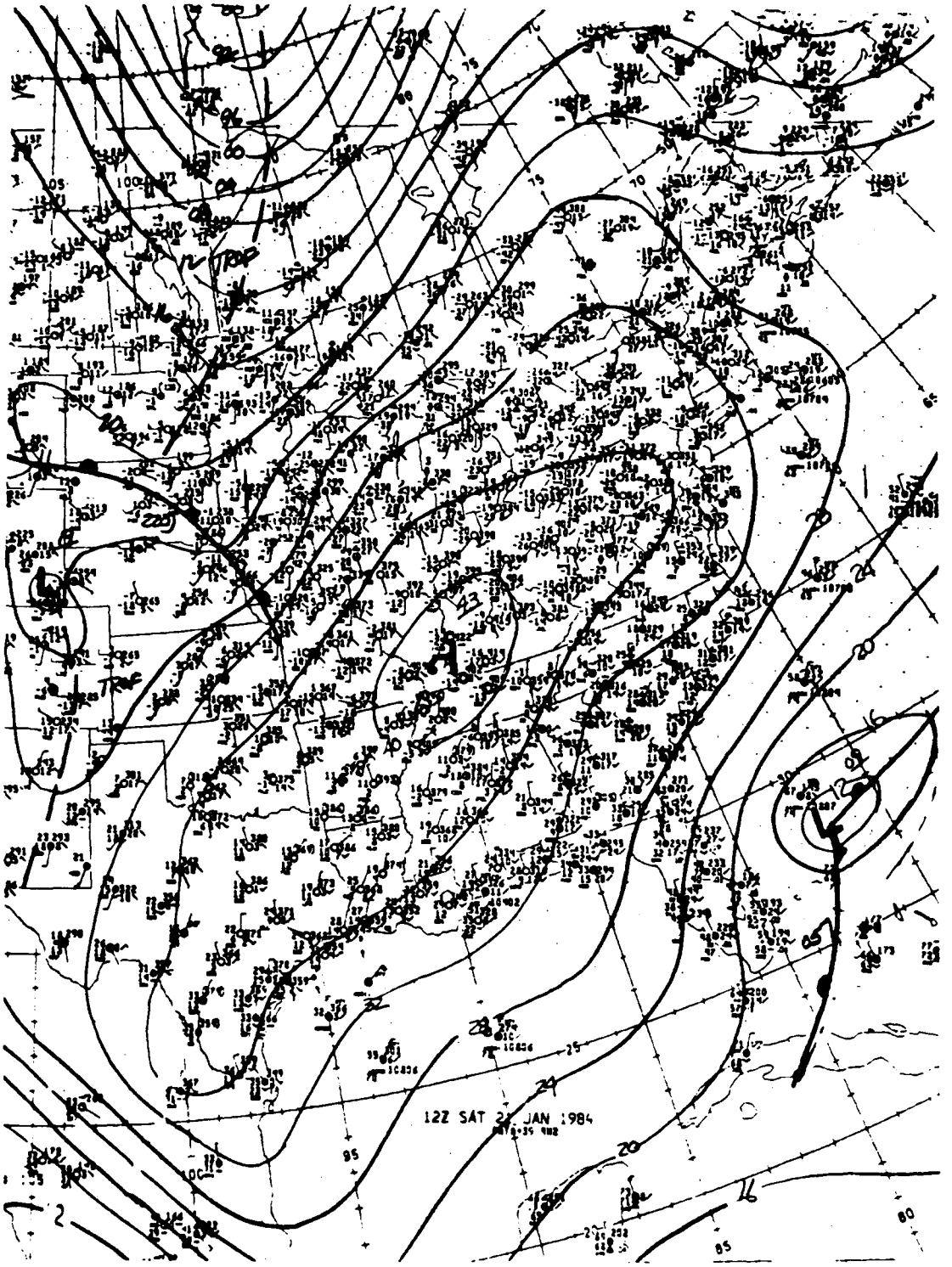

Fig. 6.1. NMC surface analysis valid at 1200 UTC, 21 January 1984.

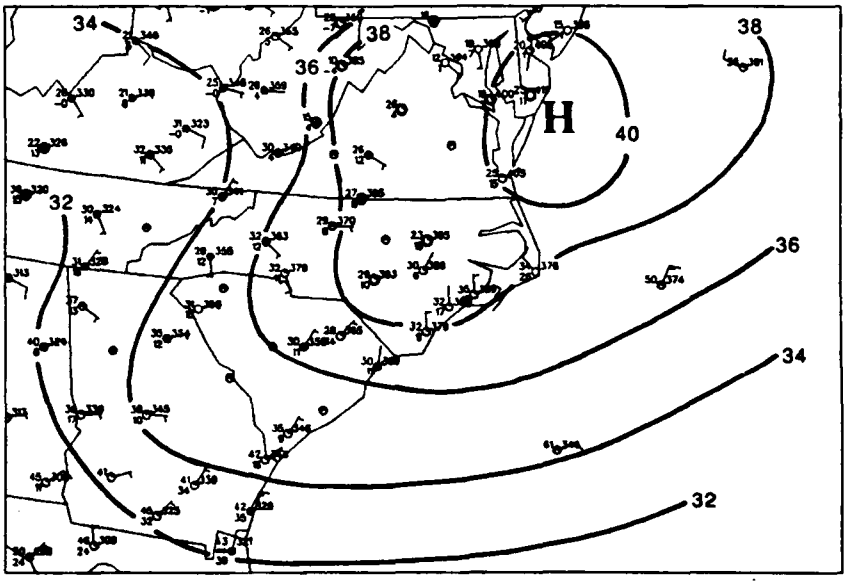

Fig. 6.2. Surface pressure analysis valid at 0000 UTC, 23 January1984.

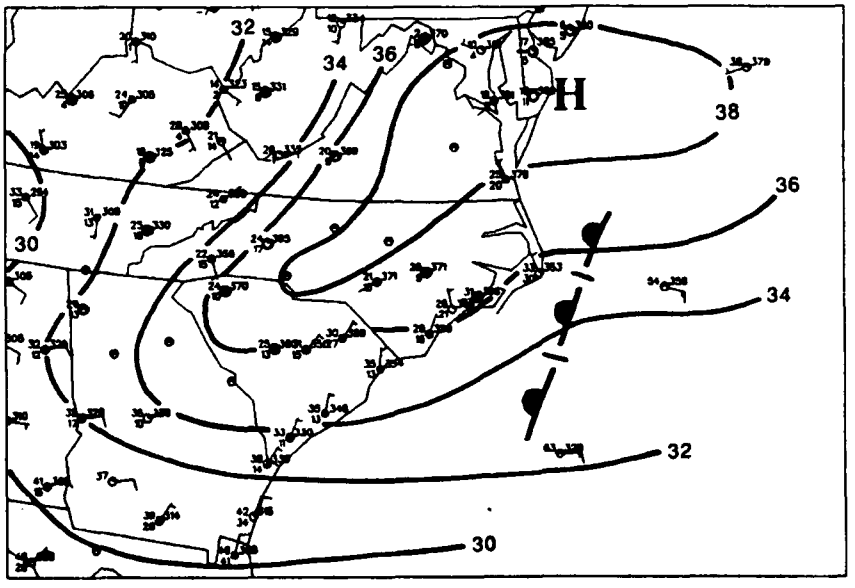

Fig. 6.3. Surface analysis valid for 0600 UTC, 23 January 1984.

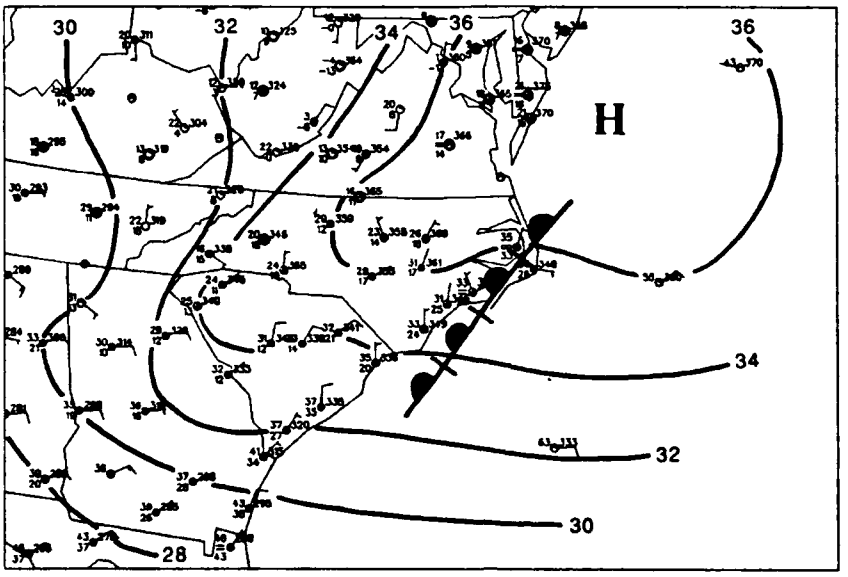

Fig. 6.4. Surface analysis valid at 1200 UTC 23 January 1984.

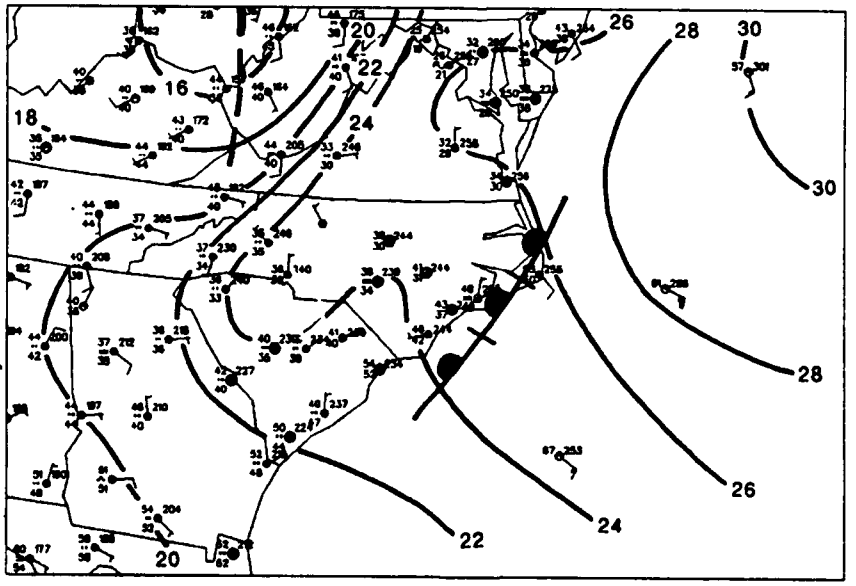

Fig. 6.5. Surface pressure analysis valid at 0900 UTC 24 January 1984.

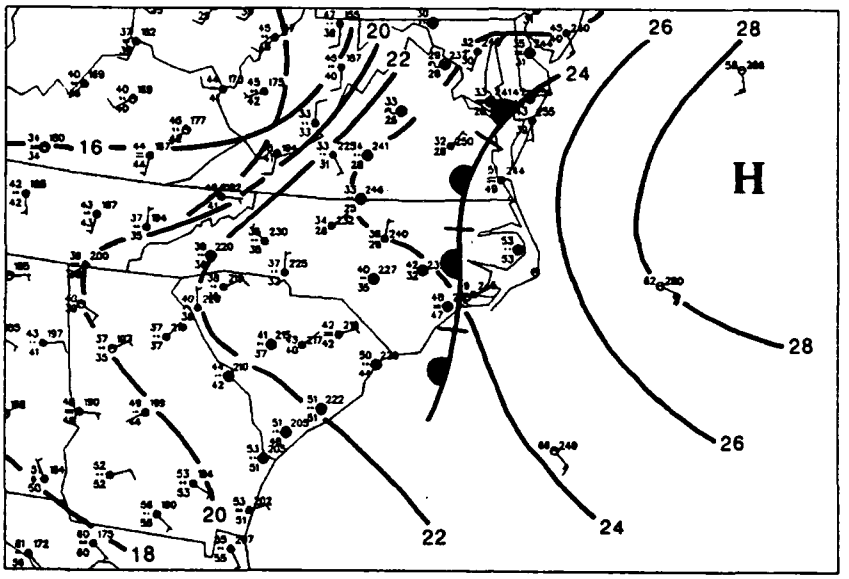

Fig. 6.6. Surface pressure analysis valid at 1200 UTC 24 January 1984.

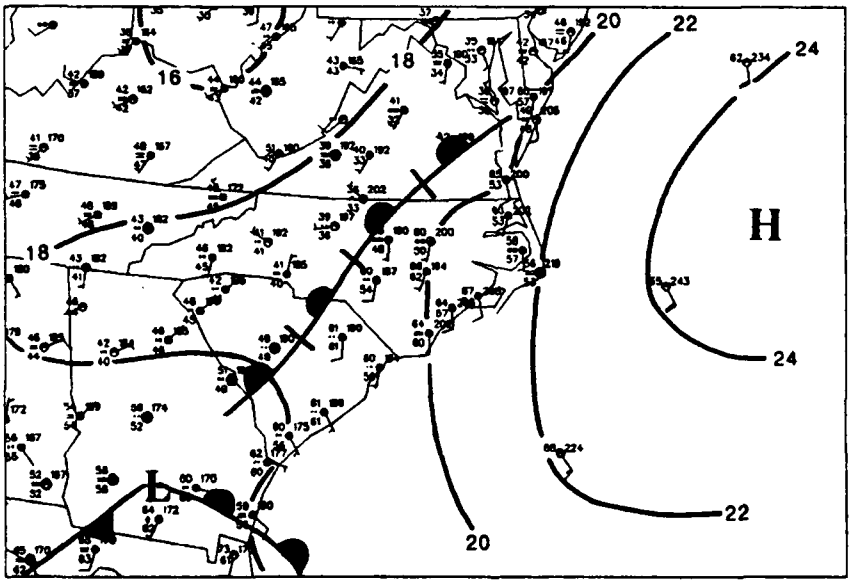

Fig. 6.7. Surface pressure analysis valid at 1800 UTC 24 January 1984.

(Fig. 6.3) the pressure ridge is now well defined, and while the buoy wind directions have turned to nearly due east, the coastal stations are still reporting north-northwesterly winds. These observations plus the mesoscale pressure analysis coastal frontogenesis offshore. By 1200 UTC on the 23rd (Fig. 6.4) the inverted ridge is beginning to show signs of weakening (i.e. higher pressure values are retreating northward) and the observation from HAT shows a wind shift to the east while Dare County Gunnery Range (2DP) is still reporting northeasterly flow. This would suggest that a frontal passage has occurred at HAT although this is not reflected in the reported temperature. Over the next 21 hours (not shown) the inverted ridge continues to weaken and the front oscillates slightly across the outer banks retreating east of HAT twice before re-crossing HAT by 0900 UTC on the 24th (Fig. 6.5), and making landfall three hours later (Fig 6.6). The front then proceeds inland and stalls along a line from just east of Richmond, Virginia (RIC) to just east of Columbia, South Carolina (CAE) by 1800 UTC on the 24th (Fig. 6.7). The terminal position of the front appears to coincide with a veering of the winds east of the front to a virtually due south direction. Such an orientation would produce a very weak, to non-existent, u-component for the winds, and so theoretically the front simply loses its' westward push.

6.3. Case of 25 January 1986.

This case occurred during GALE IOP-2 and has already been extensively examined by Egentowich (1989) and Riordan (1990). Fig. 6.8 shows the conditions approximately 12 hours prior to damming. At this time the center of high pressure is located north of Lake Superior. There is no evidence yet of an inverted ridge over the coastal plain and the winds there appear to be consistent with the expected dynamics for unaccelerated flow near the surface. The winds over the ocean do not indicate any coastal confluence.

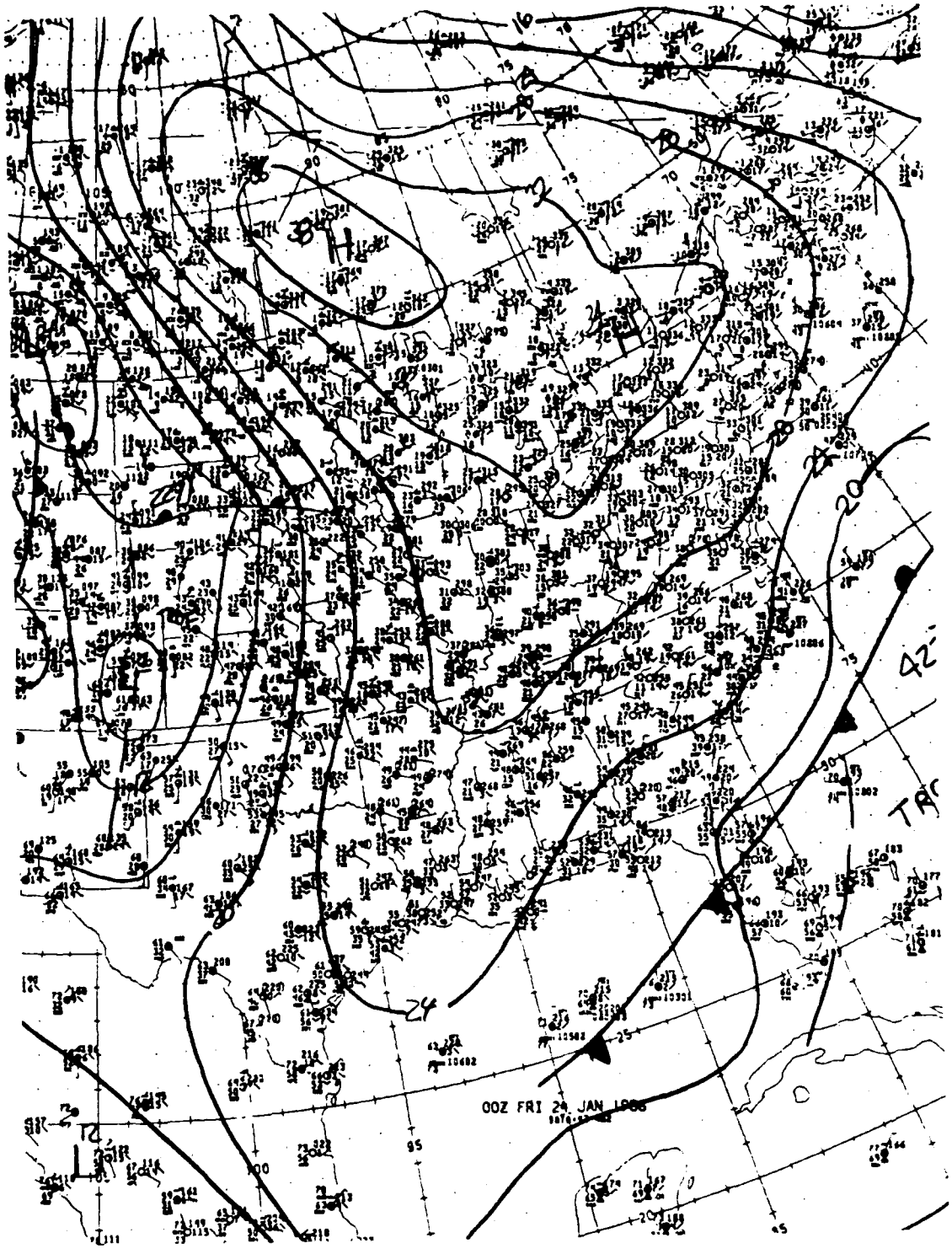

Fig. 6.8. NMC surface analysis valid at 0000 UTC 24 January 1986.

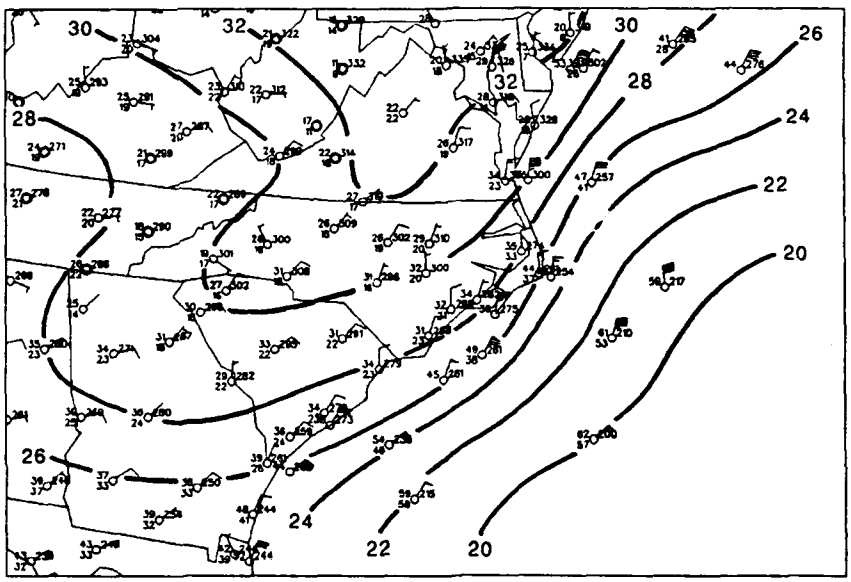

Fig. 6.9. Surface pressure analysis valid at 1200 UTC 24 January 1986.

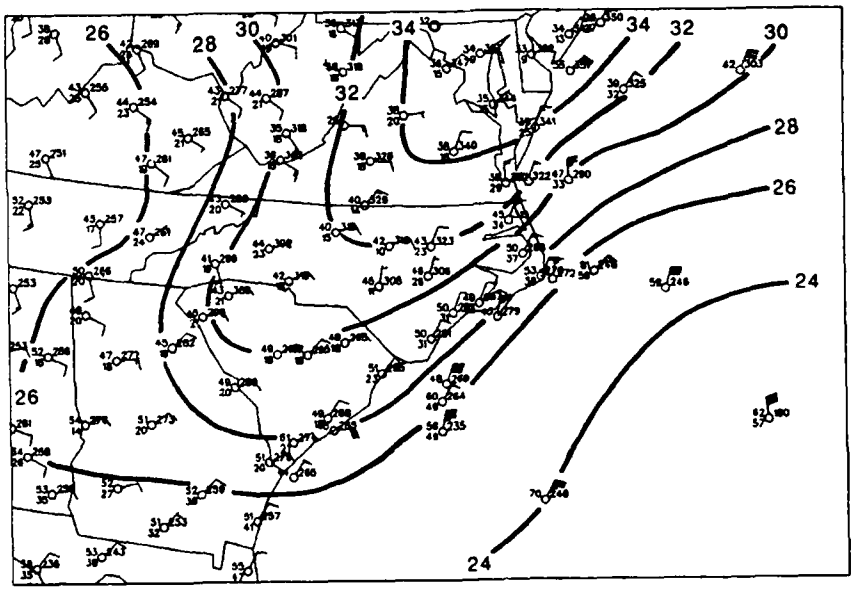

Fig. 6.10. Surface pressure analysis valid at 1800 UTC 24 January 1986.

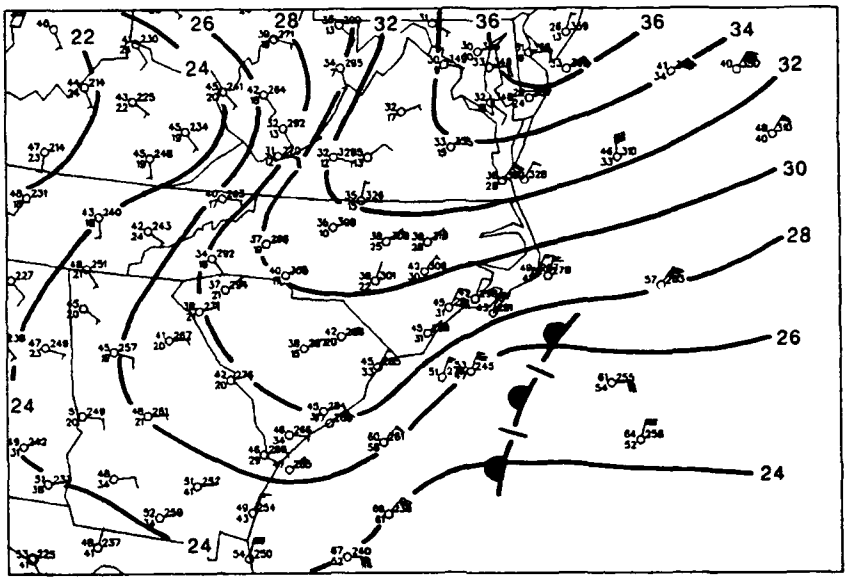

Fig. 6.11. Surface pressure analysis valid at 0000 UTC 25 January 1986.

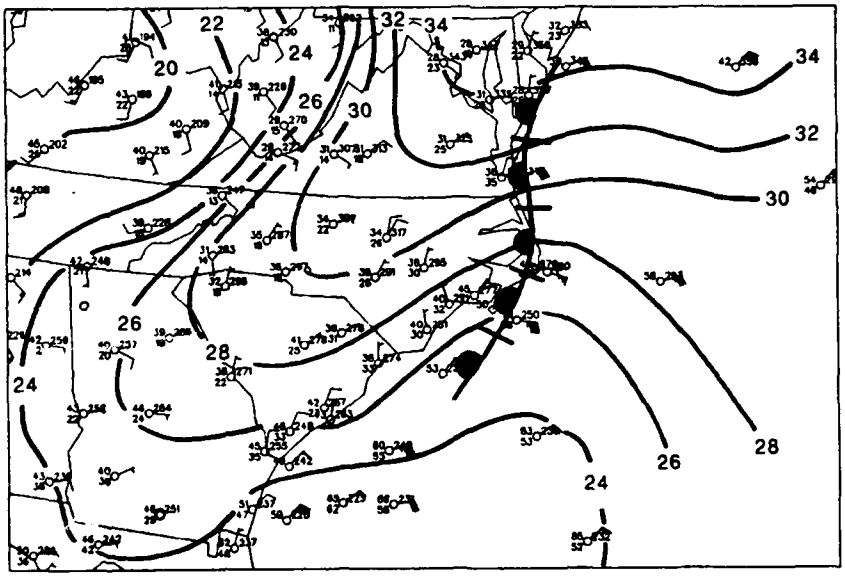

Fig. 6.12. Surface pressure analysis valid at 0600 UTC 25 January 1986.

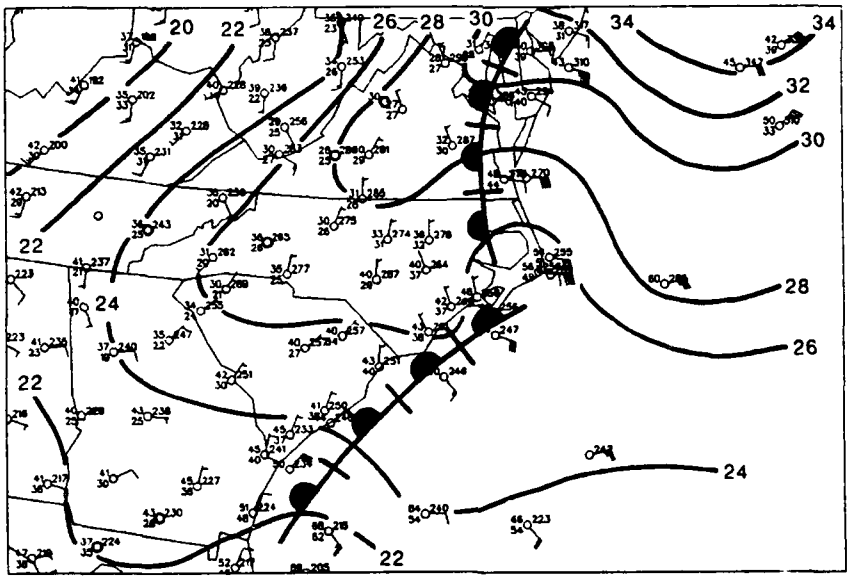

Fig. 6.13. Surface pressure analysis valid at 1200 UTC 25 January 1986.

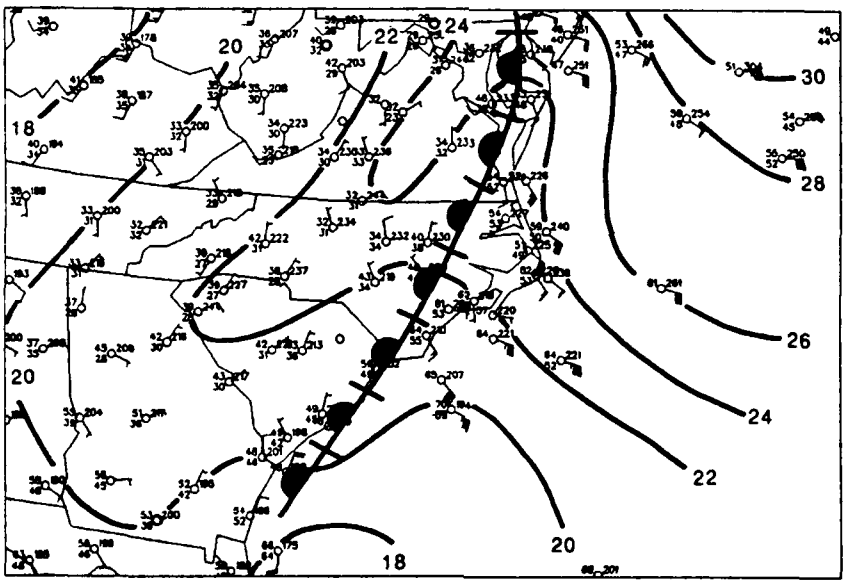

Fig. 6.14. Surface pressure analysis valid at 1800 UTC 25 January 1986.

Little change occurs until 1200 UTC on the 24th (Fig. 6.9) when the high center has moved eastward into the province of Quebec. An inverted ridge is already apparent and the winds over the central and western portions of the Carolinas and Virginia are now flowing virtually perpendicular to the isobars. Offshore wind reports still show no confluence along the coast.

By 1800 UTC on the 24th (Fig. 6.10) an inverted ridge remains well evident and damming is indicated with wind directions still crossing the isobars at angles in excess of 90 degrees. However, coastal and marine observations still show no evidence of offshore confluence or a coastal front. During the six hours which follow, weak confluence does begin to form and by 0000 UTC on the 25th (Fig. 6.11) an inverted trough and the initial stages of a coastal front become apparent offshore. At 0500 UTC (not shown, see Fig 6.12) the observation from HAT reports the winds have shifted to a due easterly direction, thereby suggesting a frontal passage (note that this contrasts with Egentowich's approximation of 0800 UTC). The coastal front then remains stationary just west of HAT until approximately 1200 UTC (Fig. 6.13) when the northern portion appears to "jump" inland between northeastern North Carolina to southern New Jersey. The southern segment, meanwhile, remains quasi-stationary along the coast from North Carolina to Georgia. The northern front promptly stalls, and no frontal passage is evident in southeastern North Carolina until at least 1800 UTC (Fig 6.14). At that time the observation from Wilmington, North Carolina (ILM) shows the winds there have veered to the southeast. Also note that by 1800 UTC the inverted ridge is no longer as sharply defined as it was six hours ago. At that time the front is onshore from approximately Myrtle Beach, South Carolina to Philadelphia, Pennsylvania. This line represents the terminal inland position of the front. From this point the cold dome

continues to dissolve while the front retreats seaward and dissipates in advance of a cold front approaching from the west.

6.4. Case of 18 January 1987.

At 0000 UTC on 17 January 1987 (Fig 6.15) a high pressure center is situated over Georgian Bay in the southeastern corner of the Canadian province of Ontario, at the same time a cold front has just recently moved offshore of the Carolinas. Precipitation in the form of light, continuous rain is falling from western Georgia to central Virginia. As it is early in this event, an inverted ridge is not present and the wind fields are still being dominated by the pressure field associated with a synoptic cold front. Within three hours (Fig. 6.16) an inverted pressure ridge has begun to form and rainfall continues within the damming region. By 1500 UTC on the 17th (Fig. 6.17) the rainfall has ceased, except in coastal regions of South Carolina and southern Georgia, while the inverted ridge has become sharply defined and at some locations the winds are crossing the contours at angles greater than 90 degrees. The maritime winds, however are still dominated by the pressure field in the wake of a slow moving cyclone now centered southeast of buoy 41001.

Very little change occurs through 0000 UTC on the 18th (Fig 6.18) with the exception that confluent angles between the buoys and coastal Carolina stations have increased slightly. In addition light precipitation is now occurring in isolated pockets along the coast of the Carolinas and Georgia, while light to moderate rain is moving eastward out of Alabama in association with a low pressure system in the northwestern Gulf of Mexico The confluence continues to strengthen and by 0600 UTC on the 18th (Fig 6.19) an inverted trough has formed along the coast of the Carolinas and a coastal

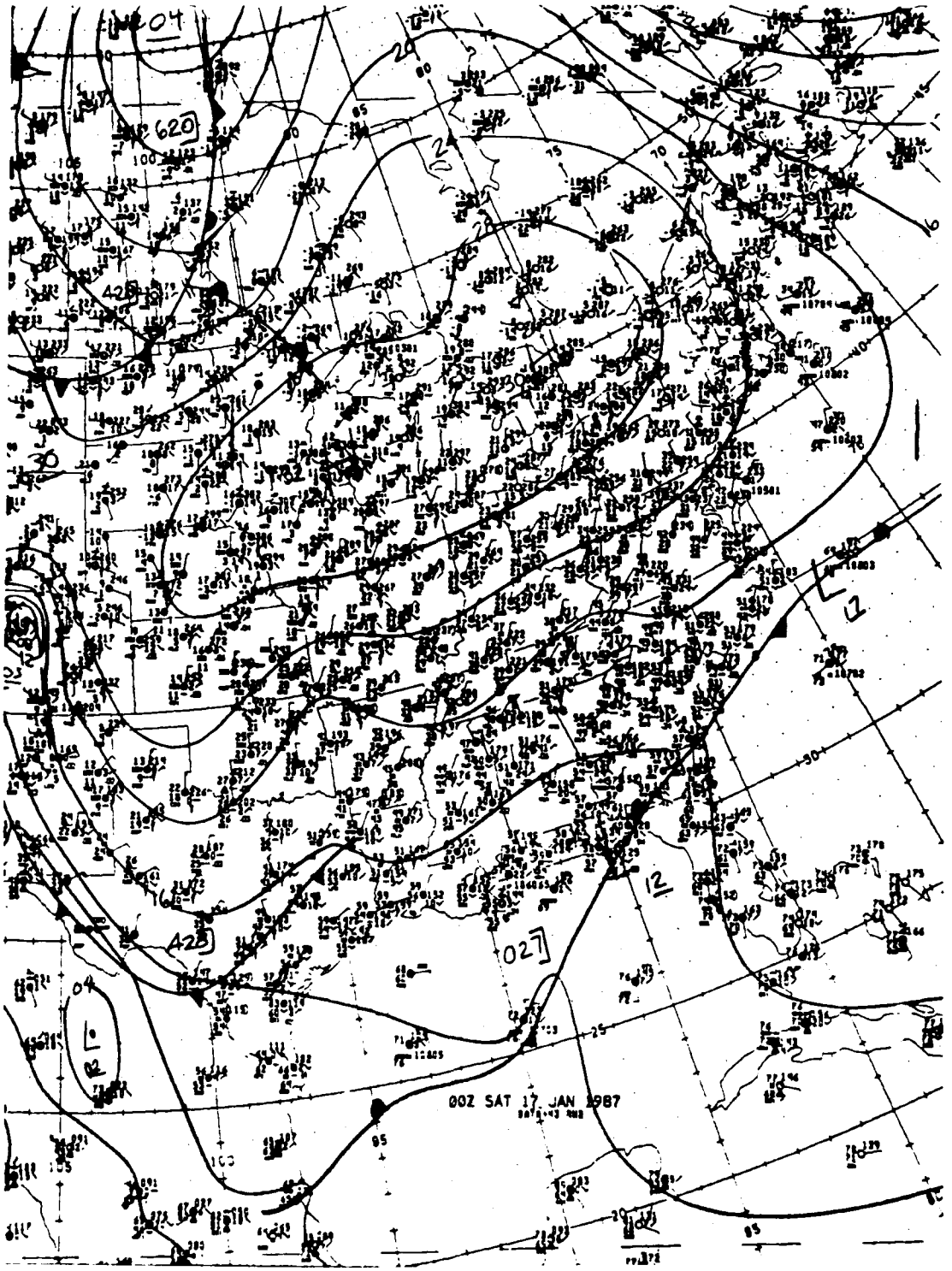

Fig. 6.15. NMC surface analysis valid at 0000 UTC on 17 January 1987.

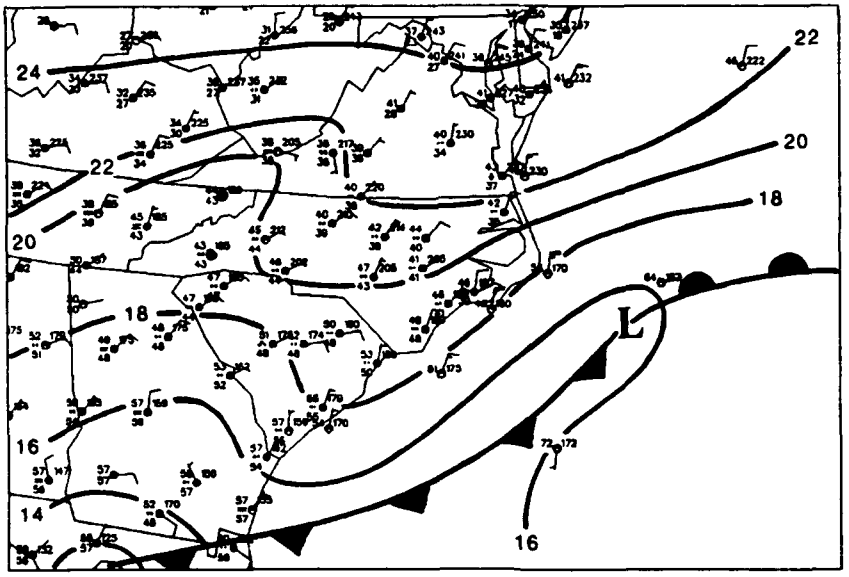

Fig. 6.16. Surface pressure analysis valid at 0300 UTC 17 January 1987.

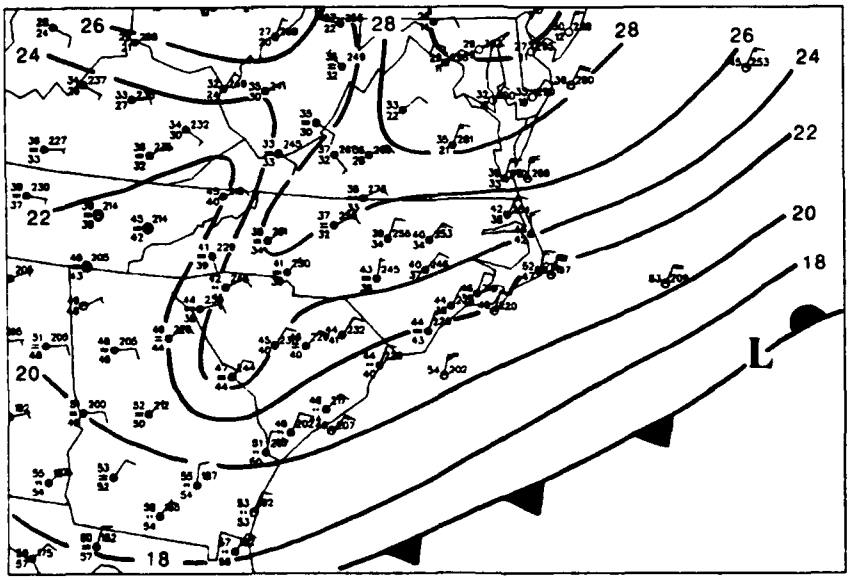

Fig. 6.17. Surface pressure analysis valid at 1500 UTC 17 January 1986.

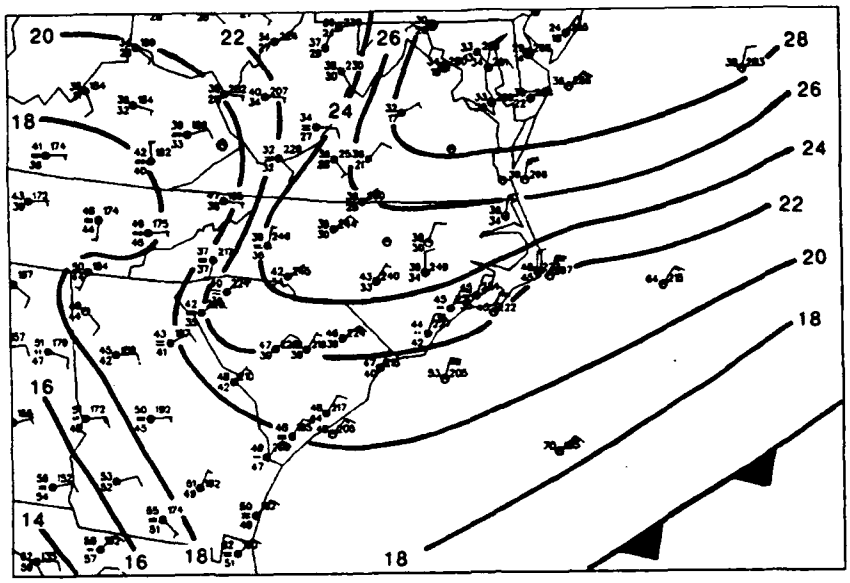

Fig. 6.18. Surface pressure analysis valid at 0000 UTC 18 January 1987.

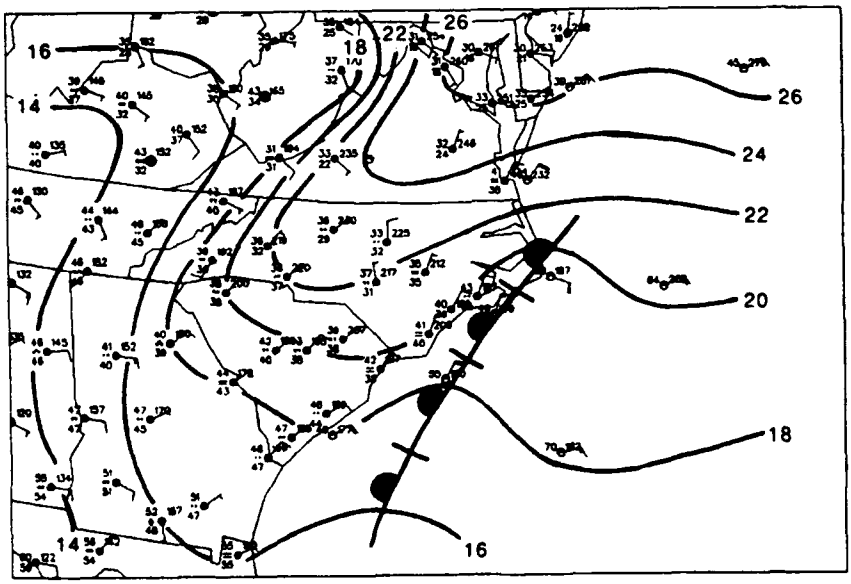

Fig. 6.19. Surface pressure analysis valid at 0600 UTC 18 January 1987.

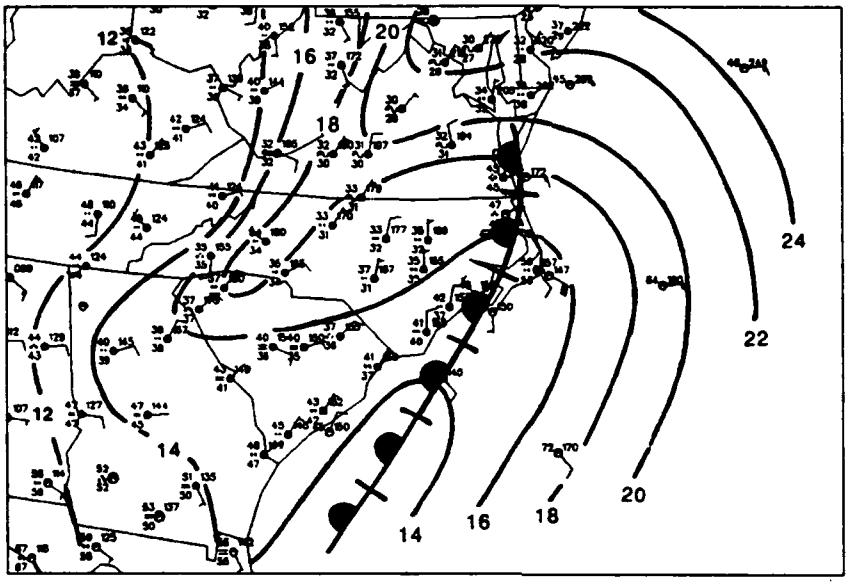

Fig. 6.20. Surface pressure analysis valid at 1200 UTC 18 January 1987.

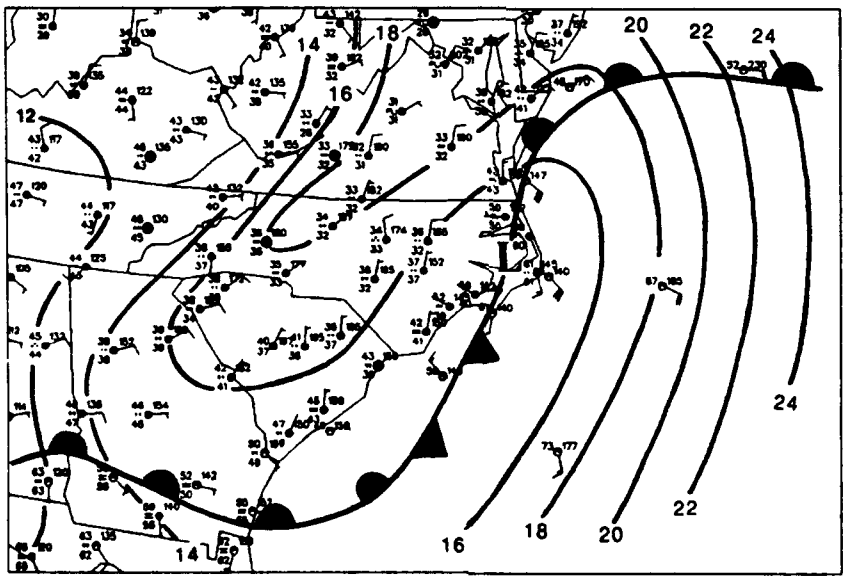

Fig. 6.21. Surface pressure analysis valid at 1500 UTC 18 January 1987.

frontal passage has occurred at Diamond Shoals (DSLN7). At the same time the rainfall continues to spread northeastward into central North Carolina with the advance of the system from the Gulf, coupled with a disturbance moving across the lower Ohio and Mississippi valleys.

By 1200 UTC (Fig. 6.20) the inverted ridge is no doubt undergoing dissipation, and the front has moved over the outer banks, and probably passed 2DP. It is interesting to note that at this time the heaviest precipitation is occurring at locations immediately west of the coastal front's position (ORF, ECG, MQI) and that the airmass over Virginia has cooled suffciently to permit light, freezing rain. Also note that the inverted trough offshore has deepened such that the maritime winds in the vicinity of the Carolinas have veered to a south-southeasterly direction. This deepening of the trough culminates in the formation of a low over HAT by 1500 UTC (Fig 6.21). Following the formation of this low, the winds over the Carolina coastal plain back to a north-northwesterly direction, pushing the coastal front further away from the shore. As the low continues to deepen and track northward, the coastal front is replaced by a seaward-moving cold front.

6.5. Case of 23 March 1989.

Fig 6.22 shows the synoptic conditions for 0600 UTC on 22 March 1989. At this time high pressure is centered over Wisconsin while a cold front, extending from a low over Newfoundland, is moving across Alabama, Georgia, and South Carolina. Precipitation associated with this front is still falling over Georgia and the Carolinas. Over the ensuing 12 hours the high center moves eastward into western New York state while the cold front slowly pushes southeastward into Florida. Even though the high

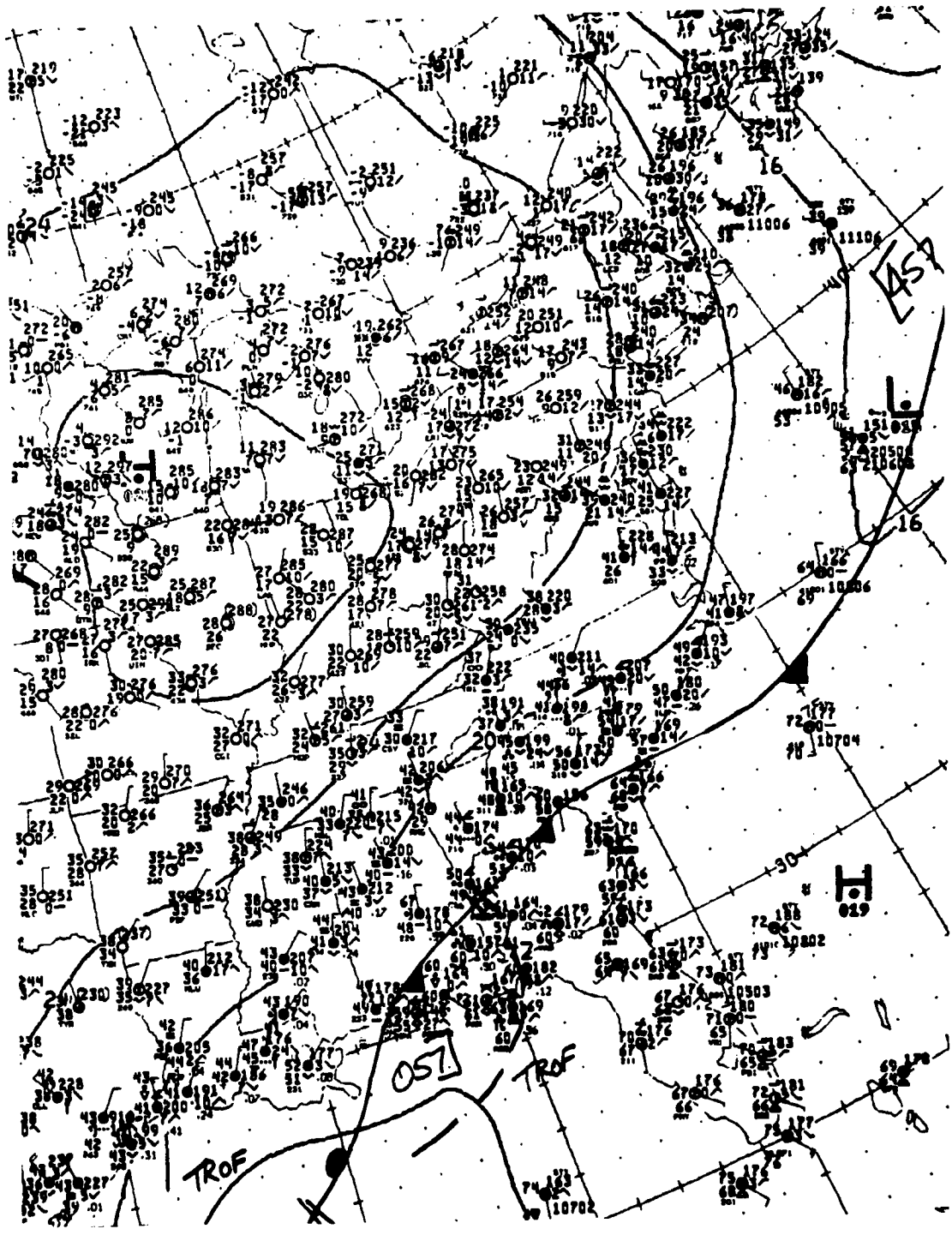

Fig. 6.22. NMC surface analysis valid at 0600 UTC 22 March 1989.

center is still positioned significantly farther west and south of the classic damming location, at 1800 UTC on the 22nd (Fig. 6.23) cold air damming is evident over the mid-Atlantic states and some winds in South Carolina are already crossing the isobars at angles of approximately 90 degrees. Precipitation continues to fall from central South Carolina to the northeast coast of North Carolina. By 0600 UTC on the 23rd (Fig. 6.24) an inverted trough has begun forming offshore of the Carolinas, and precipitation continues to be recorded within the damming region. At 1200 UTC on the 23rd (Fig 6.25) a well defined, inverted coastal trough is now in place offshore from Georgia to Virginia. Diamond Shoals observation is now indicating winds from a due easterly direction, while those at HAT remain from the north. This would place the coastal front immediately east of HAT and along the coast. Additionally, rainfall has spread northward into southern Virginia as the Gulf low moves into the panhandle of Florida and a warm front approaches the southeast coast.

The coastal front then remains stationary east of HAT until 2100 UTC on the 23rd (Fig. 6.26) when observations at HAT indicate a frontal passage. Although the synoptic warm front has drawn closer to the coast, it does not appear to be responsible for the wind shift. Note that buoy 41001 is also showing an easterly wind instead of the southerly winds expected behind the warm front. The coastal front remains west of HAT until 2300 UTC (not shown) when it retreats eastward as evidenced by the backing of the winds reported at HAT (see Fig. 6.27). From this point onward the coastal front undergoes dissipation as it is overwhelmed by the approaching warm front. The analysis valid at 0600 UTC on the 24th (Fig. 6.28) shows that the warm front has moved into coastal North Carolina, but that a "new" coastal front is now ashore from the Delmarva peninsula to southern New Jersey.

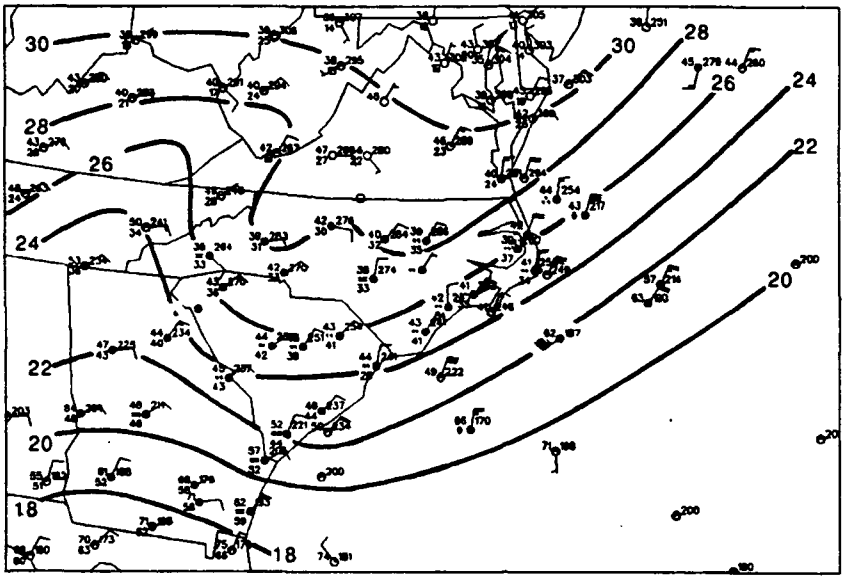

Fig. 6.23. Surface pressure analysis valid at 1800 UTC 22 March 1989.

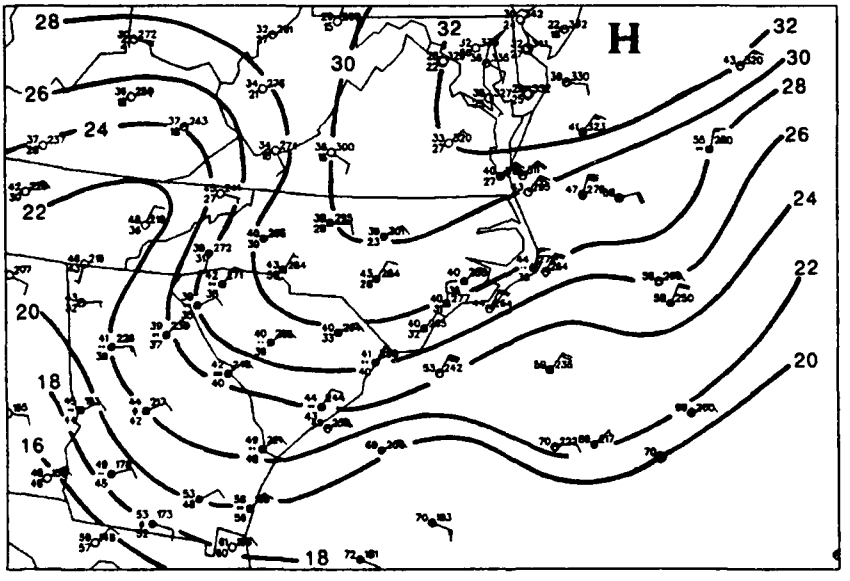

Fig. 6.24. Surface pressure analysis valid at 0600 UTC 23 March 1989.

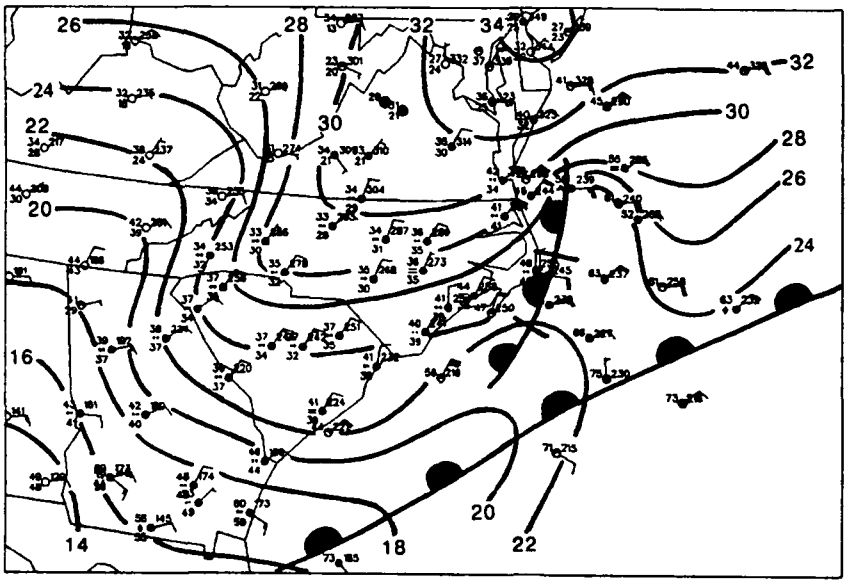

Fig. 6.25. Surface pressure analysis valid at 1200 UTC 23 March 1989.

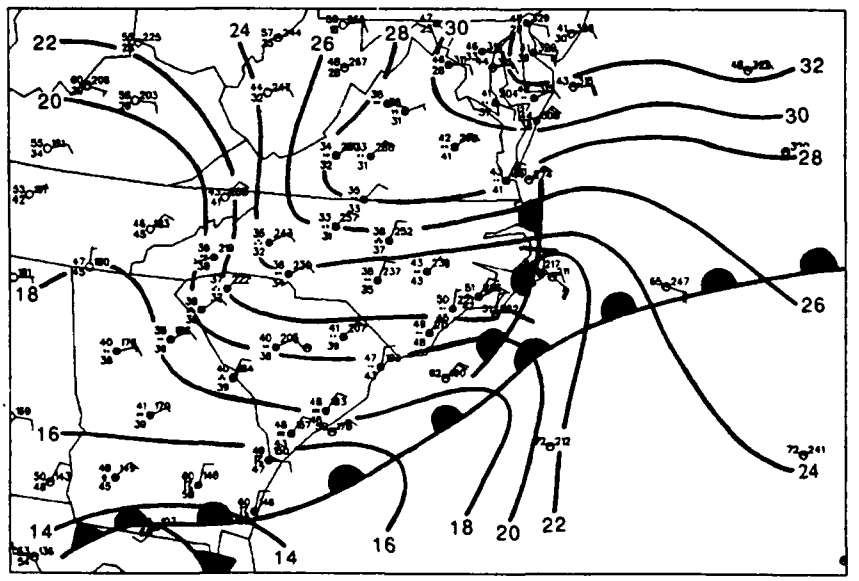

Fig. 6.26. Surface pressure analysis valid at 2100 UTC 23 March 1989.

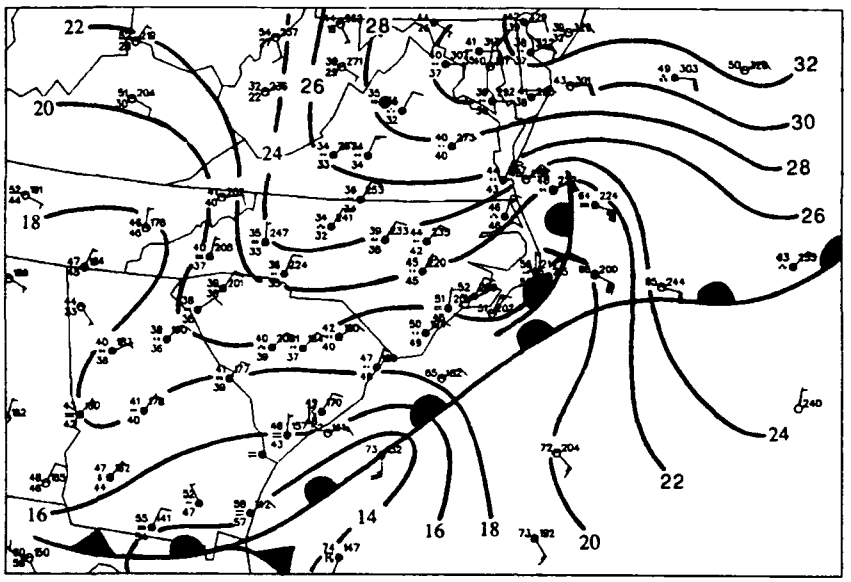

Fig. 6.27. Surface pressure analysis valid at 0000 UTC 24 March 1989.

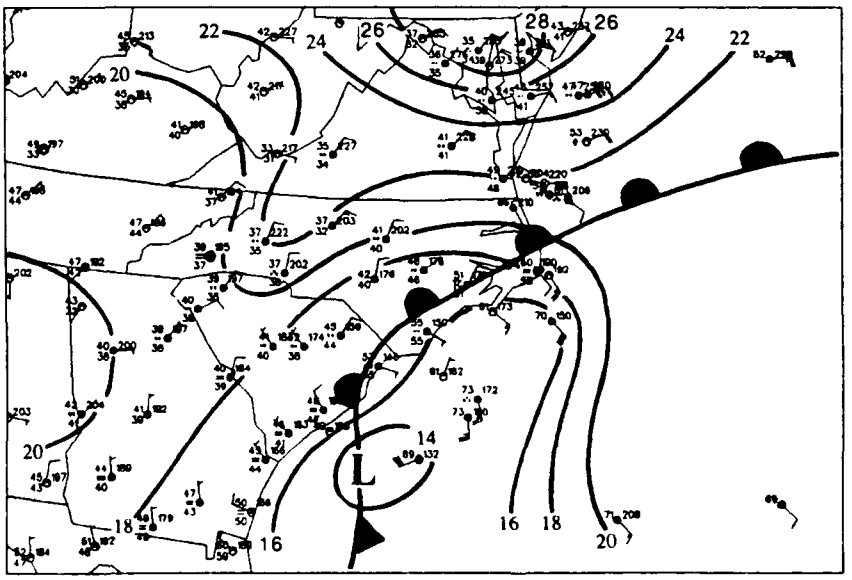

Fig. 6.28. Surface pressure analysis valid at 0600 UTC 24 March 1989.

7. DETERMINING COLD DOME STRENGTH.

7.1. Overview.

In order to test the hypothesis that a relationship exists between the intensity of the damming and the movement of the coastal front, a method was required to illustrate the magnitude of the cold dome. Techniques which depended on a knowledge of the lapse rate (i.e. static stability) were deemed inappropriate due to the poor spatial and temporal resolution of the radiosonde network, as well as the shallowness of the dome itself. Methods involving the quantification of mixing or instability (i.e. Richardson number) were especially undesirable due to doubts cast upon them by density current theory.

Egentowich (1989) had surmised that the westward movement of the front was due to the erosion of the eastern edge of the cold dome through turbulent mixing processes. However, as Nielsen and Neilley (1990) noted, the cold pool is characterized by a low level flow of cold air directed toward the front. Upon reaching the front the air is forced to ascend and mix turbulently with the warm air in the overlying inversion. By this observation, and laboratory simulations of density currents, turbulence and mixing should always be present immediately west of the front in a well developed cold dome. This then would imply that the eastern edge would be continuously eroded, and the front should be constantly moving in an onshore direction. Since coastal fronts have been observed to both stagnate and move seaward, the theory of frontal movement based solely on influences from mixing would not appear to be a valid approach. Density current theory, however, can explain the observed stationary and regressive behavior and would therefore appear to offer a better model of coastal front propagation.

The force balance structure within the dome as examined by Bell and Bosart (1988) lends credence to this argument. Their results showed that a northeasterly LLMPJ formed as a result of the damming, and Nielsen and Neilley (1990) stated that the jet provided a continual influx of cold air which offset losses due to drainage and mixing. It should be obvious then that although mixing must no doubt play a role in the eventual destruction of the cold dome, its effects would not dominate until the damming, and consequently the LLMPJ, begins to weaken. Furthermore, with regard to the work of Nielsen (1989), the eastern edge of the dome, and therefore the coastal front, cannot progress appreciably inland until the damming begins to weaken, the cold dome begins to shrink, and the near-shore winds are flowing normal to the coastline.

Three methods were proposed to objectively resolve the magnitude of cold air damming, 1) a directional analysis of the ageostrophic wind field, 2) a Laplacian analysis of the SLP field, and 3) a measurement of the mountain-parallel pressure differential.

7.2. Ageostrophic Wind Direction.

From the work of Schwerdtfeger (1975) and Bell and Bosart (1988) it is known that one result of damming is a readjustment of the wind field to a highly cross-isobar, mountain-parallel direction. Simply stated, as damming forms and intensifies the winds which are directed toward the mountains at low levels will undergo an increasing deflection to the left (northern hemisphere). In theory then the magnitude of the damming may be illustrated by the degree of wind deflection, or ageostrophy. In order to examine this hypothesis, gridded fields of the surface geostrophic and observed winds were produced through a two pass Barnes objective analysis, afterwhich the

angular difference between the wind vectors was calculated at each grid point. Once plotted and contoured, a time evolution of the charts (see Fig. 7.1 and section 12.2) showed the gradual development of an elongated region of highly ageostrophic winds. This pattern seemed to correspond well with the initial stages of damming. However, once established the areas of greatest ageostrophy became entrenched over the eastern portions of the mountains, and usually remained there regardless of the status of cold air damming.

Unfortunately for the four events examined, there did not appear to be any relationship between the degree of ageostrophy and the movement of the coastal front. In virtually all cases the greatest angular differences occurred over the higher elevations, while those over the coastal plain were usually always less than 60 degrees, a finding which agrees well with Richwein's work (see Richwein, Fig. 10). In other words, agesotrophy simply increases westward and reaches a maximum over the highest elevations.

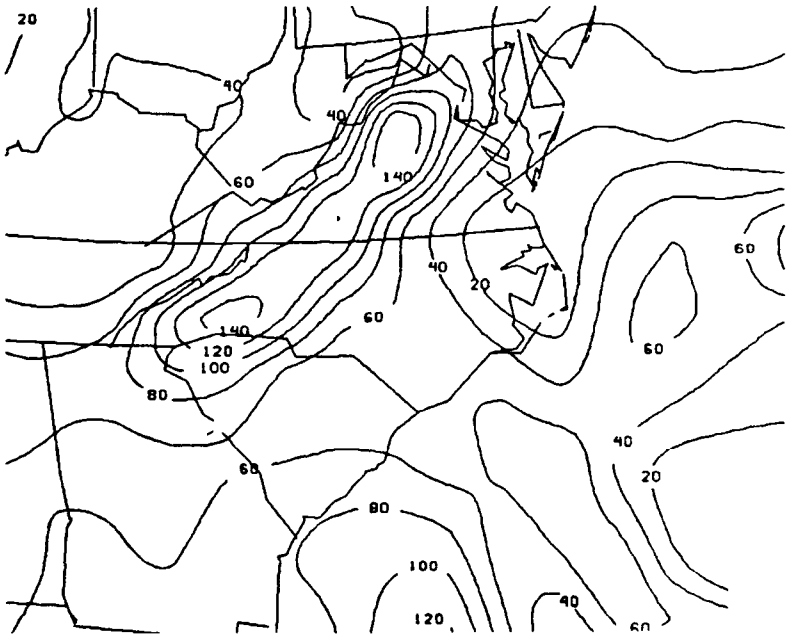

Fig. 7.1 Isopleths of angular difference between geostrophic and observed winds for 1200 UTC, 25 January 1986. Contour interval is 20 degrees.

In a comparison of the two onshore cases it was noticed that landfall could occur during periods of maximum ageostrophy over the mountains, and these large values typically persisted in the region well after the damming event had concluded. Apparently then other factors, such as light and variable winds and complex terrain, are also responsible for the appearance of ageostrophic flow in the damming region. Given these observations it is difficult to guage the magnitude of cold air damming solely by the degree of agesotrophy. Therefore, even though ageostrophy is an attendent feature of damming, it does not appear to have any discernable relationship with coastal front propagation and consequently would not offer any predictive value.

7.3. Laplacian of Surface Pressure.

Baker (1970) stated that the characteristic inverted ridge pattern was simply a reflection of the depth of the cold air trapped against the windward side of the mountains. Since the greatest surface pressures would occur beneath the deepest cold air, and the greatest surface pressure changes should occur outward from these locations, a Laplacian analysis of surface pressure was chosen to illustrate the horizontal dimensions (along with relative maxima and minima), and accordingly the magnitude, of the cold dome. To this end Barnes analyses of the surface pressure field were constructed and Laplacian values were computed at each grid point. Once again a time evolution of the charts depicted a gradually evolving, elongated pattern of contoured values (see Fig. 7.2 and section 12.3). However, unlike the analysis for ageostrophic wind angles, the Laplacian contours were centered not over the mountains, but somewhat east of them over the Piedmont plateau. This particular arrangement suggests that the Laplacian method provides a reasonable illustration of damming magnitude since the cold dome itself resides east of the mountains.

Fig. 7.2 Isopleths of the Laplacian of sea level pressure values for 1200 UTC, 25 January 1986. Values are given in units of mb m^{-2}.

A comparison of the Laplacian field values with surface analyzed positions of the front does hint at a relationship with inland movement. Both of the onshore cases experienced inland propagation of the front when Laplacian values over the Carolinas had increased to values greater than -12×10^{-11} mb m^{-2}, which suggests a possible critical threshold. A similar comparison for the hour of HAT frontal passage, however, does not indicate a relation to Laplacian field values. Movement across HAT occurred with Laplacian values ranging from -8 to -16, intimating that either the effects of the

with Laplacian values ranging from -8 to -16, intimating that either the effects of the cold dome do not reach the outer banks, or that they are negligible at that distance from the mountains.

An attempt at forecasting frontal movement from trends in the Laplacian values did not meet with success. A time series of maximum laplacian values over the Carolinas is shown in Figure 7.3. The traces themselves provide no clues as to which events will see landfall and which will not. Note that the January 1984 case does show steadily increasing Laplacian values from six hours prior to frontal passage at HAT through the end of the event. However, the values for the January 1986 case do not begin increasing until approximately three hours after HAT frontal passage. In comparison, values in the March 1989 case are increasing as early as 12 hours prior to movement across HAT, but the trend then levels off and decreases during the first three hours after frontal passage. Thereafter the values increase as seen for the two onshore events. By contrast, the January 1987 case shows decreasing values up to the time of HAT frontal passage and an increasing trend thereafter, but its values never cross the estimated critical threshold.

The possibility exists that the March 1989 case may have resulted in an onshore event had it not been for the approaching coastal cyclone and synoptic warm front. This may explain the similarity to Laplacian traces for the onshore events, and would serve to reduce the apparent inconsistencies. Nevertheless the fact that onshore movement only occurred with Laplacian values greater than -12×10^{-11} mb m^{-2} (in the March 1989 case, values are above this threshold at approximately the same time as the synoptic warm front is moving onshore) suggests that the method may have predictive value.

One drawback to this method is the method itself, namely the requirement for gridded fields of Laplacian values. While this may yet be a useful tool, the lack of a real time means to employ it would relegate this method to the category of hindcasting. Another troublesome factor is the apparently short lead time, or warning, the method gives before landfall occurs. In both instances of landfall the onshore movement occurs within one

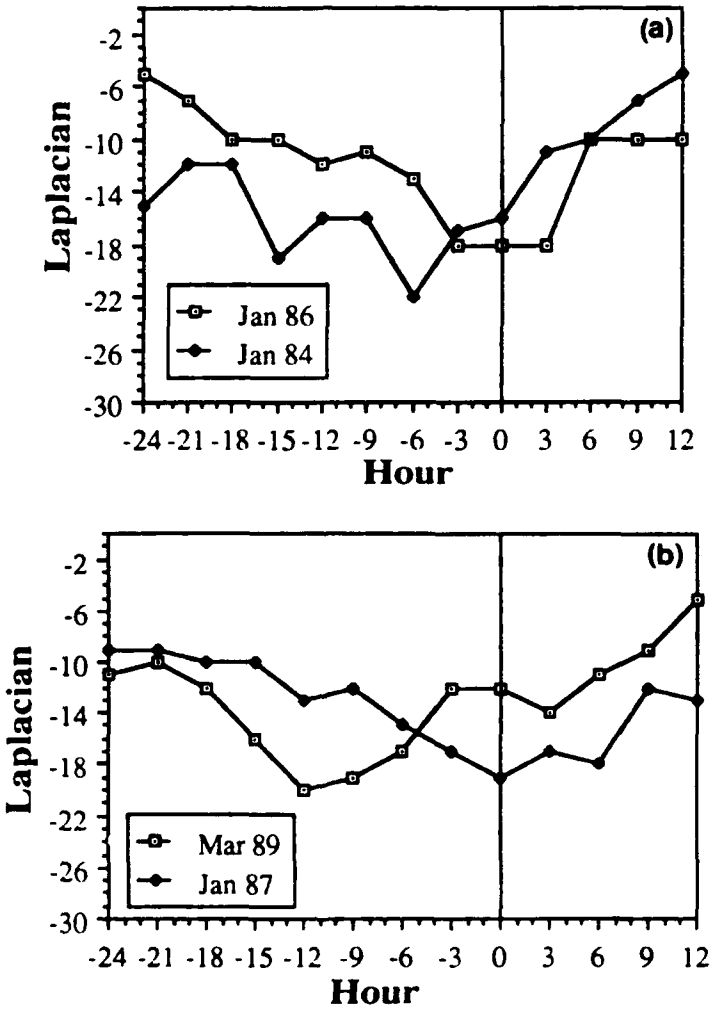

Fig. 7.3. Time series of laplacian values for onshore events (a) and offshore events (b) observed over the Carolinas. Time period covers the 24 hours prior to frontal passage at HAT through the 12 hours which followed. The values are in units of 10^{-11} mb km^{-1}, and represent the maximum value observed in either North or South Carolina.

hour after the values crossed the estimated threshold. Under these scenarios the front was essentially moving onshore as the Laplacian method was just indicating conditions were favorable for inland movement. Once again this would cause the method to act as a response to frontal movement rather than as a forewarning, and would appear to offer no predictive value.

7.4. Mountain Parallel Pressure Differential.

As stated earlier, the classic indication of cold air damming on surface pressure charts is the inverted ridge pattern on the windward side of the blocking terrain. Given the relationship between the depth of the cold air and the surface pressure beneath it, one would expect that as the depth of the cold air increases, the inverted ridge should become more pronounced, i.e. more amplified, and the pressure gradient along the ridge axis should also increase. It was then hypothesized that a simple measurement of the surface pressure differential, Δp, between two points along the axis may provide a quick and simple method to determine damming strength, and that a time series of values might provide indications of whether the damming magnitude was increasing or decreasing. Based upon the Laplacian analysis of the four cases presented, it was determined that the inverted ridge axis was best approximated by a line from Washington, DC to Athens, Georgia. The two points chosen for the measurement were Dulles International Airport (IAD) and Greensboro, North Carolina (GSO) because initial investigations showed that measurements done over greater distances (i.e. to AHN) were subjected to influences from the cyclones which invariably form, or pass through the southeast corner of the United States This resulted in pressure gradient values which were higher than would have been caused by damming alone.

The pressure differential was calculated by simply taking the algebraic difference between the reported surface pressures at IAD and GSO (i.e. IAD minus GSO). Figure 7.4 shows a time series of index values, for all four cases, from 24 hours prior to frontal passage at HAT through the 12 hours which followed. The differences between the onshore and offshore events are immediately evident. Only in the two onshore cases do the differential values decrease steadily for the hours following the frontal passage at HAT. Additionally frontal passage in these two cases occurs at Δp values less than 2.5 mb which may be indicative of the existence of a critical threshold. By contrast the two offshore cases show a steady to rising differential for the same time interval. Although a time series of the maximum Carolina Laplacian values did not indicate a relationship with frontal movement, Fig.7.4 suggests that during onshore events there may be a distinct downward trend in Δp values within six hours of frontal passage at HAT, and perhaps as much as 12 hours prior to landfall. To test whether or not this supposition was true, Δp values for 10 additional onshore and offshore events were plotted and examined (see Fig. 7.5).

Although Fig. 7.4 indicated a clear relationship, the behavior exhibited in Fig. 7.5 appears to be nothing short of chaotic. Upon closer inspection it can be seen that at the time of frontal passage at HAT the Δp values for both groups fall within the range of -0.5 to 8.9 mb. Such a wide range should completely dispell any theory of a critical threshold. It may be possible that, as noted with the Laplacian values, the effects of the cold dome are negligible at such a distance from the blocking terrain. However, remember that by the theory proposed one would expect to see decreasing values for onshore events, and increasing values or perhaps values which decrease at a slower rate for offshore events. Nevertheless, by inspection of the actual data values it becomes apparent that there is virtually no differences between the two groups.

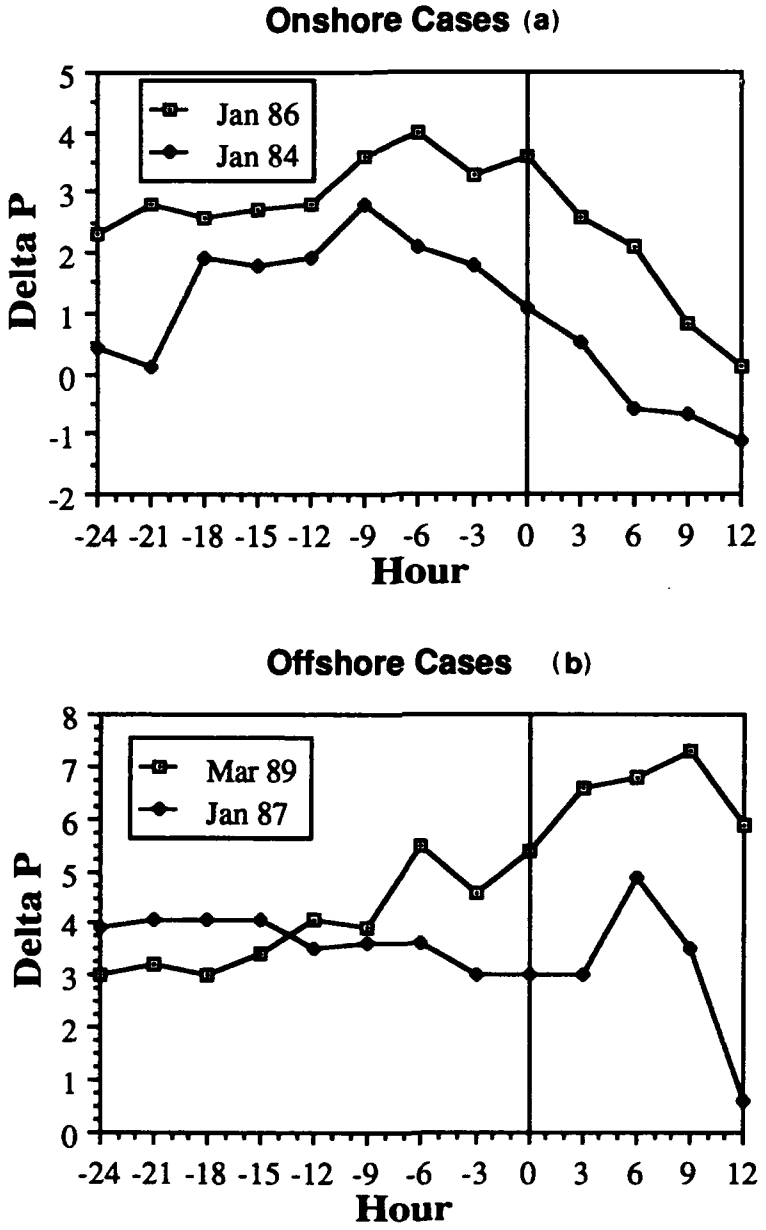

Fig 7.5. Time series of mountain-parallel delta - P values for onshore events (a) and offshore events (b). Time period covered is the same as in figure 7.3.

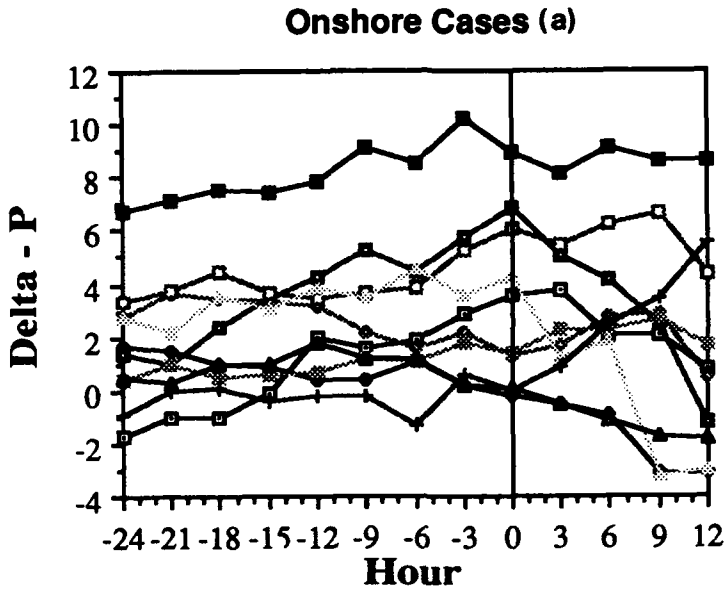

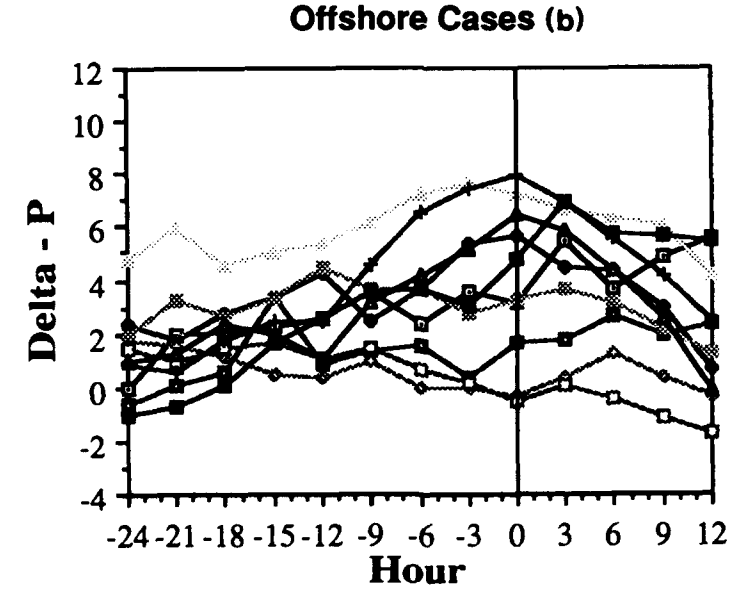

Fig 7.5. Time series of delta - P values for ten additional onshore (a) and offshore (b) events.

During onshore cases the Δp values began decreasing after frontal passage at HAT only five times out of the ten events. One case showed a relatively steady Δp trend, and in the remaining four cases the values actually increased. The results for the offshore cases are just as dubious. For these events the Δp values increased after a frontal passage at HAT in only three of the cases and decreased in the remaining seven.

In regard to the idea that offshore cases may exhibit a slower rate of decreasing Δp values, the following was noted. In the five onshore events which showed decreasing values, four of these began their descent, or were already decreasing by the time of frontal passage at HAT, while the remaining case waited until approximately three hours later. For the offshore events once again four cases were decreasing at or by the time of HAT frontal passage. However the remaining cases waited until either three (2 cases) or six (1 case) hours after frontal passage. Thus, there doesn't appear to be any significant indication of a slower rate of decrease during offshore events.

Finally an examination of the data for the time of onshore movement shows that Δp values range from -0.5 to 8.9 mb, nearly the same interval shown for HAT frontal passage. This is particularly disturbing in view of the fact that Carolina coastal fronts often "stall" in the vicinity of HAT for several hours. Obviously then if there is no significant difference between onshore and offshore phases then this method would appear to be without value. Given the poor results obtained thus far it would seem that either the Laplacian and Δp are simply not representative of the damming magnitude or there is at least one additional variable which has not been accounted for.

8. EFFECTS OF THE LOCAL WINDS.

Recalling that Nielsen's (1989) 1-D model of New England coastal front movement showed an initial dependence on ambient wind direction, streamline analyses of the four cases presented were examined. Nielsen's model indicated onshore movement once the winds were crossing the coast at angles greater than 50 degrees. This, of course, simply shows inland movement to be a consequence of an increasing magnitude of the u component of the wind in the negative x direction (assuming conventional orientation of x-y plane). Building on this then there should be a critical interval of wind directions centered about 90 degrees which would accompany inland migration. Figure 8.1 shows a time series of average maritime wind directions within 200 km of the North Carolina coast for the period 24 hours prior to HAT frontal passage through the 12 hours which followed.

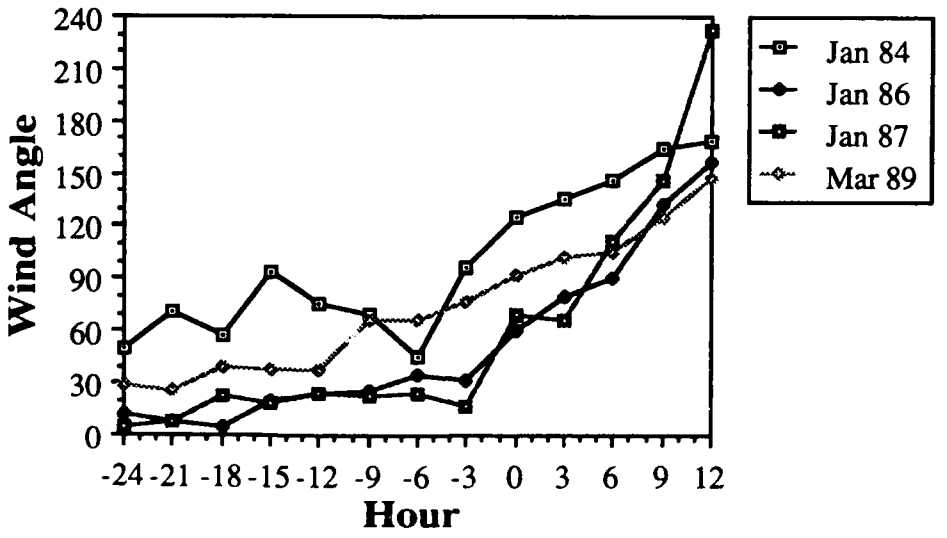

Fig. 8.1. Time series of average onshore wind angles off the coast of North Carolina for onshore and offshore events. Time period covers the 24 hours prior to frontal passage at HAT through the 12 hours which f( )wed.

It can be seen that frontal passage at HAT occured with average wind angles ranging from 55 to 125 degrees, and in the two onshore cases landfall occurred with wind angles of 90 and 135 degrees. Figures 8.2 through 8.5 show a comparison of the wind angles with the laplacian of SLP and mountain-parallel pressure differential values. In the comparisons with the Laplacian it can be seen that, during onshore events, wind directions greater than 50 degrees and Laplacian values greater than -12×10^{-11} mb m^{-2} do not coincide until one hour prior to landfall. A similar comparison for offshore events shows that for the March 1989 case the two values are not within the specified region until at least five hours after frontal passage at HAT. At that point the coastal front was already being overwhelmed by an approaching warm front. In the January 1987 case the winds begin flowing from a favorable direction one hour prior to frontal passage at HAT, but the Laplacian values never climb above the estimated critical value of -12×10^{-11} mb m^{-2}. A review of the comparison between wind direction and mountain-parallel Δp only yields mixed results. In the January 1986 case, landfall occurs two hours after the wind direction and the Δp values reach favorable values. However by the same standards, the January 1984 case achieved favorable values four hours prior to the last HAT frontal passage, or seven hours before the front made landfall. An attempt to equate the magnitude of the winds and onshore movement in all four cases proved to be unavailing. Results based upon only four cases cannot be considered conclusive, however in the four cases investigated the incorporation of onshore wind direction does not improve the already weak performance of the Laplacian and ΔP methods.

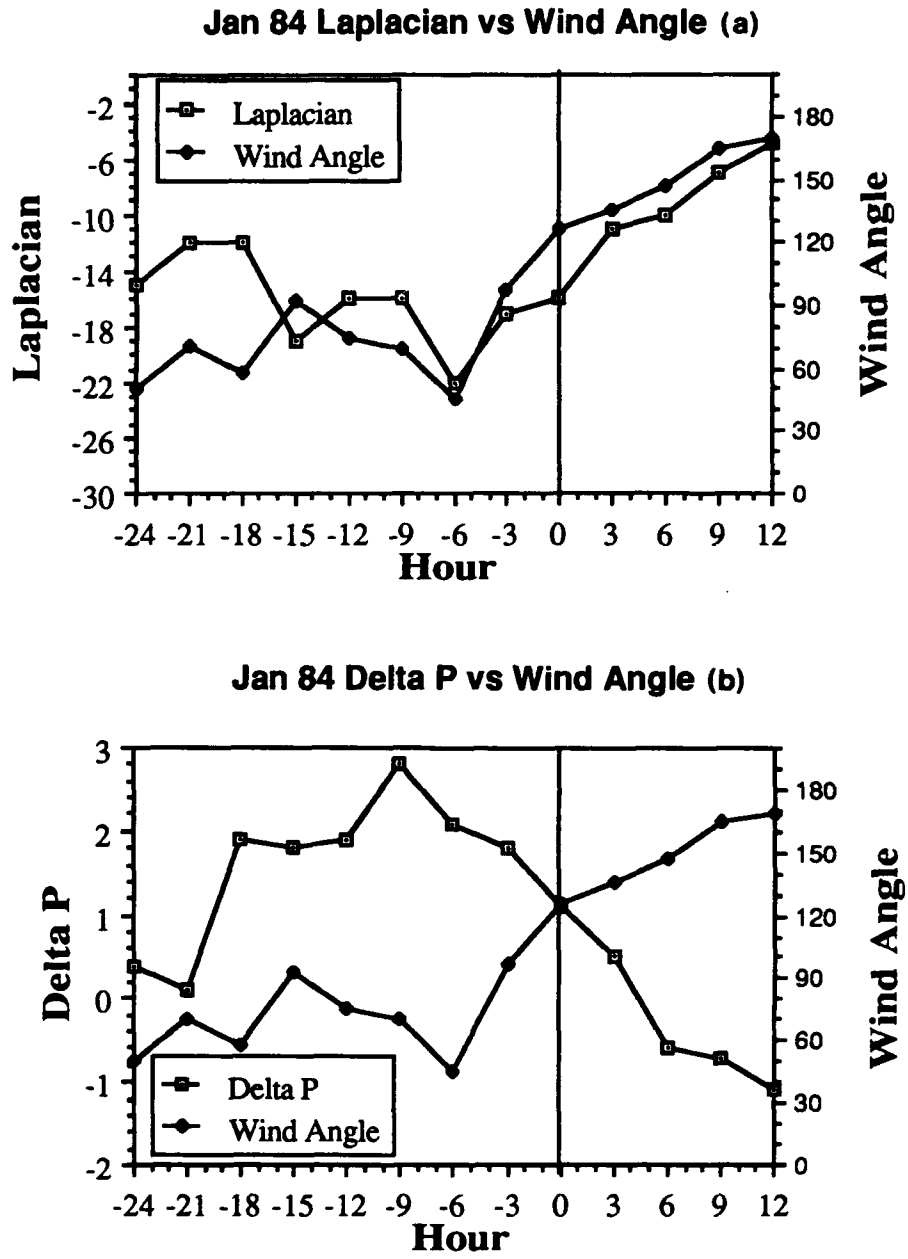

Fig. 8.2. Comparison of onshore wind angles with maximum laplacian values (a), and mountain-parallel ΔP values (b) for the 24 Jan 84 onshore event. Time period covered is the same as in figure 8.1.

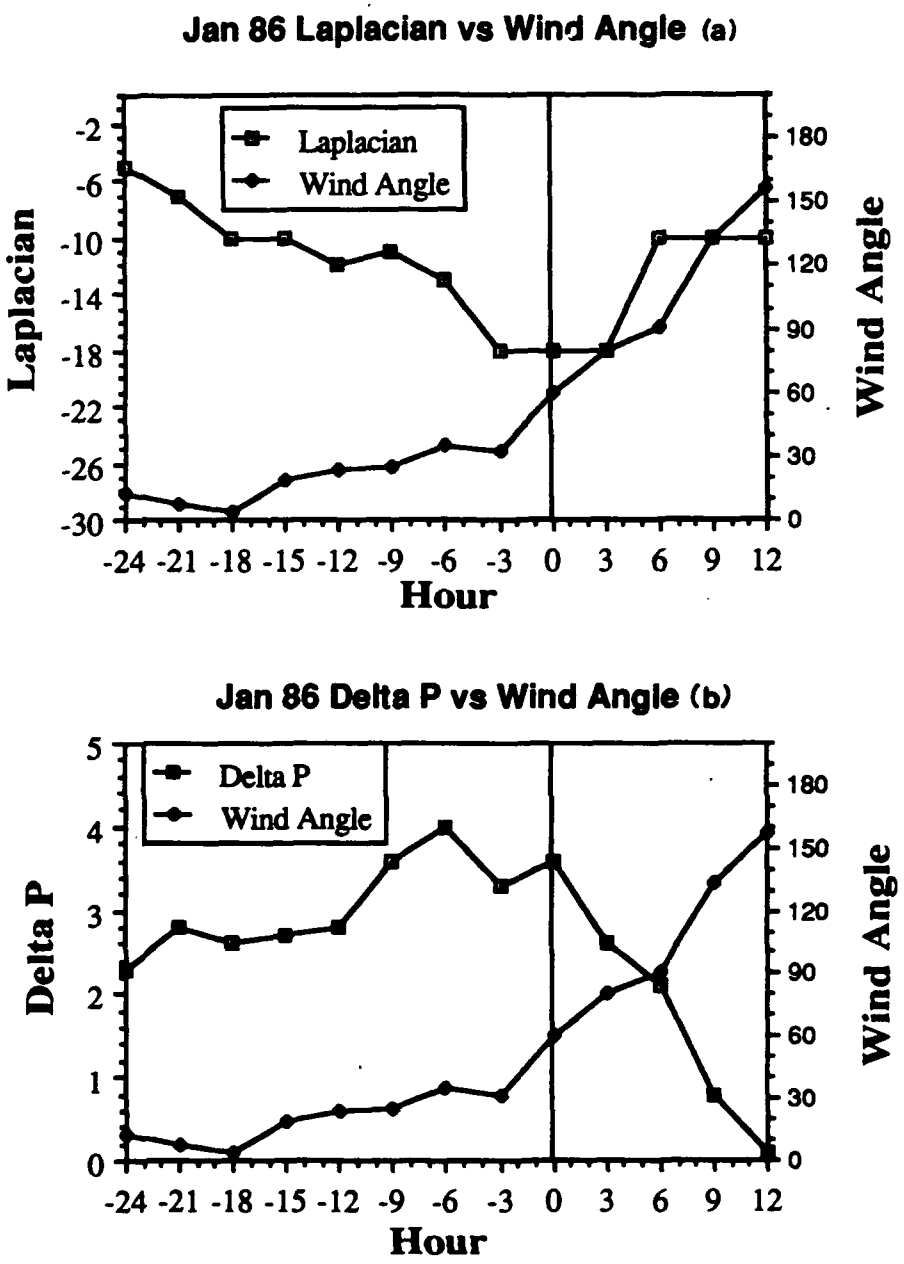

Fig. 8.3. Comparison of onshore wind angles with maximum laplacian values (a), and mountain-parallel ΔP values (b) for the 25 Jan 1986 onshore event. Time period covered is the same as in figure 8.1.

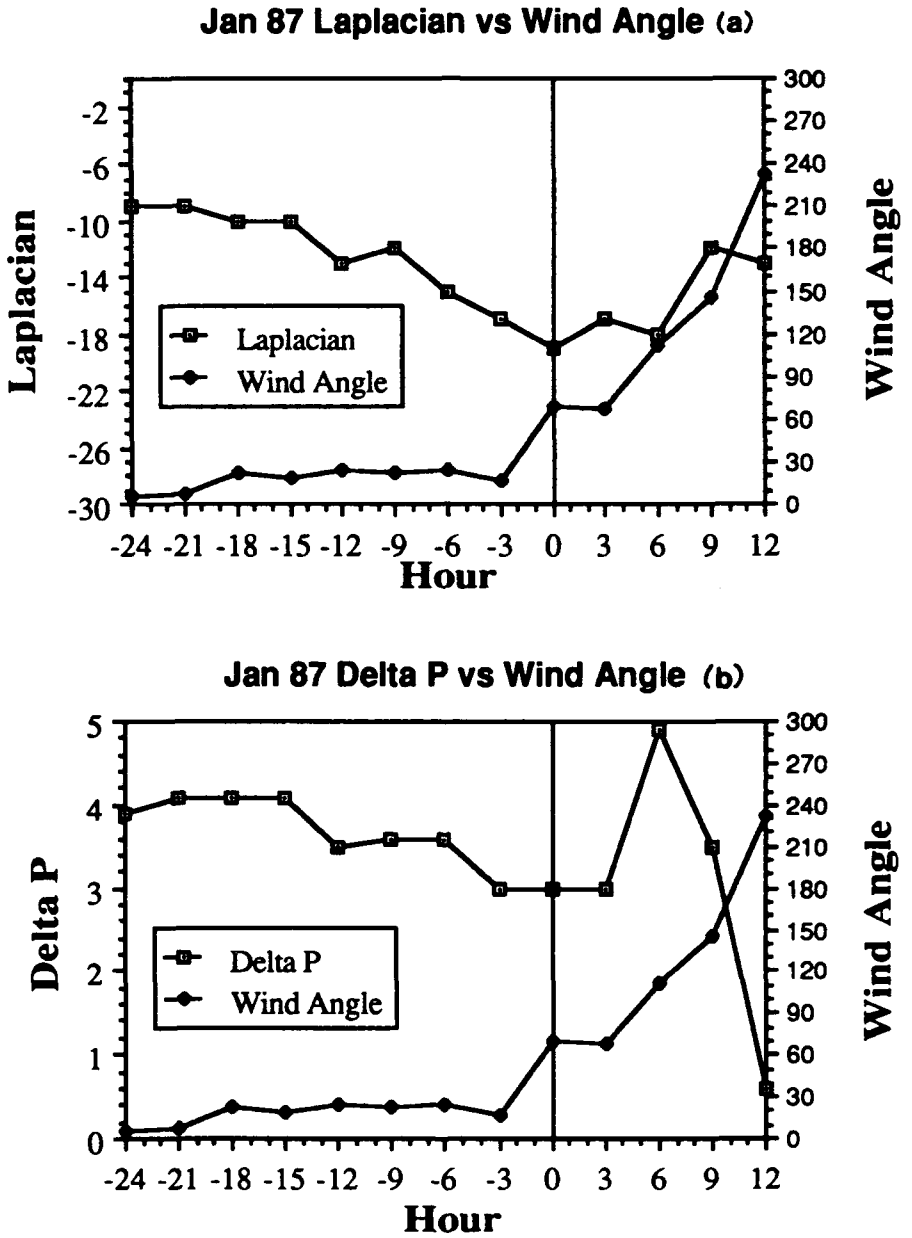

Fig. 8.4. Comparison of onshore wind angles with maximum laplacian values (a), and mountain-parallel ΔP values (b) for the 18 Jan 1987 offshore event. Time period covered is the same as in figure 8.1.

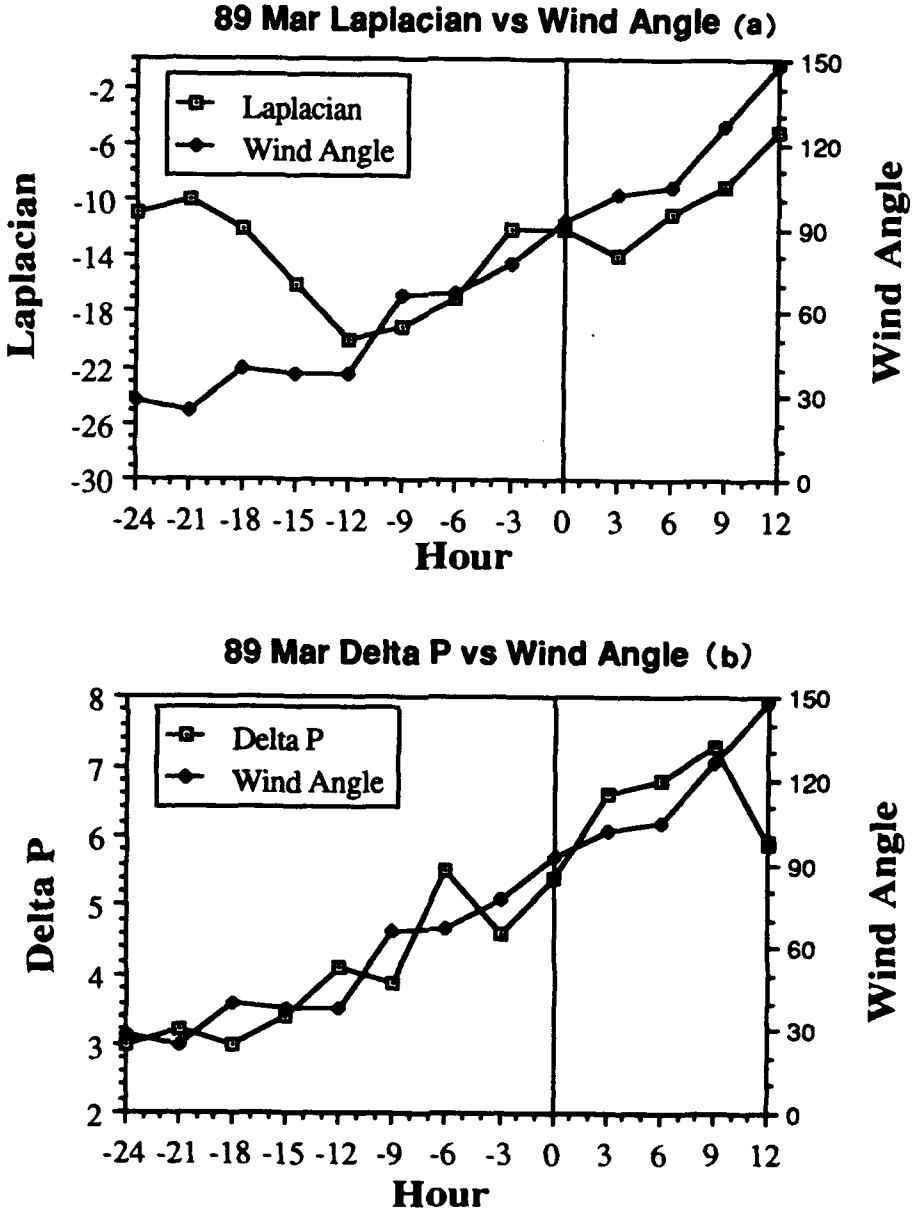

Fig. 8.5. Comparison of onshore wind angles with maximum laplacian values (a), and mountain-parallel ΔP values (b) for the 23 Mar 1989 offshore event. Time period covered is the same as in figure 8.1.

9. SUMMARY AND CONCLUSIONS.

Fifty one Carolina coastal front cases, spanning 15 years, were examined in terms of their ambient pressure and wind fields, in the hopes that an objective forecasting method could be devised based upon careful observation of conditions within the damming area. Climatological analyses for monthly occurrences and onshore hour frequency were comparable to the results found by Anderson (1991). Examination of terminal onshore positions of 35 coastal fronts suggests that in the absence of forcing by coastal cyclones, Carolina coastal fronts tend to stagnate along an axis from Hampton, Virginia to Myrtle Beach, South Carolina, passing through the vicinity of Goldsboro, North Carolina. Such a finding is analagous to a stagnation line found by Bosart (1972) for New England coastal fronts.

The construction of hemispheric composite and climatic deviation charts yielded some curious results. Although no true gauge of their significance is available, the cases, when divided into onshore (35 cases) and offshore (16 cases) groups, suggested that particular variations in the positioning, and perhaps strength of synoptic scale pressure features may accompany the onshore and offshore behavior of the front. Specifically the charts appeared to bear out the supposition that onshore movement is preceded by a weakening in the magnitude of damming against the mountains. These results may simply be a reflection of a slower moving anticyclone during offshore events. This would be consistent with stronger, or more persistent damming, and in itself may prove significant. However it must be emphasized that the results are possibly just an aberration arising from too small a sample size. Only in a much more comprehensive climatic study can this issue be properly addressed.

Three methods were explored to objectively measure the strength of the damming and proved to be unsuccessful. Analyses of the wind fields showed that increasingly ageostrophic wind angles did coincide with the initial stages of damming. However, the maximum values always resided in the mountains and usually showed highly ageostrophic directions well after it was evident, by SLP analysis, that the damming event was subsiding or had concluded. The persistence of the ageostrophy appears to be equally attributable to influences in addition to damming, such as light and variable winds, and complex terrain. Stated simply then, the analysis of ageostrophic wind angles was a good indicator of the presence cross-contour flow, but not neccessarily of damming.

Laplacian analysis of the SLP initially seemed to offer a good indicator of damming strength. Contoured values appeared and diminished in good agreement with the inverted ridge pattern. Comparisons with four cases suggested that inland migration of the front occurred when the maximum Lapacian value over the Carolinas increased to values greater than -12×10^{-11} mb m^{-2}. However, when comparing Laplacian values and the location of the front, it was discovered that the front moved inland at approximately the same time the Laplacian values first reached the estimated favorable levels. Thus the method was flawed by a lack of forewarning. The examination of a mountain-parallel pressure differential ostensibly offered a simpler method of discerning the cold dome magnitude and fronts' intentions; however an expanded analysis showed virtually no difference between values for onshore and offshore events.

Due to the poor results with the two pressure methods, an attempt was made to correlate their behavior with onshore maritime wind angles and frontal movement. A comparison between Laplacian values and the streamline angles found that although the

winds could be at favorable values one to five hours prior to a HAT frontal passage, onshore movement still did not occur until the Laplacian values increased through the estimated threshold. The same comparison for the two offshore cases showed that while the winds reached favorable values at one to eleven hours prior to HAT frontal passage, the Laplacian value either did not cross the critical threshold (January 1987) or waited until approximately five hours after fronal passage at HAT (March 1989). The comparison between wind angles and mountain-parallel pressure differential was also disappointing since it did nothing to improve the already dismal performance, and offered no explanation why the fronts often wait so long before moving onshore.

In the search for reasons as to why the proposed pressure methods failed two explanations are immediately plausible. First the mountain-parallel pressure differential, while easier to compute and monitor, is perhaps not as indicative of damming strength since it is only a one-dimensional estimation of a three-dimensional phenomenon. The Laplacian, although a two dimensional method, may only be a good indicator of the presence of damming but not sensitive enough to monitor its intensity. Secondly, damming strength and onshore wind angles may merely be neccessary but not sufficient conditions for inland movement. Other factors, such as coastal cyclones, and precipitation within the cold dome, may play some role in determining whether a front moves onshore or not. It was noted that coastal cyclones appeared to have no significant influence on the final inland position of coastal fronts. However, although coastal cyclones were observed in nine of the 35 cases of onshore events (26%), a coastal cyclone was present, at some point, in all 16 of the offshore cases. This recalls Bosart's (1975) classification of fronts in terms of advancing cyclones, and bears further inspection for the Carolinas.

10. SUGGESTIONS FOR FUTURE RESEARCH.

It is recommended that any pursuit of a Laplacian method should involve an attempt to use model output data to produce forecasted Laplacian fields. Depending upon the accuracy of the data, this might solve the short lead-time problem shown by this method. Also future attempts may benefit from the incorporation of data from aloft (i.e. sounding data, upper level vorticity patterns, etc) if available from intense experiments, such as GALE, and provided it does not suffer from the usual poor spatial and temporal resolution. Similarly attempts to locate, measure, and monitor the LLMPJ may be beneficial since a decrease in the supply of cold air to the dome should be an important precursor to the dissipation of the dome itself. However, the same conditions as with the upper level data would apply.

Barring the continuation of the methods examined here, it is suggested that any future review of coastal front cases over the Carolinas should include a reclassification of each front in terms of formation mechanism (cold air damming, coastal cyclone, etc.), type of event (onshore or offshore), and other database type information such as formation/dissipation time, time of HAT frontal passage, and landfall time. A first step in such an undertaking should be the formulation of a new objective definition of a Carolina coastal front event. Anderson's (1991) method is probably the most definitive available, but future attempts should avoid the dependence on a single offshore station. Also a stricter definition of what constitutes an onshore and offshore event is needed. The current study favors the evidence of frontal passage at mainland stations, however as was pointed out this is an imperfect system since those sites are located a considerable distance from the mainland coast.

Additionally, it has become obvious from this research that synoptic scale cyclones, either over land or offshore, exert an influence on the behavior of the coastal fronts. That is to say it has been the authors' observation that a cyclone in the vicinity of the coastal front either "pushes" it ashore, "pulls" it offshore, or simply destroys it altogether. Any forecasting method, and/or future review of cases would do well to pay attention to this fact and incorporate it accordingly.

Perhaps the most intriguing outcome of this research was the suggestion that specific synoptic pressure patterns might be associated with onshore and offshore events. It is quite possible that these findings are merely the result of too small a sample size. Of the 51 cases considered only 16 were offshore events, thus the sample size is significantly less than would be desired for a true statistical investigation. However the total number of known Carolina coastal front events currently numbers 186 (for the period 1975 - 1989), and this would provide a sufficiently large enough data base to undertake a more in-depth investigation. Once a review was accomplished a true determination of synoptic pattern dependence should be possible through the grouping of events by the various parameters and examination with the aid of tools such as the NMC CD ROM program.

11. REFERENCES.

Anderson, J. T., 1991: Carolina coastal fronts: a case study, climatology, and simple prediction scheme. M.S. Thesis, Dept. of Marine, Earth, and Atmospheric Sciences, North Carolina State University, Raleigh, NC, 67 pp.

Ballentine, R. J., 1980: A numerical investigation of New England coastal frontogenesis. *Mon. Wea. Rev.*, **108**, 1479-1497.

Barnes, S. L., 1964: A technique for maximizing details in numerical weather map analysis. *J. Appl. Meteor.*, **3**, 396-409.

Baker, D. G., 1970: A study of high pressure ridges to the east of the Appalachian Mountains. Ph.D. Thesis, Dept of Meteorology, Massachusetts Institute of Technology, Cambridge, MA, 127 pp.

Bell, G. D., and L. F. Bosart, 1988: Appalachian cold air damming. *Mon. Wea. Rev.*, **116**, 137-161.

Benjamin, T. B., 1968: Gravity currents and related phenomena. *J. Fluid Mech.*, **31**, 209-248.

Bosart, L. F., C. J. Vaudo and J. H. Helsdon, Jr., 1972: Coastal frontogenesis. *J.Appl. Meteor.*, **11**, 1236-1258.

____, 1975: New England coastal frontogenesis. *Quart. J. Roy. Meteor. Soc.*, **101**, 957-978.

____, 1981: The president's day snowstorm of 18-19 February 1979: A subsynoptic scale event. *Mon. Wea. Rev.*, **109**, 1542-1566.

____, and S. C. Lin., 1984: A diagnostic analysis of the president's day storm of February 1979. *Mon. Wea. Rev.*, **112**, 2148-2177.

Carson, R. B., 1950: The Gulf Stream front: A cause for stratus on the lower Atlantic coast. *Mon. Wea. Rev.*, **78**, 91-100.

Dunic,R. L., 1989: A method for correcting and reducing the pressure data recorded at the PAM II stations during GALE. M.S. Thesis, Dept. of Marine, Earth, and Atmospheric Sciences, North Carolina State University, Raleigh, NC, 72 pp.

Dunn, L., 1987: Cold a . damming by the front range of the Colorado Rockies and its relationship to locally heavy snows. *Wea. Forecasting*, **2**, 177-189.

Egentowich, J. M., 1989: Inland evolution of the coastal front during IOP-2, 25 January 1986. M.S. Thesis, Dept. of Marine, Earth, and Atmospheric Sciences, North Carolina State University, Raleigh, NC, 92 pp.

Forbes, G. S. , R. A. Anthes and D. W. Thomson, 1987: Synoptic and mesoscale aspects of an Appalachian ice storm associated with cold air damming. *Mon. Wea.Rev.* **115**, 564-591.

Huang, C. Y., 1990: A mesoscale planetary boundary layer numerical model for simulations of topographically induced circulations. Ph.D. dissertation, Dept. of Marine, Earth, and Atmospheric Sciences, North Carolina State University, Raleigh, NC, 253 pp

Marks, F. D., Jr., and P. M. Austin, 1979: Effects of the New England coastal front on the distribution of precipitation. *Mon. Wea. Rev.*, **107**, 53-67.

Mitsumoto, S., H. Ueda and H. Ozoe, 1983: A laboratory experiment on the dynamics of the land and sea breeze. *J. Atmos. Sci.*, **40**, 1228-1240.

Musick, D. R., 1991: A case study of a prolonged sleet event: 16-17 Feb, 1987 and a climatology of sleet events for North Carolina, 1949-1989. M.S. Thesis, Dept. of Marine, Earth, and Atmospheric Sciences, North Carolina State University, Raleigh, NC, 73 pp.

Neilley, P. P., 1984: Application of a density current model to aircraft observations of the New England coastal front. M.S. thesis, Department of Meteorology, Massachusetts Institute of Technology, Cambridge, MA, 64 pp.

Nielsen, J. W., 1989: The formation of New England coastal fronts. *Mon. Wea. Rev.*, **117**, 1380-1401.

____, and P. P. Neilley, 1990: The vertical structure of New England coastal fronts. *Mon. Wea. Rev.*, **118**, 1793-1807.

Parish, T. R., 1982: Barrier winds along the Sierra Nevada Mountains. *J. Appl. Meteor.*, **21**, 925-930.

Pielke, R. A., and J. M. Cram, 1987: An alternate procedure for analyzing surface geostrophic winds and pressure over elevated terrain. *Wea. Forecasting*, **2**, 229-236.

Pierrehumbert, R. T., and B. Wyman, 1985: Upstream effects of mesoscale mountains. *J. Atmos. Sci.*, **42**, 977-1003.

Raman, S., and A. J. Riordan, 1988: The Genesis of Atlantic Lows Experiment: The planetary boundary layer subprogram of GALE. *Bull. Amer. Meteor. Soc.*, **69**, 482-491.

Richwein, B. A., 1980: The damming effect of the southern Appalachians. *Natl. Wea. Dig.*, **5**(1), 2-12.

Riordan, A. J., 1990: Examination of the mesoscale features of the GALE coastal front of 24-25 January 1986. *Mon. Wea. Rev.*, **118**, 258-282.

Sanders, F., 1983: Observations of fronts. Mesoscale meteorology - Theories, Observations, and Methods. D. K. Lilly, T. Gal-Chen, Eds., D. Reidel, 175-203.

____, 1955: An investigation of the structure and dynamics of an intense surface frontal zone. *J. Meteor.*, **12**, 542-553.

Schwerdtfeger, W., 1975: The effect of the Antarctic Peninsula on the temperature regime of the Weddell Sea. *Mon. Wea. Rev.*, **103**, 45-51.

Simpson, J. E., 1969: A comparison between laboratory and atmospheric density currents. *Quart. J. Roy. Meteor. Soc.*, **95**, 758-765.

____, 1982: Gravity currents in the laboratory, atmosphere, and ocean. *Ann. Rev. Fluid Mech.*, **14**, 213-234.

____, and R. E. Britter, 1980: A laboratory model of an atmospheric mesofront. *Quart. J. Roy. Meteor. Soc.*, **106**, 485-500.

Wallace, J. M., and P. V. Hobbs, 1977: Atmospheric Science. An Introductory Survey. Academic Press. Orlando, Florida.

Xu, Q., 1990: A theoretical study of cold air damming. *J. Atmos. Sci.*, **47**, 2969-2985.

Young, G. S. and J. M. Fritsch, 1989: A proposal for general conventions in analysis of mesoscale boundaries. *Bull Amer. Meteor.* Soc., **70**, 1412-1421.

12. APPENDICES.

12.1. Cases Examined.

The following is a list of the selected Carolina coastal front cases used in this research. The cases are divided into onshore and offshore events as determined by the date and the approximate hour (UTC) of frontal passage at Cape Hatteras, North Carolina. Onshore cases denoted by an asterisk (*) represent cases whose terminal inland position was suspected of being influenced by the presence of a coastal cyclone. Those cases marked with a plus symbol (+) are cases which were not included in the composite analysis provided by the CD ROM program due to incomplete data.

12.1.1. Onshore Cases.

1. 12 Jan 1989 / 0300.*
2. 15 Jan 1989 / 0000.
3. 19 Feb 1988 / 1200.*
4. 01 Nov 1988 / 0000.
5. 19 Nov 1988 / 1500.
6. 28 Feb 1987 / 1200.
7. 25 Jan 1986 / 0500.
8. 02 Nov 1986 / 0300.
9. 20 Nov 1986 / 1500.*
10. 23 Nov 1986 / 2100.
11. 02 Dec 1986 / 0000.
12. 23 Dec 1986 / 1800.*
13. 24 Jan 1984 / 0900.
14. 03 Mar 1984 / 1200.*
15. 10 Jan 1983 / 0000.*
16. 22 Jan 1983 / 1500.*
17. 05 Jan 1983 / 0300.*
18. 12 Dec 1983 / 0000.*+
19. 03 Jan 1982 / 1500.*
20. 13 Jan 1982 / 1800.*
21. 03 Feb 1982 / 0000.
22. 28 Nov 1982 / 1500.*

23. 14 Dec 1981 / 1800.
24. 11 Jan 1980 / 0300.*
25. 13 Mar 1980 / 0600.*
26. 17 Nov 1980 / 1800.
27. 03 Nov 1977 / 0900.*
28. 06 Dec 1976 / 1800.+
29. 07 Jan 1976 / 1200.*
30. 18 Jan 1975 / 0600.*
31. 04 Feb 1975 / 0000.
32. 22 Feb 1975 / 2100.*
33. 18 Mar 1975 / 2100.
34. 25 Dec 1975 / 1800.*
35. 30 Dec 1975 / 1500.*

12.1.2 Offshore Events.

1. 03 Mar 1989 / 0300.
2. 23 Mar 1989 / 2100.
3. 08 Jan 1988 / 0300.
4. 23 Nov 1988 / 0300.
5. 18 Jan 1987 / 0600.
6. 15 Nov 1986 / 0600.
7. 10 Jan 1985 / 1500.
8. 01 Mar 1985 / 1500.
9. 22 Mar 1985 / 1500.
10. 06 Feb 1983 / 1800.
11. 13 Jan 1980 / 1500.
12. 27 Nov 1980 /1500.
13. 28 Dec 1980 / 0000.
14. 01 Nov 1979 / 0000.
15. 13 Jan 1978 / 0600.
16. 11 Feb 1975 / 0300.

12.2. Time Evolution of Ageostrophic Wind Angles.

This section provides a time series of the evolution of the angular difference between the objectively analyzed geostrophic and observed surface winds. The result is the departure from geostrophy (i.e. agesotrophic wind angle with respect to north) in degrees. The analyses shown in figures 12.1 to 12.8 are from the 25 January 1986 GALE case, and are representative of other onshore cases examined.

Fig. 12.1. Analysis of ageostrophic wind angles (in degrees) valid at 0600 UTC 24 January 1986. Contour interval is 20 degrees.

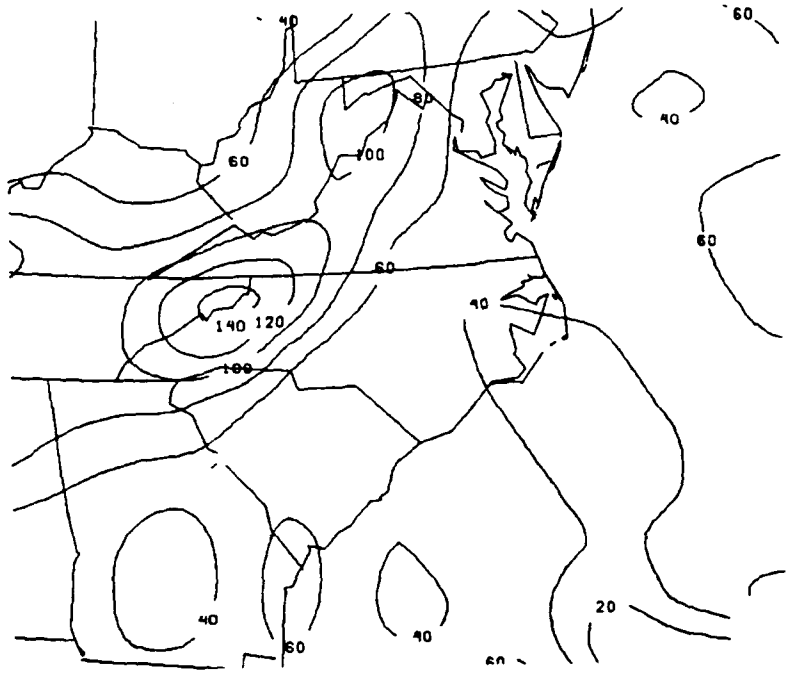

Fig. 12.2. Analysis of ageostrophic wind angles (in degrees) valid at 1200 UTC 24 January 1986. Contour interval is 20 degrees.

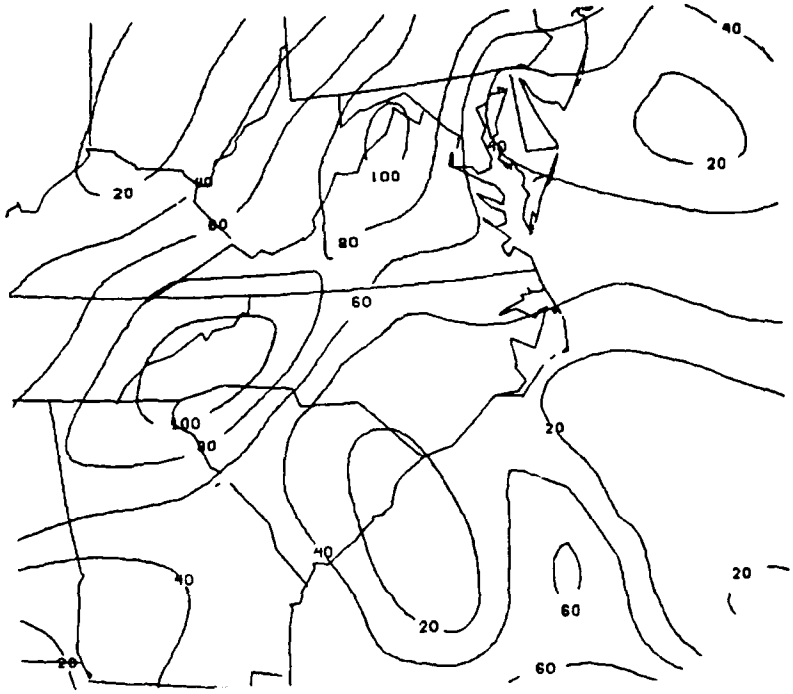

Fig. 12.3. Analysis of ageostrophic wind angles (in degrees) valid at 1800 UTC 24 January 1986. Contour interval is 20 degrees.

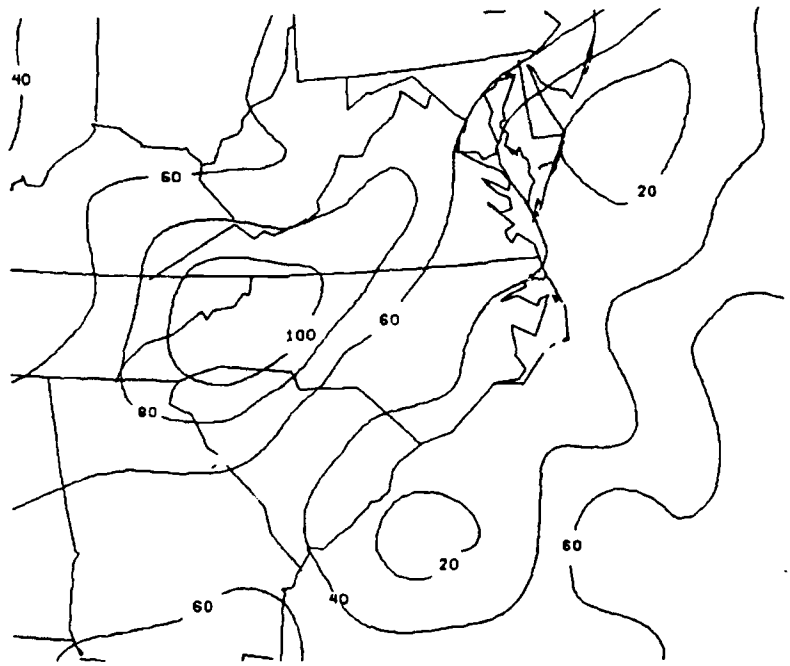

Fig. 12.4. Analysis of ageostrophic wind angles (in degrees) valid at 0000 UTC 25 January 1986. Contour interval is 20 degrees.

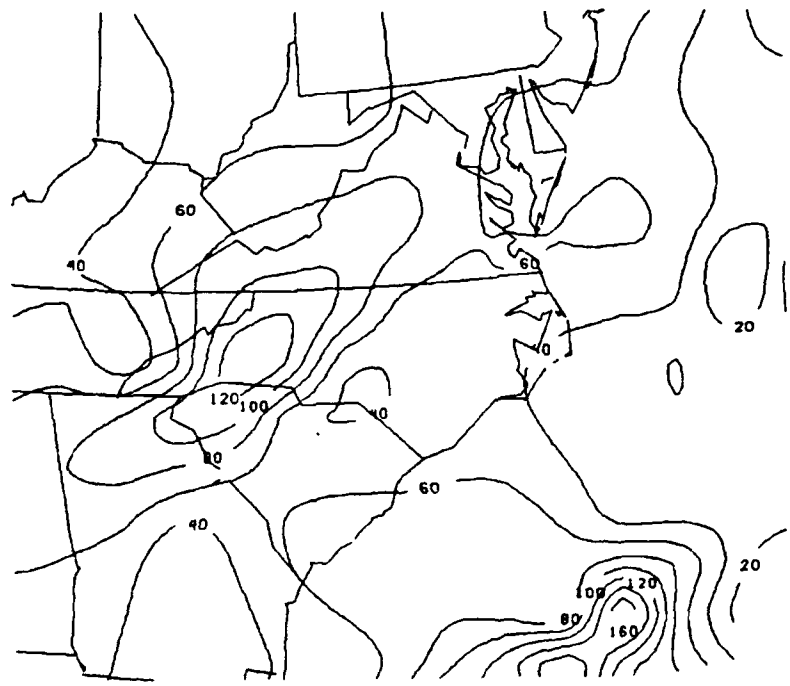

Fig. 12.5. Analysis of ageostrophic wind angles (in degrees) valid at 0600 UTC 25 January 1986. Contour interval is 20 degrees.

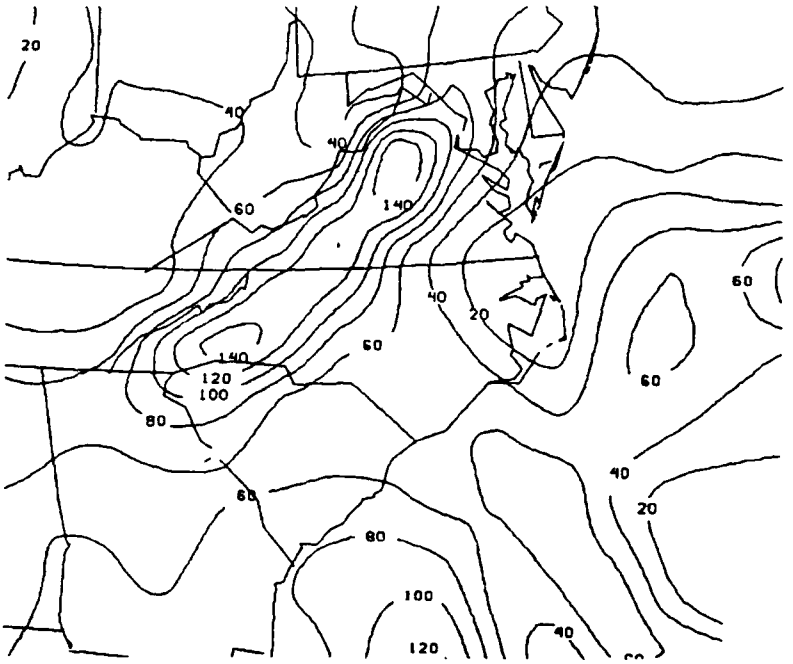

Fig. 12.6. Analysis of ageostrophic wind angles (in degrees) valid at 1200 UTC 25 January 1986. Contour interval is 20 degrees.

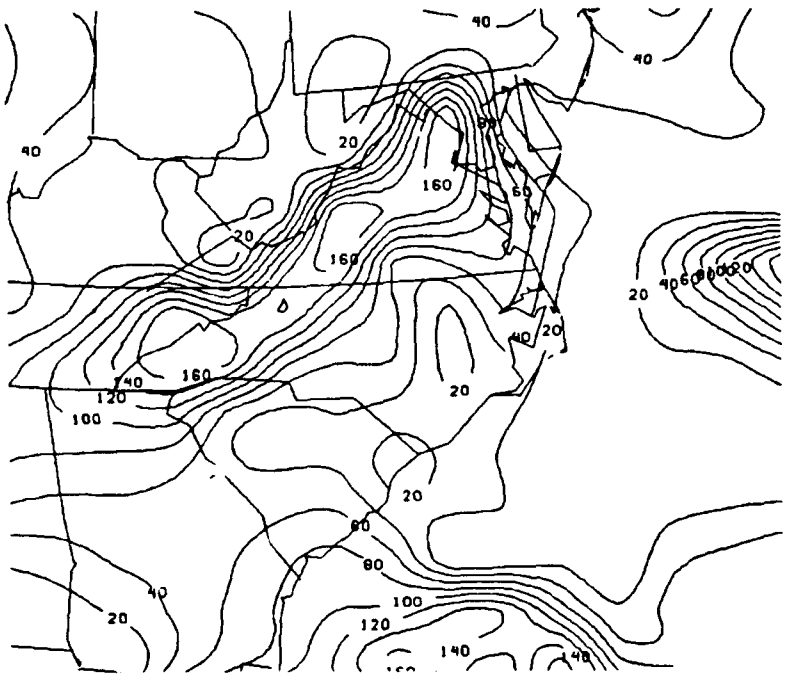

Fig. 12.7. Analysis of ageostrophic wind angles (in degrees) valid at 1800 UTC 25 January 1986. Contour interval is 20 degrees.

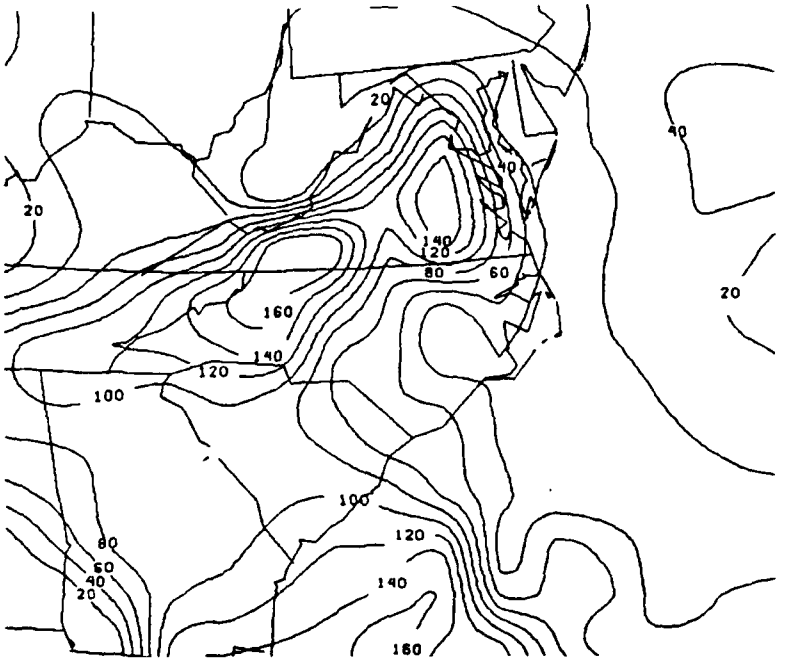

Fig. 12.8. Analysis of ageostrophic wind angles (in degrees) valid at 2100 UTC 25 January 1986. Contour interval is 20 degrees.

12.3. Time Evolution of the Laplacian of Sea Level Pressure.

This section provides a time series of the evolution of the objectively analyzed Laplacian of sea level pressure. The analyses shown in figures 12.9 to 12.16 are from the 25 January 1986 GALE case and are representative of other onshore cases examined. To avoid visual clutter, only the negative values of the Laplacian are shown.

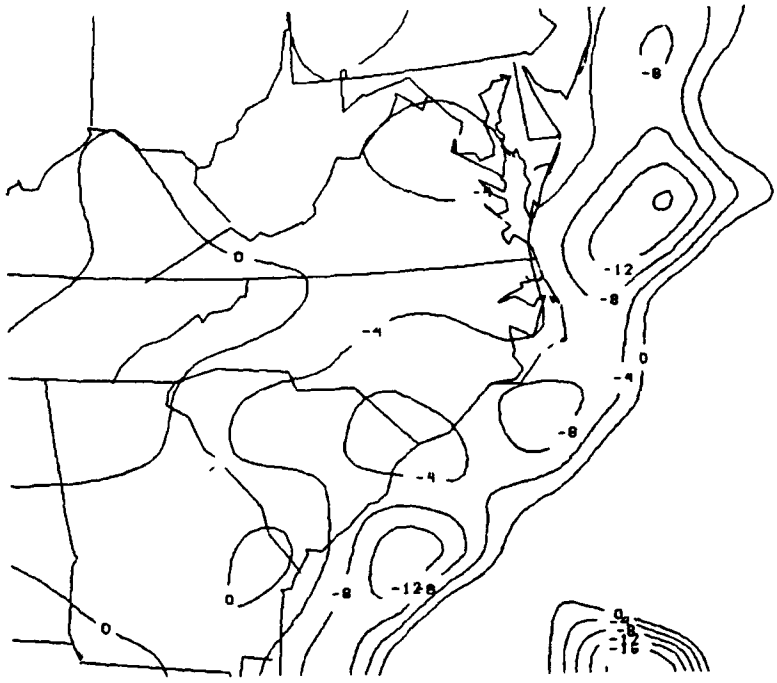

Fig. 12.9. Analysis of the Laplacian of sea level pressure valid at 0600 UTC 24 January 1986. Values given are x 10^{-11} mb m^{-2}, and the contour interval is four units.

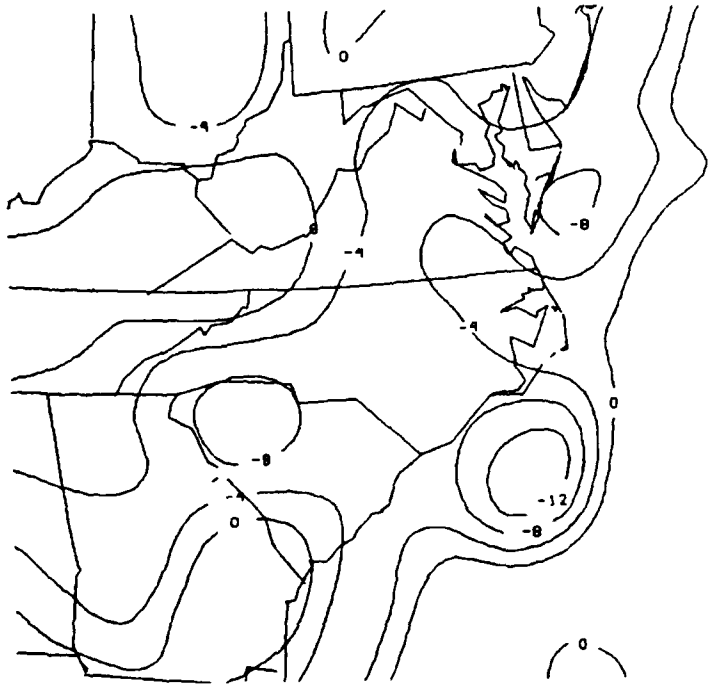

Fig. 12.10. Analysis of the Laplacian of sea level pressure valid at 1200 UTC 24 January 1986. Values given are x 10^{-11} mb m^{-2}, and the contour interval is four units.

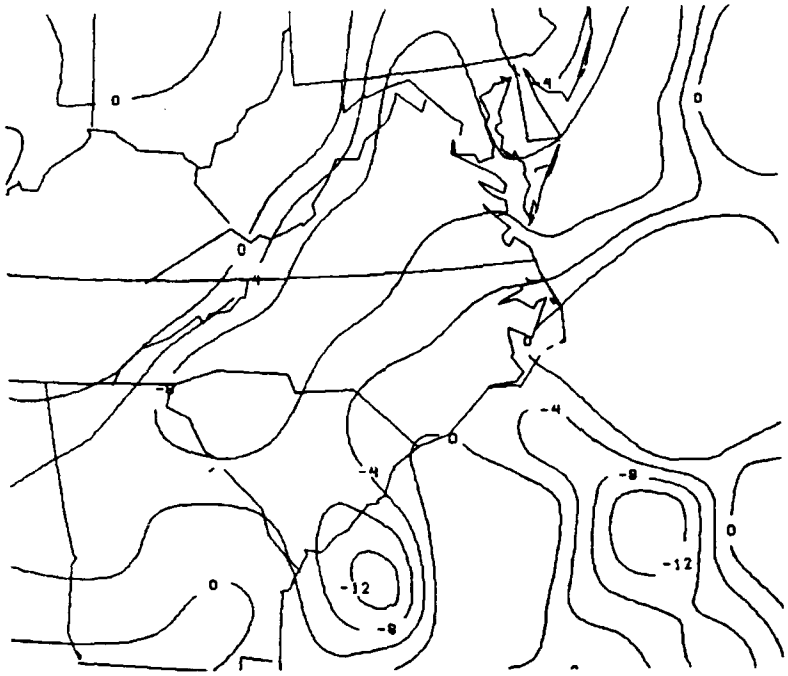

Fig. 12.11. Analysis of the Laplacian of sea level pressure valid at 1800 UTC 24 January 1986. Values given are x 10^{-11} mb m^{-2}, and the contour interval is four units.

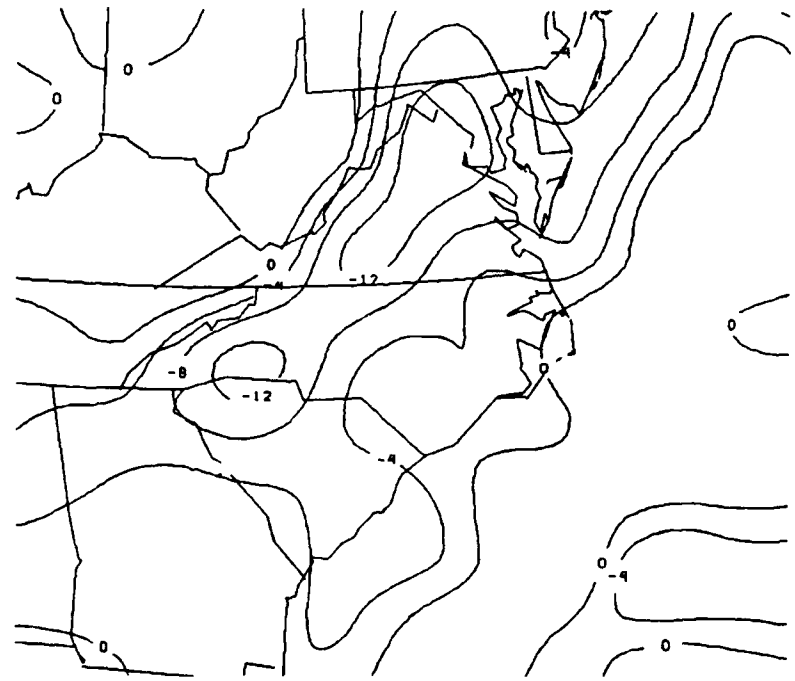

Fig. 12.12. Analysis of the Laplacian of sea level pressure valid at 0000 UTC 25 January 1986. Values given are x 10^{-11} mb m^{-2}, and the contour interval is four units.

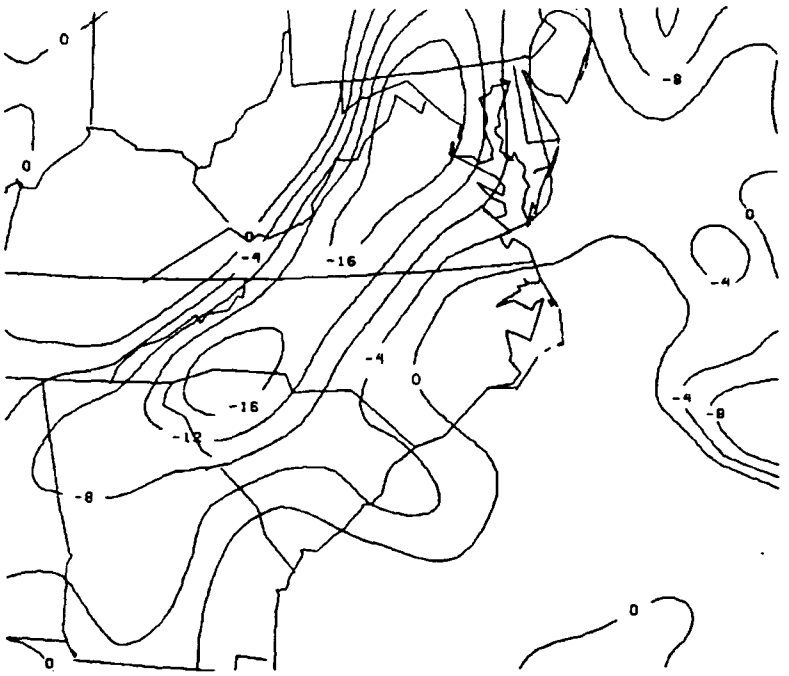

Fig. 12.13. Analysis of the Laplacian of sea level pressure valid at 0600 UTC 25 January 1986. Values given are x 10^{-11} mb m^{-2}, and the contour interval is four units.

Fig. 12.14. Analysis of the Laplacian of sea level pressure valid at 1200 UTC 25 January 1986. Values given are x 10^{-11} mb m^{-2}, and the contour interval is four units.

Fig. 12.15. Analysis of the Laplacian of sea level pressure valid at 1800 UTC 25 January 1986. Values given are x 10^{-11} mb m^{-2}, and the contour interval is four units.

Fig. 12.16. Analysis of the Laplacian of sea level pressure valid at 2100 UTC 25 January 1986. Values given are x 10^{-11} mb m^{-2}, and the contour interval is four units.